Majorana Fermions in Synthetic Quasi One-Dimensional Systems

Quantum Computer Driven Simulation Tools

DAVID GAYOWSKY

Thesis submitted to the University of Ottawa in partial fulfillment of the requirements for the degree of

Master of Science

in

PHYSICS

Department of Physics
Faculty of Science
University of Ottawa

"But don't stop looking. The triptych is about ways of never stopping. It is culture. On the right we have the boys. Two forms, but one shape, could be female, could be male, we can just about decipher four little legs and four little arms (the newborn calf of the right-hand panel!) and tiny little hopeful faces. And sense is suddenly made of the previous panels, this is pure mathematics, this is ancient logic. It is nature."

- MAX PORTER, GRIEF IS THE THING WITH FEATHERS

Abstract

Majorana fermions promise potential applications in quantum computing, superconductivity, and related fields. In this thesis, an analysis of A. Y. Kitaev's "Kitaev Chain", a quasi-one-dimensional quantum wire in contact with a p-wave superconductor, designed as a model exhibiting unpaired Majoranas, is performed. Described by tunneling of spinless fermions between quantum dots, and formation of Cooper pairs on neighboring dots, Kitaev's chain Hamiltonian serves as a basis for emergent Majorana Zero Modes (zero energy Majorana fermions localized at either end of the chain) and artificial gauges (phases) to appear.

By exact diagonalization, energy spectra and wavefunctions of a chain of spinless fermions on discrete quantum dots described by Kitaev's Hamiltonian are generated. By transforming the system into a basis of Majorana fermions and "bond fermions", where Majoranas on neighboring dots are paired, emergent Majorana Zero Modes (MZMs) are found at the ends of the chain. These emergent MZMs are paired in a non-local, zero energy bond fermion, which is found to allow degenerate energy states of the system to occur.

Joining the ends of the chain by allowing tunneling and pairing of fermions on end sites, a ring topology is considered, where an "artificial gauge" emerges. This artificial gauge, or phase, causes a phase change on tunneling and Cooper pairing Hamiltonian matrix elements as a result of operator ordering within the Hamiltonian's ring terms. These required operator orderings are derived by comparison of energy spectra of the Kitaev ring in the fermion and bond fermion bases. Matching of calculated energy spectra in the Majorana and fermionic bases is used to confirm the presence of the

artificial gauge, where this phase is found to be necessary in order to maintain a consistent energy spectra across the transformation between bases.

This analysis is performed in order to understand the concept of Majorana Zero Modes and the emergence of Majorana fermions in 1D chains. By doing so, it is determined what Majorana fermions are, where they come from, and why Majorana Zero Modes are considered to be zero energy. These results contribute to the understanding of Kitaev chains and rings, as well as serve as a starting point for discussions regarding physical implications of the artificial gauge's effect, fermion statistics, and the emergence of Majorana Zero Modes in quasi-one-dimensional systems.

Table of Contents

List of Figures

Constants, Abbreviations, and Symbols

Constants

$\hbar$	Reduced Planck Constant (Natural Units)	1
c	Speed of Light (Natural Units)	1

Abbreviations

1D	One-Dimensional
2D	Two-Dimensional
3D	Three-Dimensional
CI	Configuration-Interaction
JW	Jordan-Wigner
MZM	Majorana Zero Mode
NN	Nearest Neighbor
NNN	Next Nearest Neighbor
NP	Non-deterministic Polynomial Time
QD	Quantum Dot
VQE	Variational Quantum Eigensolver

Symbols

$\equiv$	Is Equivalent To

$\forall$ For All

$\gamma^\dagger$, γ Majorana Fermion Creation & Annihilation Operators (Respectively)

$\iff$ If And Only If

$\implies$ Implies

$\in$ In

$\wedge$ And

$\mathbb{N}$ Set of Natural Numbers $\{0, 1, 2, 3, ...\}$

$\mathbb{Z}^+$ Set of Positive Integers $\{1, 2, 3, ...\}$

$|$ Such That

σ_x, σ_y, σ_z Pauli Spin Matrices

$\subset$ Is a Subset Of, But Not Equal To

$\subseteq$ Is a Subset Of, And May Be Equal To

$\therefore$ Therefore

$\{X\}$ Set of "X"

$a^\dagger$, a Bond Fermion Creation & Annihilation Operators (Respectively)

$c^\dagger$, c Spinless Fermion Creation & Annihilation Operators (Respectively)

S^+, S^- Spin Up & Spin Down Operators (Respectively)

Chapter 1

Introduction

Since their conception in 1937 by Ettore Majorana [1], the potential applications of the Majorana fermion, or simply, "Majorana" - an elementary particle characterized by its existence as its own antiparticle, which arose from Majorana's proposition of a real, symmetric solution to the Dirac equation [2–4] - can be found in quantum computing [1, 3, 5, 6]. For a 1D chain of spinless fermions, Majorana fermions on nearest-neighbor sites will "bond" - leaving topologically protected Majoranas of zero energy at either ends of the chain [1, 5–10]. Although there is some evidence of their existence, both in superconducting chains and in ferromagnetic systems [11–13], these zero energy Majoranas, specifically called "Majorana Zero Modes" or "MZMs", have not been proved to exist experimentally; as many other quantum particles exhibit similar behaviour to that observed in Majorana experiments [14]. However, MZMs have continued to inspire theoretical study in part due to their resistance to decoherence and phase error in quantum systems [3, 6, 15] - making them ideal for future ventures in quantum computing [15–18].

In this thesis, the focus will be upon the in-depth analysis of Alexei Kitaev's "Kitaev chain" [6], a 1D model designed to serve as a basic example of the realization of MZMs. Inspired by the idea that phase error in quantum computing systems may be eliminated physically rather than with error correction algorithms, Kitaev's solution proposes using topologically protected, non-abelian anyons as a basis of qubits.

MZMs, which display non-abelian statistics, would form this qubit basis - leading Kitaev to conceive of the Kitaev chain, showing emergence of MZMs. Hence, within this thesis, by transforming fermions in Kitaev's chain to a system of bond fermions [19, 20], properties of MZMs for use in quantum computing [21–35] are explored.

Section 1.1 describes the Majorana fermion, while Section 1.2 introduces the Kitaev chain and offers a physical discussion of the system. Section 1.3 gives a brief overview of the role of Majorana fermions for topological quantum computing, introducing Kitaev's motivations for modeling emergent MZMs.

1.1 The Majorana Fermion

The Majorana fermion, although characterized by its status as being its own anti-particle, originally arose as a mathematical concept from Ettore Majorana's attempt to describe a strictly real solution to the Dirac equation for spin-$\frac{1}{2}$ particles [36, 37]. As a result, the Majorana fermion is characterized as its own anti-particle.

Majorana fermions, however, can be described by defining a single Majorana as a linear combination of fermionic creation and annihilation operators [6]. The concept of "breaking" a single fermion on a site i into two single Majorana fermions $\gamma_{i,1}$ and $\gamma_{i,2}$ is the key concept behind both the physical realization of Majorana fermions, as well as the usefulness of Majorana fermions.

1.2 The Kitaev Chain

Kitaev's model can be realized in a 1D InP quantum wire of N InAsP quantum dots, which may be occupied by spinless fermions. This quantum wire is in contact with a p-wave superconductor under the influence of an external magnetic field B, as shown in Fig. (1.1) below.

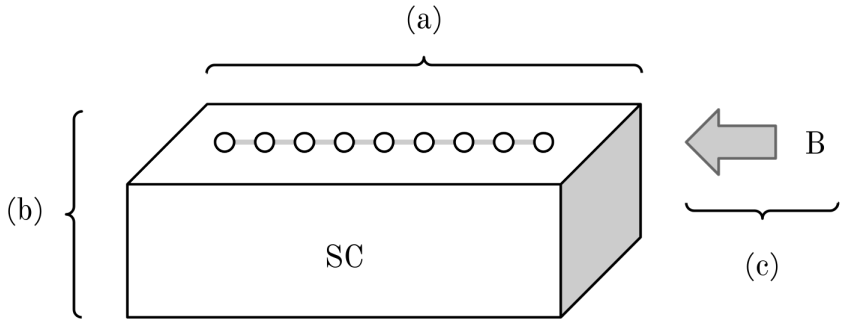

Figure 1.1: Kitaev chain consisting of a 1D quantum wire (a) in contact with a p-wave superconductor (b), under influence of an external magnetic field (c).

The configuration of this theoretical system is specifically designed in order to give rise to MZMs. Within this system, each of the quantum wire, superconductor, and magnetic field play a role, with their interaction resulting in the Kitaev chain model. Firstly, with the inclusion of the magnetic field, one spin degree of freedom is "projected away", allowing only for either spin up or spin down fermions - resulting in a system which may be considered effectively spinless, as all fermions have the same spin. In order to maintain superconductivity under the influence of this magnetic field, a p-wave superconductor is required; where a p-wave superconductor allows Cooper pairing of parallel-spin fermions (as opposed to s-wave superconductors, which only allow Cooper pairing of opposite-spin fermions). Finally, placing the quantum wire in contact with the superconductor allows superconductive properties within the quantum wire due to the proximity effect, i.e. Cooper pairs may then travel between the superconductor and quantum wire.

Firstly, consider that spinless fermions may only singly occupy sites - hence, each site, or quantum dot i, may be empty or occupied by a single fermion. An explicit diagram detailing the Kitaev chain sites and possible single fermion operators is shown in Fig. (1.2) below. In this case, fermionic operators may create or annihilate a single spinless fermion on each site.

The Kitaev Hamiltonian $\hat{H}_K$ representing this system can be written in terms of

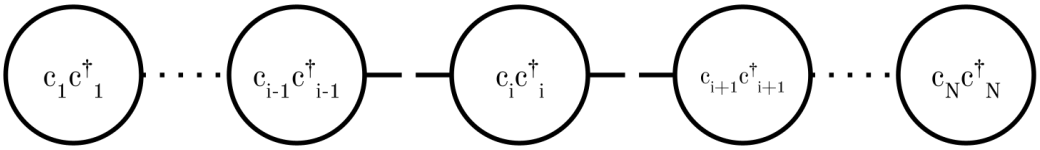

Figure 1.2: Kitaev chain of N sites, each of which site i may be occupied by a single spinless fermion.

the spinless fermionic creation and annihilation operators $c_i, c_i^\dagger$ as:

$$\hat{H}_K = t\sum_{i=1}^{N-1}(c_{i+1}^\dagger c_i + c_i^\dagger c_{i+1}) + \Delta\sum_{i=1}^{N-1}(c_{i+1}^\dagger c_i^\dagger + c_i c_{i+1}) - \mu\sum_{i=1}^{N}(c_i^\dagger c_i) \tag{1.1}$$

In this Hamiltonian, representing a chain of N sites, t is the nearest neighbor hopping (or "tunneling") integral describing the probability of a fermion hopping to an adjacent site. It should be noted that in this Hamiltonian, the nearest-neighbor (NN) approximation is assumed, i.e. fermions are considered to tunnel only to nearest-neighbor sites.

Δ is the Cooper pair energy describing the creation or annihilation of a pair of fermions on neighboring sites. Cooper pairs may travel in or out of the quantum wire due to its proximity to the p-wave superconductor, essentially "inheriting" the superconductor's pairing abilities.

μ is the chemical potential, counting the average number of electrons in the chain.

It should also be noted that the second term in each of the tunneling and pairing summations is the Hermitian conjugate of the first.

Within this thesis, the focus will be on the three-site Kitaev Hamiltonian, where the three-site chain (as shown in Fig. (1.3) below) is the minimum number of sites required to form a ring.

In addition, a smaller number of sites ensures that any calculations can be performed analytically if required, and that matrix representations of Hamiltonians do

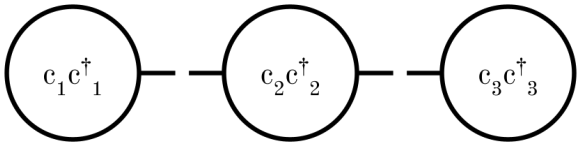

Figure 1.3: Kitaev chain of 3 sites, each of which may be occupied by a single spinless fermion.

not exceed computational ability to perform exact diagonalization. Thus, the Kitaev Hamiltonian for three sites becomes:

$$\hat{H}_K = t\sum_{i=1}^{2}(c_{i+1}^\dagger c_i + c_i^\dagger c_{i+1}) + \Delta\sum_{i=1}^{2}(c_{i+1}^\dagger c_i^\dagger + c_i c_{i+1}) - \mu\sum_{i=1}^{3}(c_i^\dagger c_i) \tag{1.2}$$

The three site Kitaev Hamiltonian may then be written explicitly as:

$$\begin{aligned}\hat{H}_K = {} & t(c_2^\dagger c_1 + c_1^\dagger c_2 + c_3^\dagger c_2 + c_2^\dagger c_3) \\ & + \Delta(c_2^\dagger c_1^\dagger + c_1 c_2 + c_3^\dagger c_2^\dagger + c_2 c_3) \\ & - \mu(c_1^\dagger c_1 + c_2^\dagger c_2 + c_3^\dagger c_3)\end{aligned} \tag{1.3}$$

Within this thesis, an investigation of the three-site Kitaev chain is done in order to show the emergence of Majorana Zero Modes. The explicit $t = \Delta, \mu = 0$ case is considered, where:

$$\begin{aligned} t &= |t| = 1 \\ \mu &= |\mu| = 0 \\ \Delta &= |\Delta| = 1 \end{aligned} \tag{1.4}$$

For the purposes of this work, only the relations of the values of t, Δ, and μ are considered. In particular, it should be noted that in the $t = \Delta, \mu = 0$ case, the Hamiltonian of Eq. (1.3) becomes exactly diagonal in the basis of bond fermions

(as shown in Sec. 3.2.1). By considering this particular set of values, one may consider this "simplest case" by calculating the system's wavefunction configurations and energy spectra exactly.

In addition, when letting one of the above values equal 1, it is then possible to define the spectra energy scale in terms of said value. In this case, it is considered that $t = 1$, and energy values will be defined simply in terms of t.

Although Kitaev's chain serves as the most basic example of MZM occurrence - and hence, contains only those parameters which are necessary to observe the emergence of MZMs - it should be noted that alternate, similar models may be considered. For instance, the Su-Schrieffer-Heeger model (which considers dimerization, or differing bonds between sites) may be used on its own or in a hybrid Kitaev model to display the emergence of MZMs on a chain [38, 39]. Alternately, models considering the system at large (e.g. including Hamiltonian terms which explicitly describe parameters such as applied magnetic field strength, spin-orbit coupling, effective mass, etc.) may be used to show the emergence of Majorana fermions in superconducting systems [7, 40, 41]. However, in order to analyze the emergence of MZMs within a simplistic "base" system, within this thesis, only the Kitaev chain model will be considered.

Hence, using these values and conventions, an analysis of the zero, one, two, and three electron states in the fermionic basis is performed, where the system's energy spectra and wavefunction configurations are calculated through exact diagonalization. The system is then transformed to the bases of Majorana and bond fermions, where spectral and wavefunction calculations are repeated in the bond fermion basis. As a result, the origin and role of the zero-energy MZM can then be observed and discussed.

1.3 Majorana Fermions for Topological Quantum Computing

Quantum computing has long been of interest due to its potential applications in efficient problem solving. In particular, when attempting to perform calculations in NP (nondeterministic polynomial time), including optimization and eigenvalue problems often required in computational physics - and which are considered to be lengthy or time consuming operations [42–45].

In quantum computation systems, however, several types of error (eg. decoherence of qubits, phase error, "bit flip" or classical error) can accumulate or occur due to interference within the system, resulting in information loss in performed calculations [46, 47]. Although many different methods of error-reducing quantum algorithms and corrections have been proposed [46–50], it has been considered that errors which arise due to interference within the system, or a qubit's interaction with the 'environment' [46], can be reduced or prevented physically rather than algorithmically in two main ways through the use of Majorana fermions. In one part by the spatial separation and topological protection of qubit sites [3, 6, 15, 16] which can occur in 1D chains of Majorana fermions; in the other, by using the inherent non-abelian statistics of individual Majoranas [1, 5, 8, 15–18, 51].

Classical error, or 'bit flip' error denoting the change of occupation of a qubit site, as well as errors resulting from accumulation of phase, are common sources of inaccurate computational results, and can occur due to electron tunneling between sites or on-site operations [6].

Kitaev's concept of spatially separated Majorana fermions on a 1D chain [6] is simple, and derives from these problems - what if these phase errors could be eliminated due to physical separation of sites? Kitaev's chain describes a superconducting system in which this separation may be found. Here, Kitaev describes individual Majorana fermions on nearest-neighbor sites pairing to form so-called "bond fermions". [1, 5–9,

52]. These nearest-neighbor pairings leave a zero-energy set of two single, unpaired Majoranas on either end of the chain, or a "non-local bond fermion". The non-local bond fermion, consisting of two Majorana Zero Modes, is hence immune to phase error due to spatial separation of the two sites (preventing interaction), and classical error due to charge conservation requirements of the system [6, 8]. In addition, in more realistic derivative models of superconducting systems, the MZMs are topologically protected within the system (meaning it is well protected against decoherence or perturbation) [5, 7, 10], and display non-abelian anyon braiding statistics [5, 8, 10, 17, 51, 53–55].

The basis of fault-tolerant quantum computation lies in the exchange of multiple particles, resulting in an accumulated phase which can be used to store information - where this information is protected from decoherence. [3, 5, 8, 10, 16, 17, 47, 51, 53]. In 2D, a process which "loops" a particle around another to return to its starting position can result in a non-trivial "winding phase", $e^{i\theta}$, on the pair wavefunction [8, 51, 53]. In the case of bosons and fermions, this "winding phase" is equivalent to $\theta = 0, 1$, respectively; however, particles called "anyons" are defined by a winding phase of $\theta \neq 0, 1$. For a so-called "abelian" anyon, each "winding" or exchange of particles creates a commutative phase, and only the total number of exchanges is important - for instance, in the case of bosons or fermions [53]. For a non-abelian anyon, however, the degenerate states of the system result in a non-commutative, higher dimensional winding phase under exchange represented as a rotation matrix between degenerate states [51]. Hence, under multiple exchanges, or "braiding" of non-abelian anyons, the accumulated phase upon the pair wavefunction acts as a "memory" of exchanges due to non-commutative matrix multiplication [8, 51, 53]. These exchanges are topologically protected from decoherence due to the topological nature of rotation matrices [5, 16, 17, 51] - and hence, a topologically protected "quantum memory" is created.

It is clear that the zero-energy, non-local MZMs are the key to fault-tolerant quan-

tum computation. Hence, in this thesis, further study of the non-local bond fermion in Kitaev's chain are undertaken, revealing the emergence of MZMs and their relation to the fermionic Kitaev chain.

1.4 Thesis Contributions

The contents of this thesis include analyses of the 3 QD Kitaev Hamiltonian in various configurations and bases, and as such are included in the following article written for publication:

David J. Gayowsky, Amintor Dusko, Jacob Manalo, Mahan Mohseni, and Paweł Hawrylak, *Kitaev chains and rings: Majorana Zero Modes and artificial gauges*, forthcoming in 2022.

For the given article, all calculations and derivations have been performed by myself in full using methodology described in Appendix A, in collaboration with Dr. Amintor Dusko. Examples of these derivations and source codes used in calculations are shown in Appendix B and C respectively.

Within this thesis, Chapter 2 and Chapter 3 are based on this article, and the various methods described in Appendix A were used to achieve its results.

If further reading is desired, a full manuscript describing the Kitaev chain and ring systems, as well as the Kitaev chain and ring in a system of spins for use in quantum algorithms, is available.

1.5 Outline

The contents of this thesis are organized as follows, beginning from the introduction in Chapter 1:

Chapter 2 focuses on a classical analysis of Kitaev's chain in the basis of fermions, starting with the tight binding (TB) model. Cooper pairing is then introduced, and its role discussed.

Chapter 3 transforms Kitaev's chain into the basis of Majorana and bond fermions, where the emergent MZM and its role are discussed.

Chapter 4 considers the Kitaev ring, where artificial gauges, or phases, are found to emerge, and their effect on movement of fermions in the ring are discussed.

The Appendix contains an in-depth discussion of methodology used to achieve the results of Chapters 2 and 3, as well as explicit example calculations, derivations, and source codes.

Chapter 2

The Fermionic Kitaev Chain

This chapter will focus on the 1D Kitaev model of spinless fermions, and will serve as a basis for comparison with such a system of Majorana and bond fermions. When comparing the system in fermions and bond fermions, it is assumed that the system will exhibit the same energy spectra regardless of basis. Therefore, it is possible to ensure the accuracy of a transformation by comparison of energy spectra, where matching spectra implies the basis transformation has been performed correctly. As a result, the focus of this chapter will be to perform an analysis of the Kitaev chain for the purpose of both gaining an initial understanding of the system, as well as to provide a base comparison to ensure validity of future transformations.

Within this chapter, Section 2.1 introduces possible configurations of the three site Kitaev chain, and derives or computationally generates Hamiltonian matrices as required. Section 2.2 then performs an analysis of the Kitaev chain, calculating energy eigenvalues and wavefunctions, focusing first on the tunneling Hamiltonian, then introducing Cooper pairing to the system.

2.1 The Three-Site Kitaev Chain

Firstly, recall the explicit Kitaev Hamiltonian on three sites of Eq. (1.3):

$$\begin{aligned}\hat{H}_K &= t(c_2^\dagger c_1 + c_1^\dagger c_2 + c_3^\dagger c_2 + c_2^\dagger c_3) \\ &+ \Delta(c_2^\dagger c_1^\dagger + c_1 c_2 + c_3^\dagger c_2^\dagger + c_2 c_3) \\ &- \mu(c_1^\dagger c_1 + c_2^\dagger c_2 + c_3^\dagger c_3)\end{aligned} \tag{1.3}$$

For such a system, it is first important to note that $\hat{H}_K$ does not conserve the number of particles - the three site Kitaev chain may be occupied by 0, 1, 2, or 3 spinless fermions. Considering all possible occupation numbers, it is then possible to explicitly write all possible electron configurations (as discussed in detail in Sec. A.2). The number of configurations of this system will hence be:

$$\begin{aligned}k &= \binom{3}{0} + \binom{3}{1} + \binom{3}{2} + \binom{3}{3} \\ &= 1 + 3 + 3 + 1 \\ &= 8\end{aligned} \tag{2.1}$$

The 8 possible electron configurations may be written explicitly, beginning with the vacuum state (zero-electron configuration):

$$|0\rangle \tag{2.2}$$

The one-electron configurations are:

$$|1\rangle, |2\rangle, |3\rangle \tag{2.3}$$

The two-electron configurations are:

$$|12\rangle, |13\rangle, |23\rangle \tag{2.4}$$

Finally, the three-electron configuration is:

$$|123\rangle \tag{2.5}$$

The set of all possible electronic configurations $\{k\}$ may then be written explicitly as:

$$\begin{aligned} &\{|0\rangle, |1\rangle, |2\rangle, |3\rangle, \\ &|12\rangle, |13\rangle, |23\rangle, |123\rangle\} \end{aligned} \tag{2.6}$$

Wavefunctions $|\psi_j\rangle$ (for $j \in \{0, 1, 2, ...7\}$) of the system can be written as a linear combination of all possible configurations, over all possible electron numbers. Hence, for the three site case, $|\psi_j\rangle$ can be written explicitly for all the above electronic configurations as:

$$\begin{aligned} |\psi_j\rangle = &A_0^j |0\rangle + A_1^j |1\rangle + A_2^j |2\rangle + A_3^j |3\rangle \\ &+ A_4^j |12\rangle + A_5^j |13\rangle + A_6^j |23\rangle + A_7^j |123\rangle \end{aligned} \tag{2.7}$$

Where in order to know the allowed wavefunctions (i.e. know the wavefunction coefficients A^j), acting on Eq. (2.7) with $\hat{H}_K$ will hence give:

$$\sum_{\{q\},Q} \langle \{p\}, P| \hat{H}_K |\{q\}, Q\rangle A^j_{Q,\{q\}} = E^j A^j_{P,\{p\}} \tag{2.8}$$

Where this is a matrix equation describing the Kitaev Hamiltonian matrix in the space of all possible electron configurations $\{q\}, \{p\} \subseteq \{k\}$ for a given electron occupation number $Q, P \in \mathbb{N} \leq N = 3$.

As such, in order to obtain the allowed wavefunctions and energy spectra of this system, the following matrix may be constructed, and exact diagonalization performed to find its eigenvalues and eigenvectors:

$$\langle \{p\}, P | \, \hat{H}_K \, | \{q\}, Q \rangle = H^K_{p,q} \tag{2.9}$$

2.1.1 Matrix Hamiltonians and Subspaces

From the set of possible configurations given by Eq. (2.6) the matrix representation of the Kitaev Hamiltonian, $H^K_{p,q}$, can be written generally as shown in Eq. (2.10) on the following page.

Thus, in order to obtain the explicit matrix Hamiltonian, it is required to explicitly calculate all $k^2 = 8^2 = 64$ matrix elements $H^K_{p,q}$. However: there are, in fact, two observations which reduce the number of calculations required to derive such matrices.

$$\hat{H}_K = \begin{bmatrix} H^K_{0,0} & H^K_{0,1} & H^K_{0,2} & H^K_{0,3} & H^K_{0,12} & H^K_{0,13} & H^K_{0,23} & H^K_{0,123} \\ H^K_{1,0} & H^K_{1,1} & H^K_{1,2} & H^K_{1,3} & H^K_{1,12} & H^K_{1,13} & H^K_{1,23} & H^K_{1,123} \\ H^K_{2,0} & H^K_{2,1} & H^K_{2,2} & H^K_{2,3} & H^K_{2,12} & H^K_{2,13} & H^K_{2,23} & H^K_{2,123} \\ H^K_{3,0} & H^K_{3,1} & H^K_{3,2} & H^K_{3,3} & H^K_{3,12} & H^K_{3,13} & H^K_{3,23} & H^K_{3,123} \\ H^K_{12,0} & H^K_{12,1} & H^K_{12,2} & H^K_{12,3} & H^K_{12,12} & H^K_{12,13} & H^K_{12,23} & H^K_{12,123} \\ H^K_{13,0} & H^K_{13,1} & H^K_{13,2} & H^K_{13,3} & H^K_{13,12} & H^K_{13,13} & H^K_{13,23} & H^K_{13,123} \\ H^K_{23,0} & H^K_{23,1} & H^K_{23,2} & H^K_{23,3} & H^K_{23,12} & H^K_{23,13} & H^K_{23,23} & H^K_{23,123} \\ H^K_{123,0} & H^K_{123,1} & H^K_{123,2} & H^K_{123,3} & H^K_{123,12} & H^K_{123,13} & H^K_{123,23} & H^K_{123,123} \end{bmatrix} \tag{2.10}$$

The first method of reducing the number of calculations has already been noted in Appendix A.6, which is that for any matrix element $H^K_{p,q}$, $H^K_{p,q} = H^{K*}_{q,p}$ so long as $\hat{H}_K$ is Hermitian (which it is). In addition, as all coefficients of $\hat{H}_K$ are real, it is not even required to find the complex conjugate - therefore we take directly that:

$$H^K_{p,q} = H^K_{q,p} \tag{2.11}$$

The second observation is realized from noting that both the tunneling and chemical potential terms of $\hat{H}_K$ conserve the number of particles in the chain - however, the pairing term, which creates or annihilates pairs of fermions on neighboring sites, alters particle numbers only in sets of 2. Therefore, any given configuration will only have interactions with configurations of the same occupation number parity (i.e. for the 3-site chain, the configuration of 3 fermions will interact only with configurations of 1 fermion, and a configuration of 2 fermions will interact only with the configuration of 0 fermions).

As a result, any matrix element describing the interaction between two configurations of different occupation number parities will be 0; or, written explicitly:

$$\begin{aligned}
\langle\{p\}, P=0|\, \hat{H}_K \,|\{q\}, Q=1\rangle &= 0 \\
\langle\{p\}, P=0|\, \hat{H}_K \,|\{q\}, Q=3\rangle &= 0 \\
\langle\{p\}, P=2|\, \hat{H}_K \,|\{q\}, Q=1\rangle &= 0 \\
\langle\{p\}, P=2|\, \hat{H}_K \,|\{q\}, Q=3\rangle &= 0
\end{aligned} \tag{2.12}$$

Thus the Hamiltonian of Eq. (2.10) can now be simplified to:

$$\hat{H}_K = \begin{bmatrix}
H^K_{0,0} & 0 & 0 & 0 & H^K_{0,12} & H^K_{0,13} & H^K_{0,23} & 0 \\
0 & H^K_{1,1} & H^K_{1,2} & H^K_{1,3} & 0 & 0 & 0 & H^K_{1,123} \\
0 & H^K_{2,1} & H^K_{2,2} & H^K_{2,3} & 0 & 0 & 0 & H^K_{2,123} \\
0 & H^K_{3,1} & H^K_{3,2} & H^K_{3,3} & 0 & 0 & 0 & H^K_{3,123} \\
H^K_{12,0} & 0 & 0 & 0 & H^K_{12,12} & H^K_{12,13} & H^K_{12,23} & 0 \\
H^K_{13,0} & 0 & 0 & 0 & H^K_{13,12} & H^K_{13,13} & H^K_{13,23} & 0 \\
H^K_{23,0} & 0 & 0 & 0 & H^K_{23,12} & H^K_{23,13} & H^K_{23,23} & 0 \\
0 & H^K_{123,1} & H^K_{123,2} & H^K_{123,3} & 0 & 0 & 0 & H^K_{123,123}
\end{bmatrix} \tag{2.13}$$

Where this matrix can then be re-arranged through simple row and column operations, and written in block-diagonal form as:

$$\hat{H}_K = \begin{bmatrix} H^K_{0,0} & H^K_{0,12} & H^K_{0,13} & H^K_{0,23} & 0 & 0 & 0 & 0 \\ H^K_{12,0} & H^K_{12,12} & H^K_{12,13} & H^K_{12,23} & 0 & 0 & 0 & 0 \\ H^K_{13,0} & H^K_{13,12} & H^K_{13,13} & H^K_{13,23} & 0 & 0 & 0 & 0 \\ H^K_{23,0} & H^K_{23,12} & H^K_{23,13} & H^K_{23,23} & 0 & 0 & 0 & 0 \\ 0 & 0 & 0 & 0 & H^K_{1,1} & H^K_{1,2} & H^K_{1,3} & H^K_{1,123} \\ 0 & 0 & 0 & 0 & H^K_{2,1} & H^K_{2,2} & H^K_{2,3} & H^K_{2,123} \\ 0 & 0 & 0 & 0 & H^K_{3,1} & H^K_{3,2} & H^K_{3,3} & H^K_{3,123} \\ 0 & 0 & 0 & 0 & H^K_{123,1} & H^K_{123,2} & H^K_{123,3} & H^K_{123,123} \end{bmatrix} \tag{2.14}$$

For any block-diagonal matrix, the set of eigenvalues and eigenvectors will simply be the union of the sets of eigenvalues and eigenvectors of its sub-matrices (or "contributing blocks"). Thus, it is then possible to divide the matrix Kitaev Hamiltonian into two separate 'subspace' matrix Hamiltonians, each representing the configurations of either even or odd occupation number parity. The subspace matrices can thus be written:

$$\hat{H}_{EK} = \begin{bmatrix} H^K_{0,0} & H^K_{0,12} & H^K_{0,13} & H^K_{0,23} \\ H^K_{12,0} & H^K_{12,12} & H^K_{12,13} & H^K_{12,23} \\ H^K_{13,0} & H^K_{13,12} & H^K_{13,13} & H^K_{13,23} \\ H^K_{23,0} & H^K_{23,12} & H^K_{23,13} & H^K_{23,23} \end{bmatrix} \tag{2.15}$$

$$\hat{H}_{OK} = \begin{bmatrix} H^K_{1,1} & H^K_{1,2} & H^K_{1,3} & H^K_{1,123} \\ H^K_{2,1} & H^K_{2,2} & H^K_{2,3} & H^K_{2,123} \\ H^K_{3,1} & H^K_{3,2} & H^K_{3,3} & H^K_{3,123} \\ H^K_{123,1} & H^K_{123,2} & H^K_{123,3} & H^K_{123,123} \end{bmatrix} \tag{2.16}$$

Where, from the above matrices and the assumption of Eq. (2.11), it can be seen that the number of required matrix element calculations has been reduced from 64 to 20 (as it is still required to calculate the diagonal elements, which occur only once in each matrix). The complete set of matrix element calculations will not be shown here, as they are repetitive, however in the style of Appendix A.4, an explicit example

from each term of $\hat{H}_K$ is shown below, using the fermionic relations in Eq. (A.16), Eq. (A.18), and Eq. (A.19).

Example 1: Tunneling Term (Two-Electron Configuration)

The Kitaev Hamiltonian tunneling matrix element $H^K_{12,13}$ is calculated as follows:

$$\begin{aligned}
H^K_{12,13} &= \langle 12|\, \hat{H}_K\, |13\rangle \\
&= \langle 12|\, t(c_3^\dagger c_2 + c_2^\dagger c_3)\, |13\rangle \\
&= t\, \langle 0|\, c_2 c_1 (c_3^\dagger c_2 + c_2^\dagger c_3) c_1^\dagger c_3^\dagger\, |0\rangle \\
&= t\, \langle 0|\, c_2 c_1 c_3^\dagger c_2 c_1^\dagger c_3^\dagger\, |0\rangle + t\, \langle 0|\, c_2 c_1 c_2^\dagger c_3 c_1^\dagger c_3^\dagger\, |0\rangle \\
&= t\, \langle 0|\, c_1 c_3^\dagger \underbrace{\cancel{c_2 c_2}}_{0} c_1^\dagger c_3^\dagger\, |0\rangle + t\, \langle 0|\, c_1 \underbrace{c_2 \cancel{c_2^\dagger}}_{1} \underbrace{\cancel{c_3 c_3^\dagger}}_{1} c_1^\dagger\, |0\rangle \\
&= 0 + t\, \langle 0|\, \cancel{c_1 c_1^\dagger}\, |0\rangle \\
&= t\, \underbrace{\langle 0|0\rangle}_{1} \\
&= t
\end{aligned}$$

Example 2: Pairing Term (Two-Electron Configuration)

The Kitaev Hamiltonian pairing matrix element $H^K_{12,0}$ is calculated as follows:

$$\begin{aligned}
H^K_{12,0} &= \langle 12|\, \hat{H}_K\, |0\rangle \\
&= \langle 12|\, \Delta(c_2^\dagger c_1^\dagger + c_1 c_2)\, |0\rangle \\
&= \Delta\, \langle 0|\, c_2 c_1 (c_2^\dagger c_1^\dagger + c_1 c_2)\, |0\rangle \\
&= \Delta\, \langle 0|\, c_2 c_1 c_2^\dagger c_1^\dagger\, |0\rangle + \Delta\, \langle 0|\, c_2 c_1 c_1 c_2\, |0\rangle \\
&= -\Delta\, \langle 0|\, \underbrace{c_2 \cancel{c_2^\dagger}}_{1} \underbrace{c_1 \cancel{c_1^\dagger}}_{1}\, |0\rangle + \Delta\, \langle 0|\, c_2 \underbrace{c_1 c_1}_{0} c_2\, |0\rangle \\
&= -\Delta\, \underbrace{\langle 0|0\rangle}_{1} + 0 \\
&= -\Delta
\end{aligned}$$

Example 3: Chemical Potential Term (Two-Electron Configuration)

The Kitaev Hamiltonian tunneling matrix element $H^K_{12,12}$ is calculated as follows:

$$
\begin{aligned}
H^K_{12,12} &= \langle 12| \hat{H}_K |12\rangle \\
&= \langle 12| -\mu(c_1^\dagger c_1 + c_2^\dagger c_2) |12\rangle \\
&= -\mu \langle 0| c_2 c_1 (c_1^\dagger c_1 + c_2^\dagger c_2) c_1^\dagger c_2^\dagger |0\rangle \\
&= -\mu \langle 0| c_2 c_1 c_1^\dagger c_1 c_1^\dagger c_2^\dagger |0\rangle - \mu \langle 0| c_2 c_1 c_2^\dagger c_2 c_1^\dagger c_2^\dagger |0\rangle \\
&= -\mu \langle 0| c_2 \underbrace{\cancel{c_1 c_1^\dagger}}_{1} \underbrace{\cancel{c_1 c_1^\dagger}}_{1} c_2^\dagger |0\rangle - \mu \langle 0| c_1 \underbrace{\cancel{c_2 c_2^\dagger}}_{1} \underbrace{\cancel{c_2 c_2^\dagger}}_{1} c_1^\dagger |0\rangle \\
&= -\mu \langle 0| \cancel{c_2 c_2^\dagger} |0\rangle - \mu \langle 0| \cancel{c_1 c_1^\dagger} |0\rangle \\
&= -\mu \underbrace{\langle 0|0\rangle}_{1} - \mu \underbrace{\langle 0|0\rangle}_{1} \\
&= -2\mu
\end{aligned}
$$

After performing all required element calculations, the Kitaev Hamiltonian in the even and odd subspace matrix representations becomes:

$$
\hat{H}_{EK} = \begin{bmatrix} 0 & -\Delta & 0 & -\Delta \\ -\Delta & -2\mu & t & 0 \\ 0 & t & -2\mu & t \\ -\Delta & 0 & t & -2\mu \end{bmatrix} \tag{2.17}
$$

$$
\hat{H}_{OK} = \begin{bmatrix} -\mu & t & 0 & -\Delta \\ t & -\mu & t & 0 \\ 0 & t & -\mu & -\Delta \\ -\Delta & 0 & -\Delta & -3\mu \end{bmatrix} \tag{2.18}
$$

Where these subspace matrices can then be diagonalized to calculate system energy spectra and wavefunctions.

2.1.2 Computational Generation of the Matrix Hamiltonians

For large N systems, the matrix representations of Kitaev Hamiltonians can be tedious to derive analytically - recall that a chain of $N = 3$ sites requires 20 calculations. However, subspace matrices can be generated computationally using a program of the form described in Fig. (A.1) of Appendix A.5.

In this case, an input of the number of sites N, numerical values of t, Δ, and μ, and whether the user would like to return the even or odd subspace matrix is given to the function call, and a numerical Kitaev Hamiltonian matrix is returned.

The function defined to generate subspace matrices of the Kitaev Hamiltonian for N sites is shown in Fig. (2.1) on the following page, with source code in Appendix C.1.

It should be noted that as the form of the Hamiltonian does not change with the number of sites N, if-else statements populating subspace matrices do not change based on N. In addition, computationally generated matrix Hamiltonians were found to match those derived analytically for $N = 2, 3, 4$.

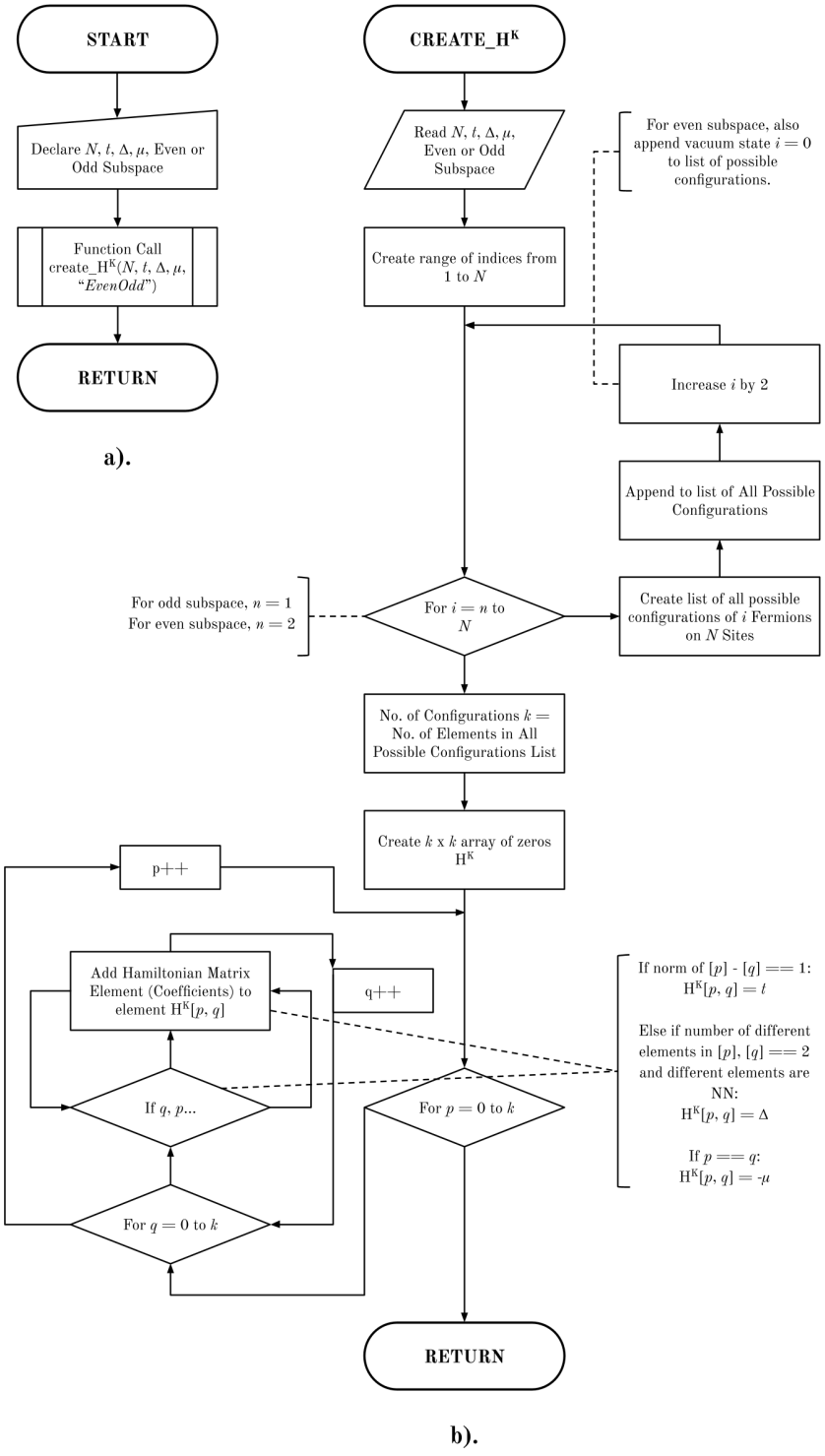

Figure 2.1: Program flowchart for computational generation of matrix Kitaev Hamiltonian for N sites. a). Main function call, b). Hamiltonian generation function.

2.2 Analysis of the Kitaev Chain

Within this section, the roles of the various terms of the Kitaev Hamiltonian are investigated, where energy spectra and system wavefunctions are generated. Initially, in Sec. 2.2.1 the tight binding, or "tunneling" Kitaev Hamiltonian is explored, then pairing terms are added in Sec. 2.2.2, and effects on system energy spectra and configurations are observed.

2.2.1 The Tight Binding Kitaev Chain Hamiltonian

Initially, consider only the first term of the Kitaev Hamiltonian. The tight binding, or "tunneling", Kitaev Hamiltonian contains only the nearest-neighbor hopping term of the Kitaev Hamiltonian in Eq. (1.2), i.e. the tunneling Hamiltonian on three sites becomes:

$$\hat{H}_K = t\sum_{i=1}^{2}(c_{i+1}^{\dagger}c_i + c_i^{\dagger}c_{i+1}) \tag{2.19}$$

Explicitly, this can be written in the form of Eq.(1.3) as:

$$\hat{H}_K = t(c_2^{\dagger}c_1 + c_1^{\dagger}c_2 + c_3^{\dagger}c_2 + c_2^{\dagger}c_3) \tag{2.20}$$

Taking the form of the even and odd subspace matrix Hamiltonians (Eq. (2.17) and (2.18), respectively) derived in Sec. 2.1.1, the matrix form of the tunneling Kitaev Hamiltonian can then be written simply by letting $\Delta, \mu = 0$ in these equations. Thus, including the numerical values and conventions imposed in Eq. (1.4) above, the even and odd tunneling matrix Kitaev Hamiltonians are:

$$\hat{H}_{ET} = \begin{bmatrix} 0 & 0 & 0 & 0 \\ 0 & 0 & t & 0 \\ 0 & t & 0 & t \\ 0 & 0 & t & 0 \end{bmatrix} = \begin{bmatrix} 0 & 0 & 0 & 0 \\ 0 & 0 & 1 & 0 \\ 0 & 1 & 0 & 1 \\ 0 & 0 & 1 & 0 \end{bmatrix} \tag{2.21}$$

$$\hat{H}_{OT} = \begin{bmatrix} 0 & t & 0 & 0 \\ t & 0 & t & 0 \\ 0 & t & 0 & 0 \\ 0 & 0 & 0 & 0 \end{bmatrix} = \begin{bmatrix} 0 & 1 & 0 & 0 \\ 1 & 0 & 1 & 0 \\ 0 & 1 & 0 & 0 \\ 0 & 0 & 0 & 0 \end{bmatrix} \tag{2.22}$$

Thus, through the use of computational matrix generation and exact diagonalization, the even and odd subspace energies, as well as even and odd wavefunction configurations, are calculated as in Fig. (2.2), (2.3), and (2.4) on the following page (respectively).

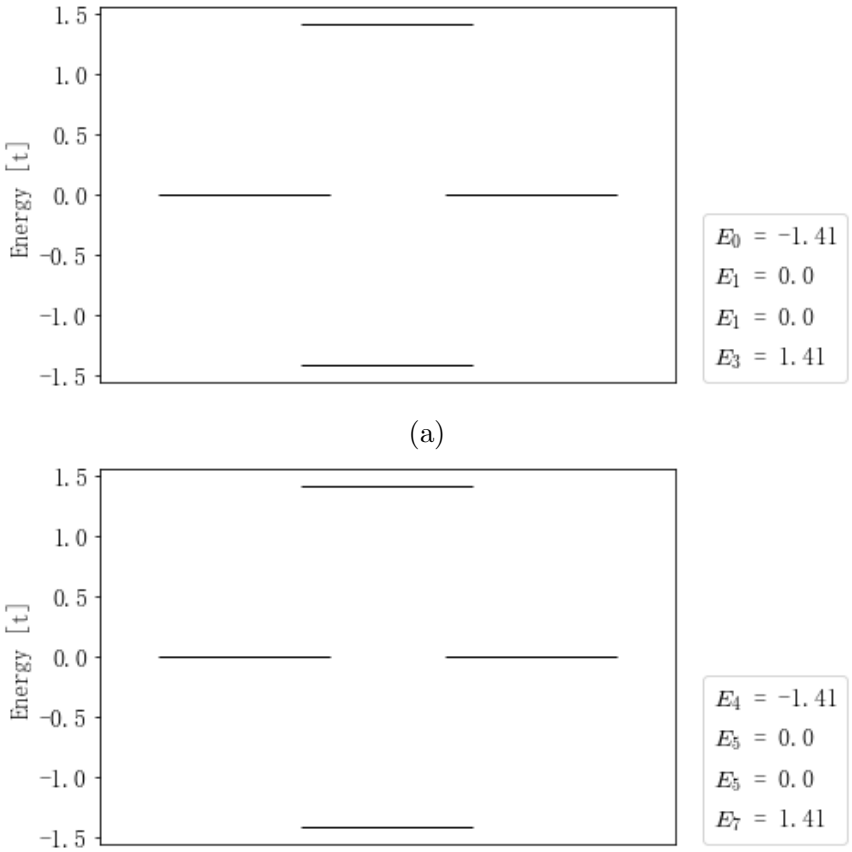

Figure 2.2: Energy spectra of three-site $\Delta, \mu = 0$ Kitaev chain, (a) even and (b) odd subspaces.

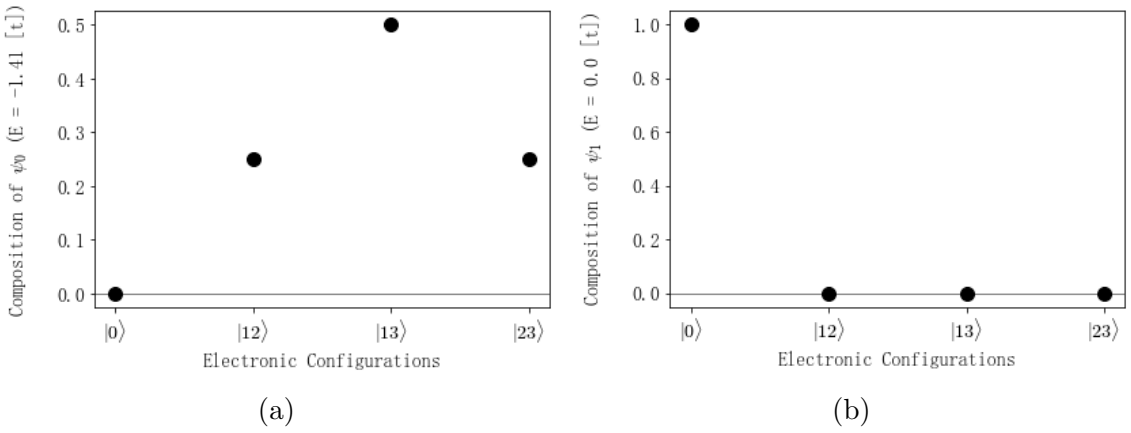

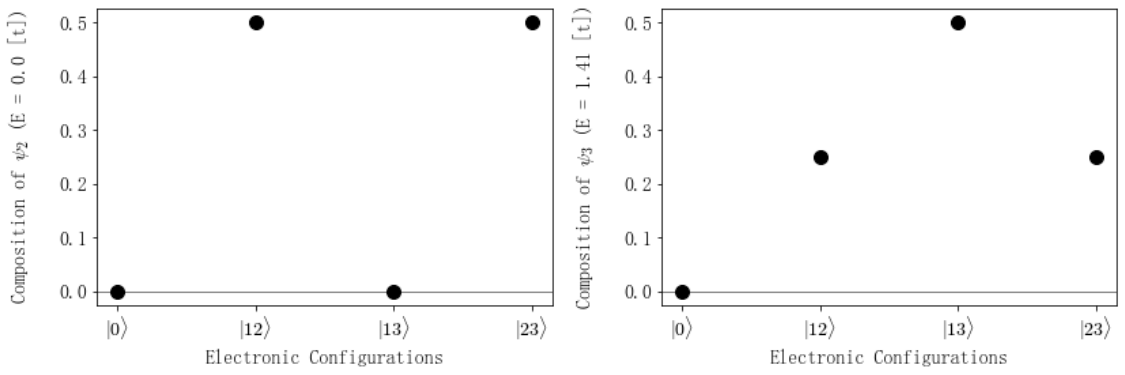

(c) (d)

Figure 2.3: Wavefunction configurations of $\Delta, \mu = 0$ Kitaev Hamiltonian, even subspace.

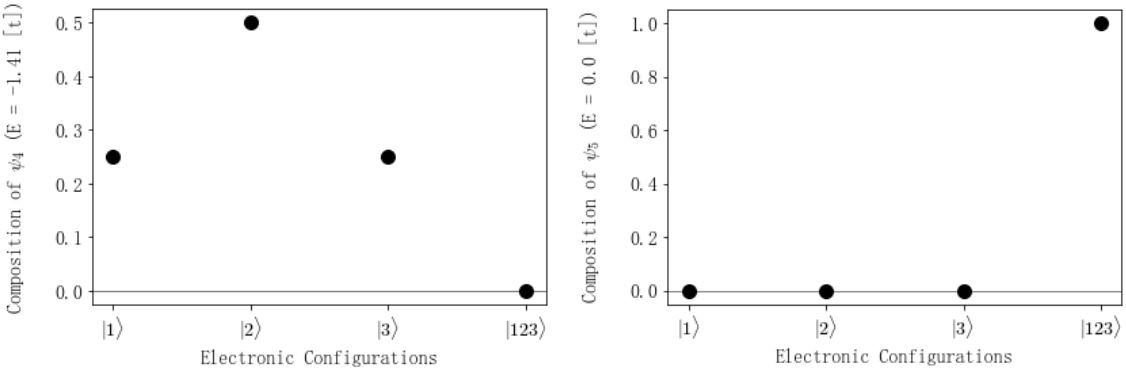

(a) (b)

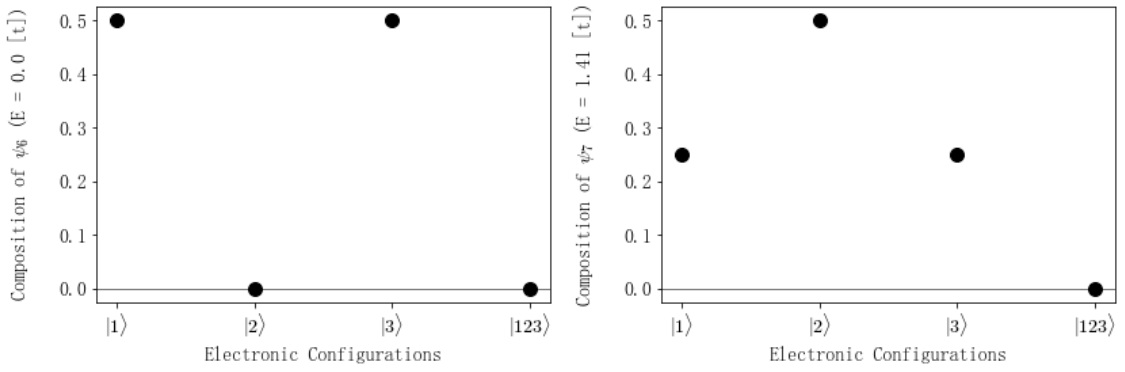

(c) (d)

Figure 2.4: Wavefunction configurations of $\Delta, \mu = 0$ Kitaev Hamiltonian, odd subspace.

From Fig. (2.2a) and (2.3) above, consider the separation of the vacuum and two electron states, and their respective energies. The vacuum state, $|0\rangle$, is completely decoupled from all two-electron states as shown in Fig. (2.3) (i.e. there is no allowed transition from the vacuum state to any two-electron configuration). However, the vacuum state is degenerate in energy with respect to $|\psi_2\rangle$, where:

$$|\psi_2\rangle = \frac{1}{\sqrt{2}}(|12\rangle + |23\rangle) \tag{2.23}$$

Expecting that emergent MZMs occur as degenerate "zero" energy states, with no change in system energy under occupation, this result is promising. Similarly to the appearance of MZMs, occupying states $|12\rangle$, $|23\rangle$ results in no change of energy with respect to the vacuum (unoccupied) state.

However, it is not yet apparent how, or if, this leads to the appearance of MZMs in the Kitaev chain, and further investigation is required. As the two electron states are not actually coupled to $|0\rangle$ through allowed transitions in the system, occupation number coupling must now be considered.

2.2.2 Effect of the Pairing Term

In this subsection, the effect of the pairing term on energy spectra and configurations of the Kitaev chain will be observed. In this case, both the pairing and tunneling terms of Eq. (1.2) will be used, and the Hamiltonian becomes:

$$\hat{H}_K = t\sum_{i=1}^{2}(c_{i+1}^\dagger c_i + c_i^\dagger c_{i+1}) + \Delta\sum_{i=1}^{2}(c_{i+1}^\dagger c_i^\dagger + c_i c_{i+1}) \tag{2.24}$$

Explicitly, this can be written in the form of Eq. (1.3) as:

$$\begin{aligned}\hat{H}_K = t(c_2^\dagger c_1 + c_1^\dagger c_2 + c_3^\dagger c_2 + c_2^\dagger c_3) \\ + \Delta(c_2^\dagger c_1^\dagger + c_1 c_2 + c_3^\dagger c_2^\dagger + c_2 c_3)\end{aligned} \tag{2.25}$$

Taking the form of the even and odd subspace matrix Hamiltonians (Eq. (2.17) and (2.18), respectively) derived in Sec. 2.1.1, the matrix form of the Hamiltonian described above in Eq. (2.24) can be written by letting $\mu = 0$ in these equations.

Recall, the $|t| = |\Delta|$ case of Eq. (1.4) will be considered. Thus, including the numerical values imposed in Eq. (1.4) above, the even and odd matrix Kitaev Hamiltonians given by $t = \Delta$ are:

$$\hat{H}_{EP1} = \begin{bmatrix} 0 & -\Delta & 0 & -\Delta \\ -\Delta & 0 & t & 0 \\ 0 & t & 0 & t \\ -\Delta & 0 & t & 0 \end{bmatrix} = \begin{bmatrix} 0 & -1 & 0 & -1 \\ -1 & 0 & 1 & 0 \\ 0 & 1 & 0 & 1 \\ -1 & 0 & 1 & 0 \end{bmatrix} \tag{2.26}$$

$$\hat{H}_{OP1} = \begin{bmatrix} 0 & t & 0 & -\Delta \\ t & 0 & t & 0 \\ 0 & t & 0 & -\Delta \\ -\Delta & 0 & -\Delta & 0 \end{bmatrix} = \begin{bmatrix} 0 & 1 & 0 & -1 \\ 1 & 0 & 1 & 0 \\ 0 & 1 & 0 & -1 \\ -1 & 0 & -1 & 0 \end{bmatrix} \tag{2.27}$$

Thus, through the use of exact diagonalization, the even and odd subspace energies, as well as even and odd wavefunction configurations, are calculated as in Fig. (2.5), (2.6), and (2.7) on the following page (respectively).

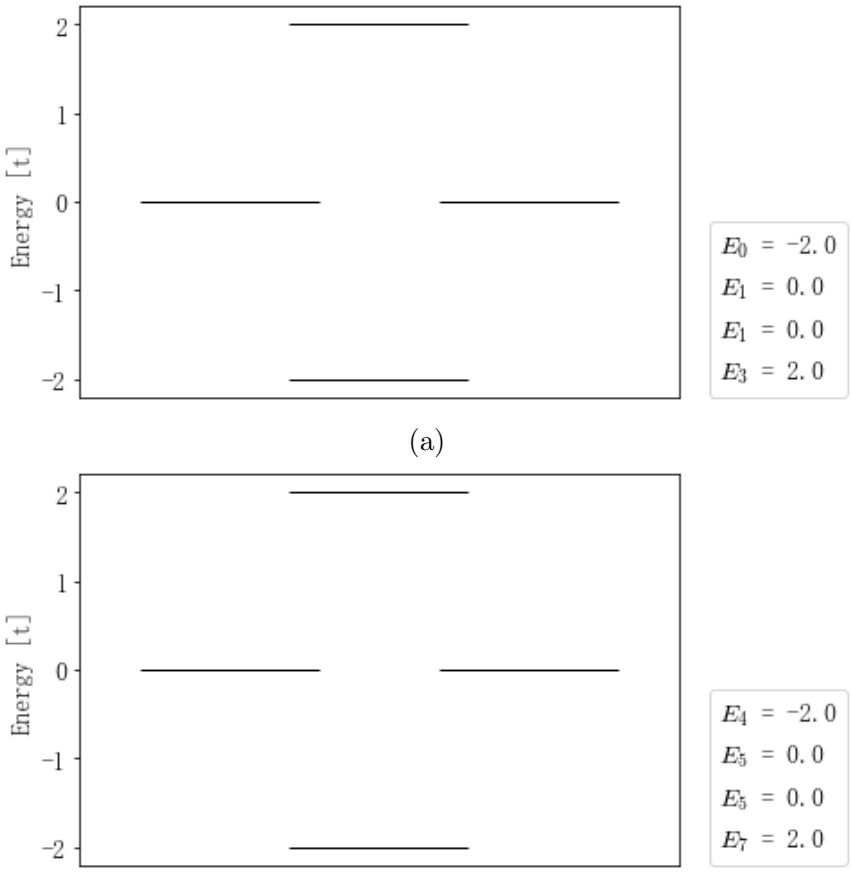

Figure 2.5: Energy spectra of three-site $t = \Delta, \mu = 0$ Kitaev chain, (a) even and (b) odd subspaces.

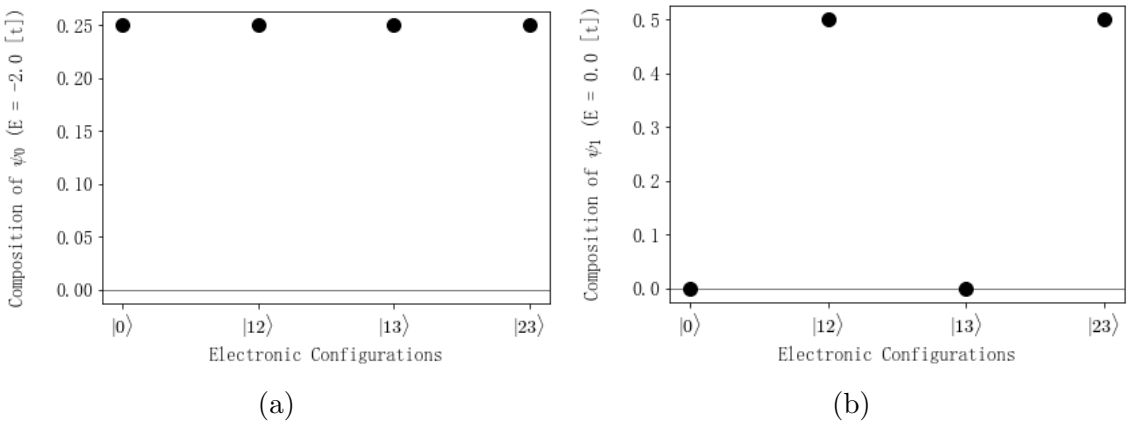

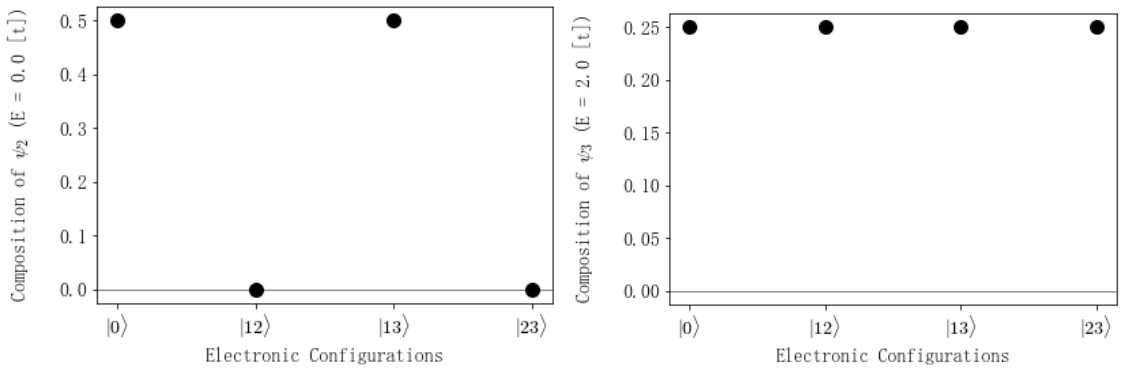

(c) (d)

Figure 2.6: Wavefunction configurations of $t = \Delta, \mu = 0$ Kitaev Hamiltonian, even subspace.

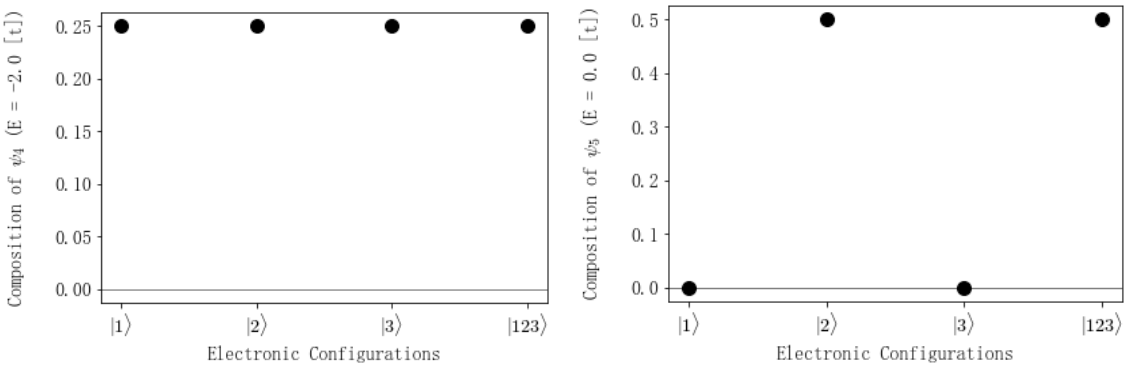

(a) (b)

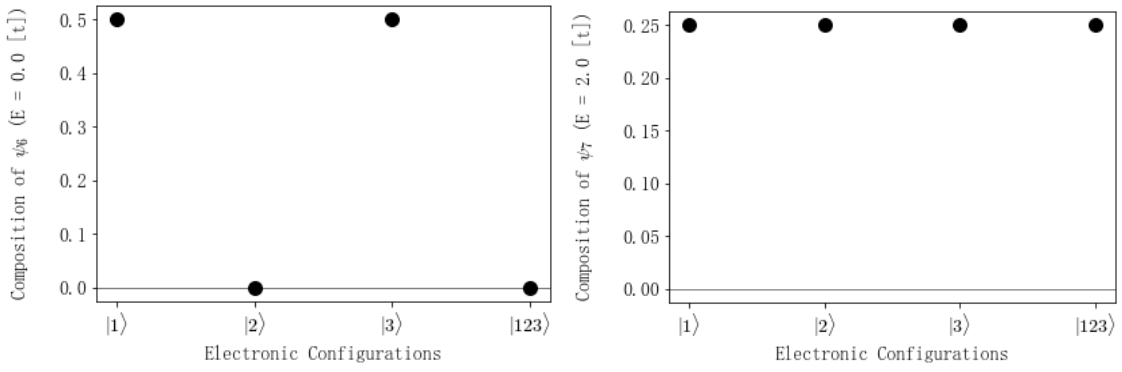

(c) (d)

Figure 2.7: Wavefunction configurations of $t = \Delta, \mu = 0$ Kitaev Hamiltonian, odd subspace.

From Fig. (2.5a) and (2.6), consider once again the potential coupling of degenerate energy states.

Previously, in Sec. 2.2.1, the two degenerate energy states of the even subspace were decoupled, with the vacuum state having no allowed transitions to any two-electron state. However, from Fig. (2.6), it can now be seen that by allowing Cooper pairing within the system, the vacuum state may now couple two-electron configurations, resulting in the two degenerate energy configurations:

$$\begin{aligned} |\psi_1\rangle \,| &= \frac{1}{\sqrt{2}}(|12\rangle + |23\rangle) \\ |\psi_2\rangle &= \frac{1}{\sqrt{2}}(|0\rangle + 0.5\,|13\rangle) \end{aligned} \tag{2.28}$$

Thus, it can be seen that two-electron configurations may be occupied without changing the system energy from the vacuum state. Although it is not immediately apparent from this result how MZMs appear in the Kitaev chain, further investigation may yield a more concrete physical explanation. Particularly in the two-electron configurations - where, as will be seen in Chapter 3, bond fermions are formed by pairing Majoranas on neighboring dots. This corresponds with two adjacent sites in the fermionic basis - hence, the continued appearance of degenerate zero-energy states is encouraging. Hence, further investigation is performed in order to realize MZMs in the 1D Kitaev system.

Chapter 3

Majorana and Bond Fermions on the Kitaev Chain

Majorana fermions, as a mathematical construct, arose from Ettore Majorana's strictly real solution to the Dirac equation, where the usual charge conjugation requirements of particles and their anti-particles were no longer valid. This resulted in the construction of a particle, which, characteristically, is its own anti-particle.

Alexei Kitaev later considered the uses of such a particle and its inherent statistics for quantum computing applications, and sought to construct a model which would exhibit such Majorana fermions - in fact, the Kitaev Hamiltonian is defined in such a way in order to allow for observation of isolated Majoranas.

Hence, within this chapter, the emergence of Majorana fermions on Kitaev's chain and ring will be examined. Initially, in Sec. 3.1, the transformation to the Majorana fermion basis is performed. Following this, a further basis transformation to that of "bond fermions" is undertaken, where neighboring Majoranas are paired, in Sec. 3.2.

3.1 Majorana Fermions

Majorana fermions can be constructed mathematically by a conversion from fermionic operators to Majorana operators - or, they may be physically defined simply as "breaking" a spinless fermion into two Majorana fermions $\gamma_{i,1}$ and $\gamma_{i,2}$ localized on

site i, as shown in Fig. (3.1) below.

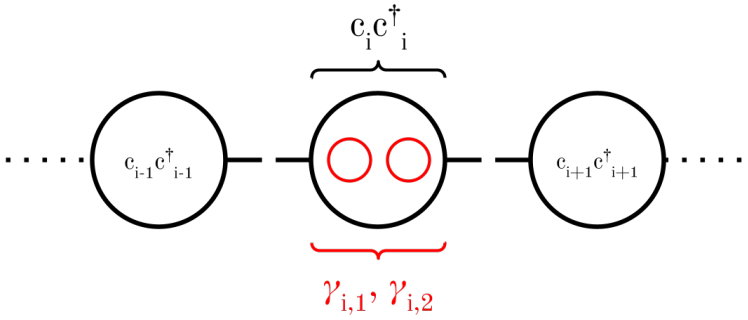

Figure 3.1: Majorana fermions $\gamma_{i,1}$ and $\gamma_{i,2}$ formed by "breaking" a spinless fermion on site i.

Majorana operators $\gamma_{i,1}$ and $\gamma_{i,2}$ may be defined as a linear combination of fermionic operators $c_i, c_i^\dagger$ for some arbitrary site i as:

$$\begin{aligned} \gamma_{i,1} &= c_i + c_i^\dagger \\ \gamma_{i,2} &= i(c_i^\dagger - c_i) \end{aligned} \tag{3.1}$$

Additionally, fermionic creation and annihilation operators can be expressed in terms of Majorana operators for some site i as:

$$\begin{aligned} c_i &= \frac{1}{2}(\gamma_{i,1} + i\gamma_{i,2}) \\ c_i^\dagger &= \frac{1}{2}(\gamma_{i,1} - i\gamma_{i,2}) \end{aligned} \tag{3.2}$$

Additionally, Majorana operators obey the following relations:

$$\begin{aligned} \gamma_{\alpha,\beta} &= \gamma_{\alpha,\beta}^\dagger \\ \gamma_{\alpha,\beta}^2 &= 1 \\ \{\gamma_{i,\alpha}, \gamma_{j,\beta}\} &= 2\delta_{ij}\delta_{\alpha\beta} \end{aligned} \tag{3.3}$$

As a result, it is then possible to use Eq. (3.2) and (3.3) to transform a given system of spinless fermions into a system of Majorana fermions.

3.1.1 The Kitaev Hamiltonian in Majorana Fermions

The Kitaev chain of N sites, each of which may be occupied by a single spinless fermion, can be transformed into Majorana fermions as shown in Fig. (3.2) below.

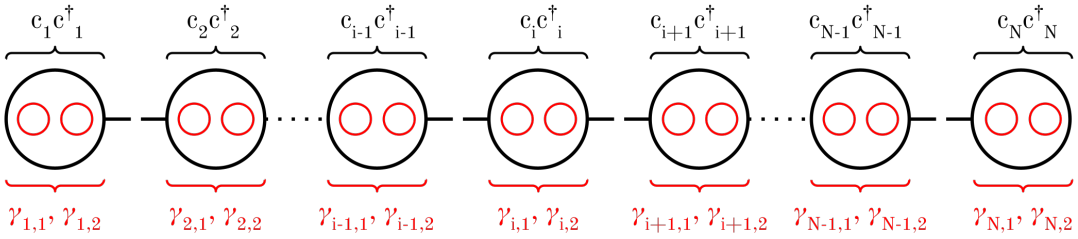

Figure 3.2: Kitaev chain of N sites, "broken" into individual Majorana fermions.

By using the fermionic and Majorana fermion relations in Eq. (3.2), as well as the Majorana fermion operator relations of Eq. (3.3), firstly the original Kitaev chain Hamiltonian for N sites given by Eq. (1.1):

$$\hat{H}_K = t\sum_{i=1}^{N-1}(c_{i+1}^\dagger c_i + c_i^\dagger c_{i+1}) + \Delta\sum_{i=1}^{N-1}(c_{i+1}^\dagger c_i^\dagger + c_i c_{i+1}) - \mu\sum_{i=1}^{N}(c_i^\dagger c_i) \tag{1.1}$$

This Hamiltonian can hence be transformed into the basis of Majorana fermions. Derived fully in Appendix B.1, the Kitaev Hamiltonian can then be written explicitly in terms of Majorana operators γ as:

$$\hat{H}_M = \frac{i(t+\Delta)}{2}\sum_{i=1}^{N-1}\gamma_{i,1}\gamma_{i+1,2} + \frac{i(t-\Delta)}{2}\sum_{i=1}^{N-1}\gamma_{i+1,1}\gamma_{i,2} - \frac{i\mu}{2}\sum_{i=1}^{N}\gamma_{i,1}\gamma_{i,2} - \frac{N\mu}{2} \tag{3.4}$$

However - this Hamiltonian is not diagonal, as it involves Majoranas on neighboring sites, as shown in Fig. (3.3) of the following page.

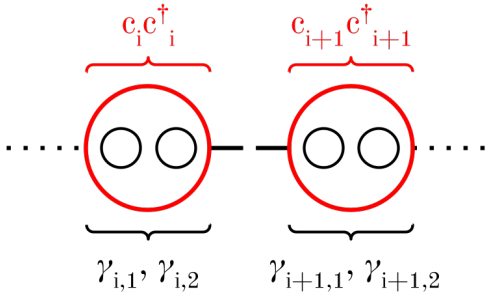

Figure 3.3: "Pairing" of individual Majorana fermions on a single site, consistent with fermionic occupation basis.

Hence, the question may be asked - is it possible to transform this Hamiltonian such that it is diagonal? To do so, a further transformation will be considered.

3.2 Majorana Pairing in Bond Fermions

In order to calculate eigenvalues and wavefunctions for the Kitaev Hamiltonian in Majoranas, it is required to transform this Hamiltonian into a basis in which it is diagonal. Luckily, this is achievable simply by defining a new Majorana pairing basis.

The Kitaev Hamiltonian may exist in two possible regimes, which describe two possible Majorana pairings - a non-topological, or "trivial" strong pairing regime, and a "topological" weak pairing regime. The "trivial" regime describes the pairing of Majorana fermions on a single quantum dot, essentially coupling Majoranas back into their original spinless fermions, as previously shown in Fig. (3.3).

The "topological" regime, however, is characterized by the coupling of Majoranas on neighboring sites, and the formation of a complete basis of states describing paired neighboring Majoranas. In this regime, the system is described by the conception of a "bond fermion", where the bond fermionic operators for a system of N sites are defined explicitly for some sites $i, i+1 \in N$ as:

$$
\begin{aligned}
a_i &= \frac{1}{2}(\gamma_{i,1} + i\gamma_{i+1,2}) \\
a_i^\dagger &= \frac{1}{2}(\gamma_{i,1} - i\gamma_{i+1,2})
\end{aligned}
\tag{3.5}
$$

Hence, bond fermions perform the action of explicitly pairing Majorana fermions $\gamma_{i,1}$ and $\gamma_{i+1,2}$ as shown in Fig. (3.4) below.

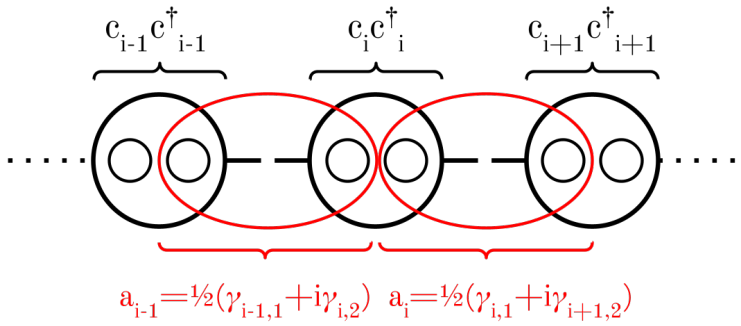

Figure 3.4: Creation of bond fermions by pairing of Majoranas on neighboring sites.

Where, as bond fermionic operators are no longer their own anti-particle and are hence characterized by fermionic statistics, once again obey the following commutation relations (for some sites $i, j \in N$):

$$
\begin{aligned}
\{a_i^\dagger, a_j^\dagger\} &= 0 \\
\{a_i, a_j\} &= 0 \\
\{a_i, a_j^\dagger\} &= \delta_{ij}
\end{aligned}
\tag{3.6}
$$

Hence, the action of the bond fermionic creation and annihilation operators on a state $|i\rangle$, and the vacuum state $|0\rangle$, are:

$$
\begin{aligned}
a_i^\dagger |0\rangle = |i\rangle \, , a_i^\dagger |i\rangle = 0 \\
a_i |i\rangle = |0\rangle \, , a_i |0\rangle = 0
\end{aligned}
\tag{3.7}
$$

Where by using these relations, the Kitaev Hamiltonian can be transformed into the basis of bond fermions, and hence diagonalized to calculate energy spectra and wavefunctions.

3.2.1 The Simplified Kitaev Hamiltonian in Bond Fermions

Initially, consider the case where $t = \Delta, \mu = 0$. Thus, the Kitaev Hamiltonian in the Majorana basis of Eq. (3.4), simplifies to:

$$\hat{H}_M = i\Delta \sum_{i=1}^{N-1} \gamma_{i,1}\gamma_{i+1,2} \tag{3.8}$$

Hence, using the Majorana and bond fermion transformation of Eq. (3.5), as well as the bond fermion commutation relations of Eq. (3.6), the simplified Kitaev Hamiltonian (as derived in Appendix B.2.1) can be written in the basis of bond fermions on N sites as:

$$\hat{H}_B = \Delta \sum_{i=1}^{N-1} (2a_i^\dagger a_i - 1) \tag{3.9}$$

Where it is noted that this Hamiltonian is now fully diagonal in the bond fermionic basis.

3.2.2 Initial Emergence of the Zero Energy State

Once again, consider the simplified Kitaev chain Hamiltonian in the bond fermionic basis, as in Eq. (3.9). Explicitly, this Hamiltonian is written for a system of three fermions as:

$$\hat{H}_B = \Delta(2a_1^\dagger a_1 - 1) + \Delta(2a_2^\dagger a_2 - 1) \tag{3.10}$$

However, there appears to be something missing here - this equation describes only *two* bond fermions, but this is supposed to be a *three* site system. In order to determine where the "missing" bond fermion has gone, consider the physical representation of this system, as shown below in Fig. (3.5).

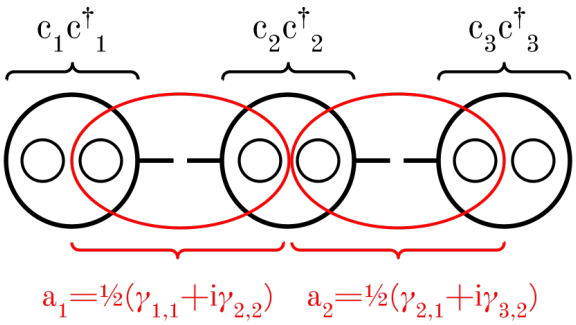

Figure 3.5: Representation of the simplified $t = \Delta$ Kitaev chain in the bond fermion basis for three sites.

From Fig. (3.5), it is observed that the Kitaev Hamiltonian creates two non-local bond fermions, a_1 and a_2, however, shows two "dangling Majoranas" on either end of the chain. These two dangling Majoranas, $\gamma_{1,2}$ and $\gamma_{3,1}$, are shown explicitly in Fig. (3.6) below.

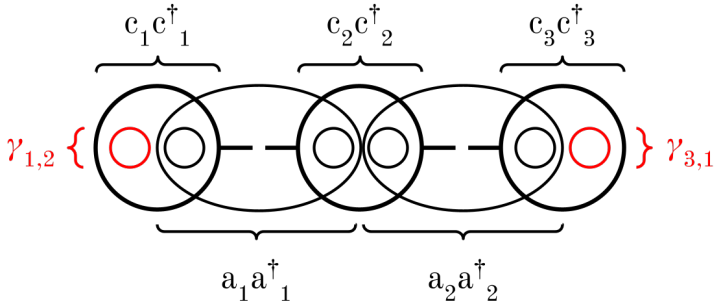

Figure 3.6: Dangling Majoranas in the simplified $t = \Delta$ Kitaev chain for three sites.

The appearance of dangling Majoranas within the Kitaev Hamiltonian is an intentional inclusion by Kitaev - in fact, the observation of dangling Majoranas is the purpose of Kitaev's toy model, as it is these particles which are essential to Kitaev's purpose in quantum computing.

However, when considering the entire physical system, it is still required to find a representation for these dangling Majoranas. In order to do so, the neat trick of forming by hand a "zero energy" bond fermion is performed. The bond fermion a_3 (as shown in Fig. (3.7) below) is mathematically constructed from the dangling Majoranas as:

$$\begin{aligned} a_3 &= \frac{1}{2}(\gamma_{3,1} + i\gamma_{1,2}) \\ a_3^\dagger &= \frac{1}{2}(\gamma_{3,1} - i\gamma_{1,2}) \end{aligned} \tag{3.11}$$

Where, by defining the Hamiltonian term representing the occupation of this bond fermion with zero energy as:

$$0(2a_3^\dagger a_3 - 1) \tag{3.12}$$

This term may be added to the Hamiltonian while leaving it essentially unchanged.

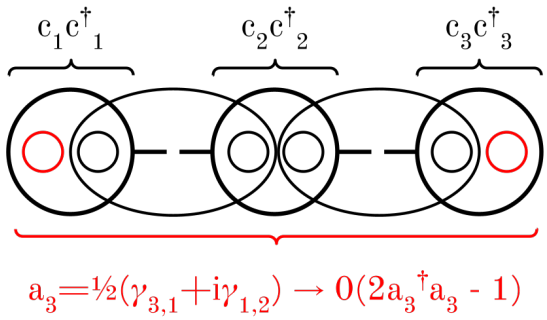

Figure 3.7: Construction of zero-energy bond fermion in the simplified $t = \Delta$ Kitaev chain for three sites.

Thus, the system Hamiltonian for a chain of three bond fermions becomes, explicitly:

$$\hat{H}_B = \Delta(2a_1^\dagger a_1 - 1) + \Delta(2a_2^\dagger a_2 - 1) + 0(2a_3^\dagger a_3 - 1) \tag{3.13}$$

Hence, this Hamiltonian may be used to calculate energy eigenvalues and wavefunction configurations of the system.

3.2.3 The Zero Energy State and Degenerate Energies of Configurations

Noting that the Hamiltonian of Eq. (3.13) is entirely diagonal, it is hence possible to calculate the system's eigenvalues and eigenvectors analytically - its eigenvectors will simply be the possible configurations of the system, and its eigenvalues the projection of the Hamiltonian on each possible state.

Hence, the energies of the system may be calculated as in the example calculation of Appendix B.2.2, giving the energy spectra and wavefunction configurations of the system as in Fig. (3.8), (3.9) and (3.10), respectively.

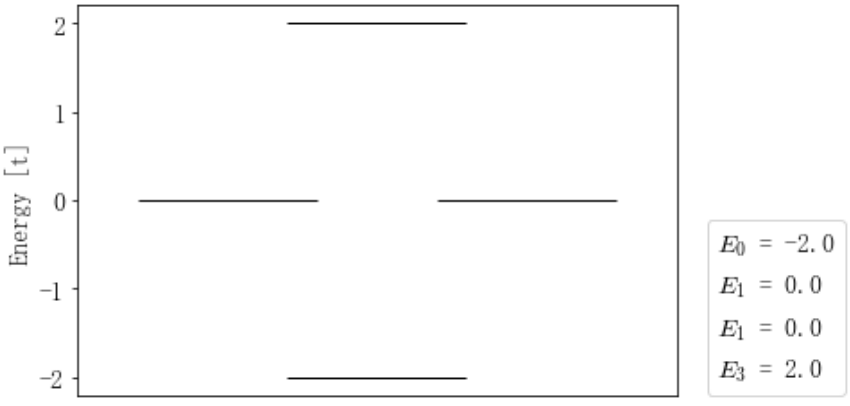

(a)

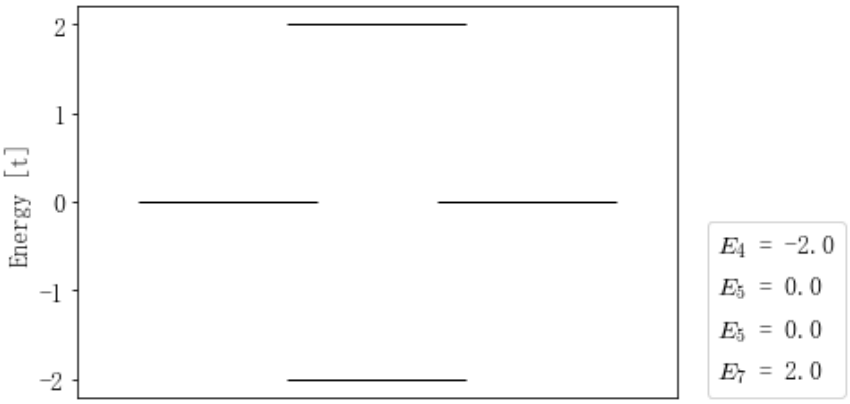

(b)

Figure 3.8: Energy spectra of three-site $t = \Delta, \mu = 0$ Kitaev chain in bond fermions, (a) even and (b) odd subspaces.

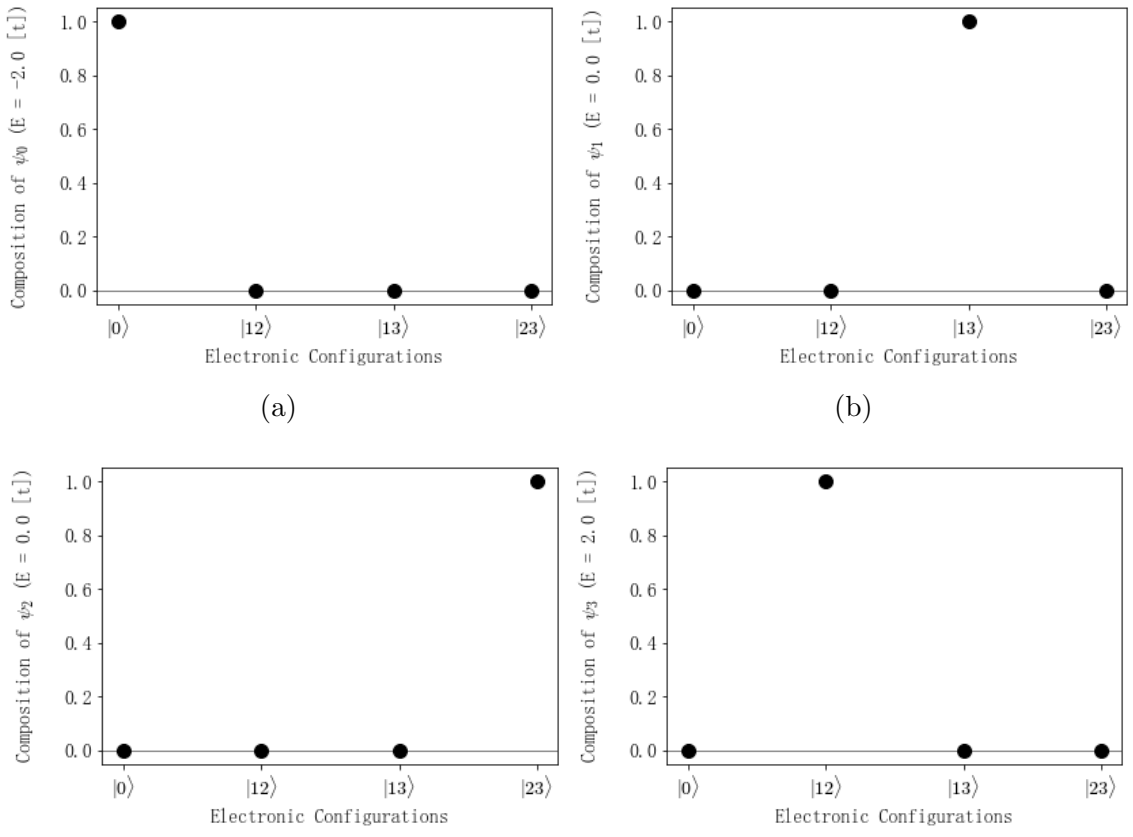

(a) (b)

(c) (d)

Figure 3.9: Wavefunction configurations of three-site $t = \Delta, \mu = 0$ Kitaev chain in bond fermions, even subspace.

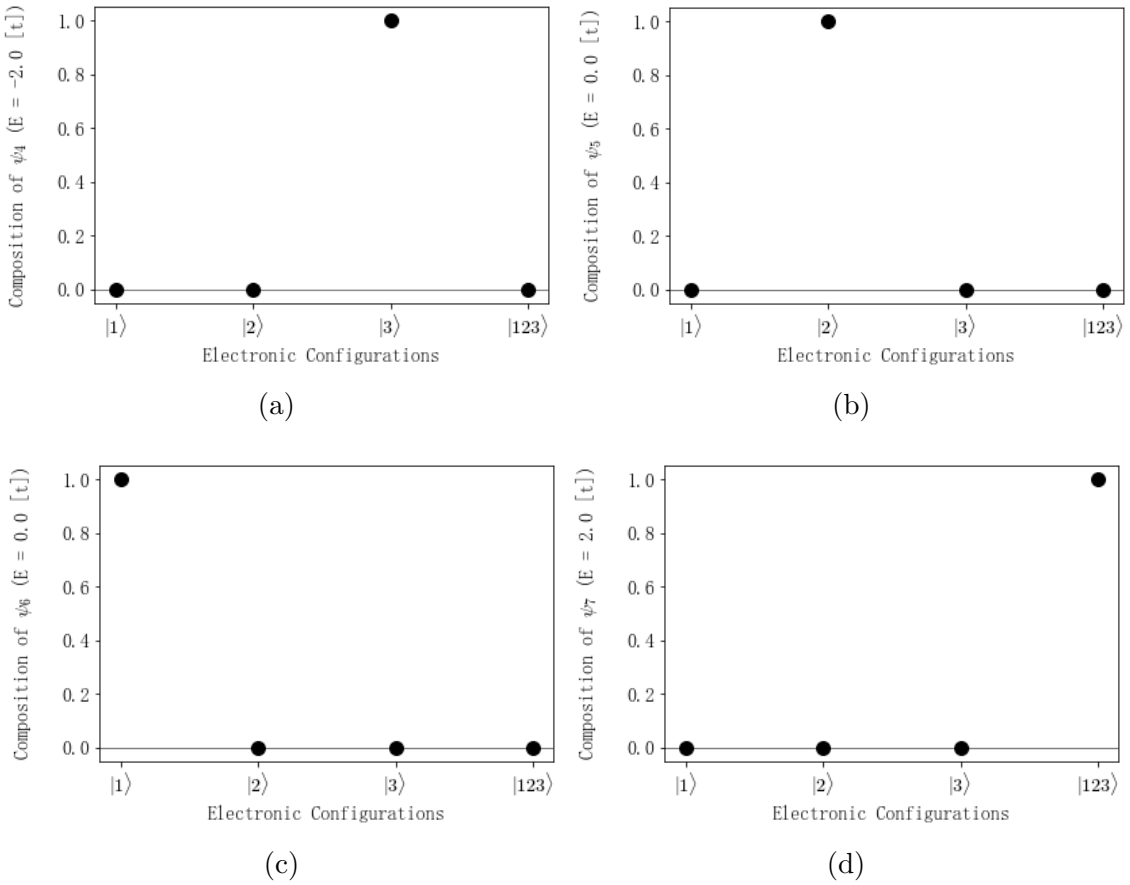

Figure 3.10: Wavefunction configurations of three-site $t = \Delta, \mu = 0$ Kitaev chain in bond fermions, odd subspace.

Firstly, it is of note that the energy spectra of the system is exactly that given in Fig. (2.5) for the three site, $t = \Delta, \mu = 0$ Kitaev chain, as demonstrated explicitly on the following page in Fig. (3.11).

Due to the matching of energy spectra in the fermion and bond fermion bases, this implies that the transformation into bond fermions is performed correctly, as, recall, the spectra of the system does not change across bases.

Importantly, it can be observed that the inclusion of this zero energy bond fermion in the possible system configurations leads directly to the calculated energy spectra (noting that without the creation of bond fermion a_3, there would be only four possible states of the system, rather than eight as shown above in Fig. (3.9) and Fig. (3.10)). Hence, this zero energy bond fermion is necessary not only to describe the system

physically, but also in order to ensure proper basis mapping between the fermionic and bond fermionic bases.

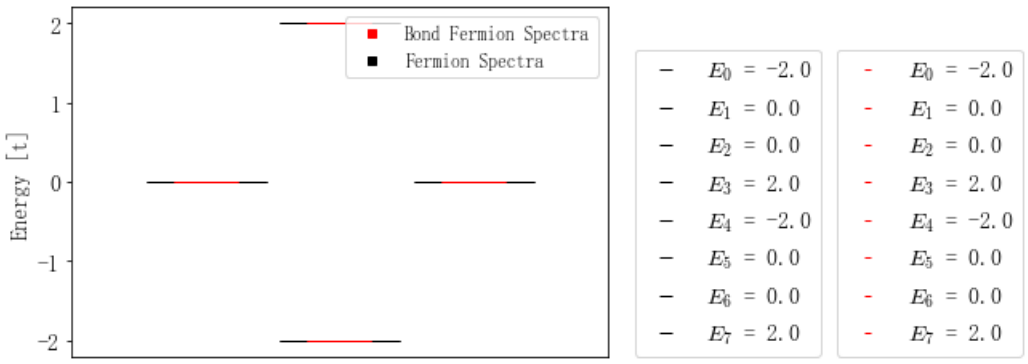

Figure 3.11: Degenerate energy spectra of three-site $t = \Delta, \mu = 0$ Kitaev chain in fermions and in bond fermions.

In addition, it may be noted that, indeed, the zero energy state described by a_3 does not change the energy of any configuration it is added to (e.g. the occupation of bond fermion a_3 creates state $|13\rangle$ from state $|1\rangle$, which share a degenerate energy value). By observation of Fig. (3.9) and Fig. (3.10), it is seen that in the space of the three site Kitaev Hamiltonian, any state in which a_3 is occupied results in a degenerate energy of configurations. Explicitly, these degenerate energies of configurations are:

$$\begin{aligned} |0\rangle, |3\rangle &\longrightarrow E = -2\,[\Delta] \\ |1\rangle, |13\rangle &\longrightarrow E = 0\,[\Delta] \\ |2\rangle, |23\rangle &\longrightarrow E = 0\,[\Delta] \\ |12\rangle, |123\rangle &\longrightarrow E = 2\,[\Delta] \end{aligned} \tag{3.14}$$

Interestingly, these are not states which are directly coupled through use of the pairing term, as they exist in separate subspaces - it is merely the occupation of bond fermion a_3 which creates energy degeneracy.

As a result, it can be said that the non-local bond fermion a_3 behaves as expected

within the system, allowing spectral matching across bases, and creating energy degeneracy within the bond fermion chain.

Chapter 4

The Kitaev Ring

4.1 The Fermionic Kitaev Ring

Within this chapter, Kitaev's chain described in Sec. 1.2 is expanded to a ring system. In this case, the model once again describes a chain of $N \in \mathbb{Z}^+$ sites, or quantum dots, each of which may be empty or occupied by a single fermion. However, in the ring model, sites 1 and N are brought into proximity as shown in Fig. (4.1) below.

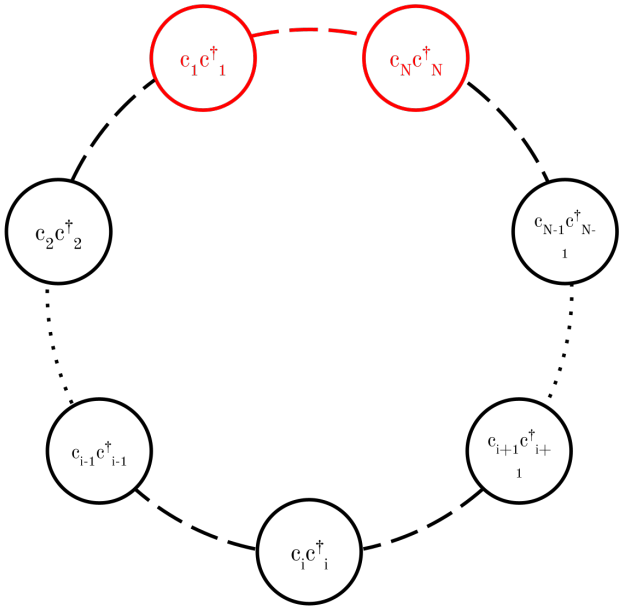

Figure 4.1: Kitaev ring of N sites, each of which site $i \in N$ may be occupied by a single spinless fermion.

The geometry of this system is characterized by allowed tunneling between sites 1 and N, and allowed creation or annihilation of a Cooper pair of fermions on sites 1 and N.

The Hamiltonian of this system is once again given in the nearest-neighbor approximation. However, in this case, the summations in the tunneling and pairing terms of the Kitaev chain for N sites (given in Eq. (1.1)) are expanded to include the N^{th} term in the summation (rather than terminating at $N-1$). As such, this allows tunneling and pairing of sites 1 and N as described above, and the Kitaev Hamiltonian $\hat{H}_{KR}$ can be written as:

$$\hat{H}_{KR} = t\sum_{i=1}^{N}(c_{i+1}^{\dagger}c_i + c_i^{\dagger}c_{i+1}) + \Delta\sum_{i=1}^{N}(c_{i+1}^{\dagger}c_i^{\dagger} + c_i c_{i+1}) - \mu\sum_{i=1}^{N}(c_i^{\dagger}c_i) \tag{4.1}$$

Recall that the three-site Kitaev ring is the minimum number of sites required to impose periodic boundary conditions for such a system. Thus, the analysis of the Kitaev ring will once again (like the chain case) be performed for three sites. Then, the Kitaev Hamiltonian for a three site ring becomes:

$$\hat{H}_{KR} = t\sum_{i=1}^{3}(c_{i+1}^{\dagger}c_i + c_i^{\dagger}c_{i+1}) + \Delta\sum_{i=1}^{3}(c_{i+1}^{\dagger}c_i^{\dagger} + c_i c_{i+1}) - \mu\sum_{i=1}^{3}(c_i^{\dagger}c_i) \tag{4.2}$$

However, the explicit form of this Hamiltonian depends on some sites i and $i+1$ - i.e. some site, and a neighboring site "greater" in index. As a result, for the ring case, it now must be considered whether site 1 or site 3 is considered to be the "greater" index when travelling around a ring. Thus, the periodic terms of the Kitaev ring Hamiltonian, denoted by the coefficients t_{13} and Δ_{13} may take two possible forms. The first, assuming that site 1 is "greater" in index than site 3:

$$\begin{matrix} t_{13}(c_1^\dagger c_3 + c_3^\dagger c_1) \\ \Delta_{13}(c_1^\dagger c_3^\dagger + c_3 c_1) \end{matrix} \tag{4.3}$$

And the second, assuming that site 3 is "greater" in index than site 1:

$$\begin{matrix} t_{13}(c_3^\dagger c_1 + c_1^\dagger c_3) \\ \Delta_{13}(c_3^\dagger c_1^\dagger + c_1 c_3) \end{matrix} \tag{4.4}$$

In both Eq. (4.3) and (4.4) above, the tunneling ring term described by t_{13} has identical terms (although in opposite order, addition of Hamiltonian terms is commutative, therefore order of terms does not matter).

However, the ordering of the Δ_{13} ring terms in Eq. (4.3) and (4.4) is opposite in terms of ordering of operators, and cannot be considered identical. In order to determine which is the correct ordering of the Δ_{13} ring terms, spectral matching will be used. As energy spectra must be consistent across basis transformations, these calculated spectra are later compared to spectra of the Kitaev ring transformed to a system of bond fermions. It follows directly from this that the matching spectra occurs in the correct canonical ordering of the Δ_{13} ring terms, at which point the correct ordering can be observed.

4.1.1 The Tunneling Kitaev Ring and Artificial Phase

The tunneling Kitaev ring contains only the nearest-neighbor hopping term of Eq. (4.2), such that the tunneling Hamiltonian for a three site ring becomes:

$$\hat{H}_{KR} = t\sum_{i=1}^{3}(c_{i+1}^\dagger c_i + c_i^\dagger c_{i+1}) \tag{4.5}$$

Where considering the case where site 1 is "greater" in index than site 3, explicitly, the tunneling ring Kitaev Hamiltonian can be written:

$$\begin{aligned}\hat{H}_{KR} &= t(c_2^\dagger c_1 + c_1^\dagger c_2 + c_3^\dagger c_2 + c_2^\dagger c_3) \\ &+ t_{13}(c_1^\dagger c_3 + c_3^\dagger c_1)\end{aligned} \tag{4.6}$$

Or, equivalently, where site 3 is "greater" in index than site 1, the tunneling ring Kitaev Hamiltonian can be written explicitly (and equivalently):

$$\begin{aligned}\hat{H}_{KR} &= t(c_2^\dagger c_1 + c_1^\dagger c_2 + c_3^\dagger c_2 + c_2^\dagger c_3) \\ &+ t_{13}(c_3^\dagger c_1 + c_1^\dagger c_3)\end{aligned} \tag{4.7}$$

While both of the above two orderings are technically correct, the analysis of the pairing term will determine the proper ordering, and t_{13} ordering will be chosen to match for consistency. However, to initially choose one indiscriminately for matrix element calculations, the site 1 "greater" in index than site 3 case will be considered.

Thus, the subspace matrix Hamiltonians will be the same as those given in Eq. (2.21) and (2.22), however, with the addition of the t_{13} matrix elements describing tunneling of a fermion between sites 1 and 3. These elements, $H_{1,3}^{KR}$ and $H_{12,23}^{KR}$, can then be calculated explicitly as given in the derivations on the following page.

(Recall that $H_{1,3}^{KR} = H_{3,1}^{KR}$ and $H_{12,23}^{KR} = H_{23,12}^{KR}$, thus symmetric matrix elements are not calculated).

Calculation: Tunneling element $H_{1,3}^{KR}$ $(= H_{3,1}^{KR})$

The Kitaev Hamiltonian tunneling matrix element $H_{1,3}^{KR}$ is calculated as follows:

$$\begin{aligned}
H_{1,3}^{KR} &= \langle 1|\, \hat{H}_{KR}\, |3\rangle \\
&= \langle 1|\, t_{13}(c_1^\dagger c_3 + c_3^\dagger c_1)\, |3\rangle \\
&= t_{13}\, \langle 0|\, c_1(c_1^\dagger c_3 + c_3^\dagger c_1)c_3^\dagger\, |0\rangle \\
&= t_{13}\, \langle 0|\, c_1 c_1^\dagger c_3 c_3^\dagger\, |0\rangle + t_{13}\, \langle 0|\, c_1 c_3^\dagger c_1 c_3^\dagger\, |0\rangle \\
&= t_{13}\, \langle 0|\, \underbrace{c_1 c_1^\dagger}_{1}\, \underbrace{c_3 c_3^\dagger}_{1}\, |0\rangle - t_{13}\, \langle 0|\, \underbrace{c_1 c_1}_{0}\, \underbrace{c_3^\dagger c_3^\dagger}_{0}\, |0\rangle \\
&= t_{13}\, \underbrace{\langle 0|0\rangle}_{1} - 0 \\
&= t_{13}
\end{aligned}$$

Calculation: Tunneling element $H_{12,23}^{KR}$ $(= H_{23,12}^{KR})$

The Kitaev Hamiltonian tunneling matrix element $H_{12,23}^{KR}$ is calculated as follows:

$$\begin{aligned}
H_{12,23}^{KR} &= \langle 12|\, \hat{H}_{KR}\, |23\rangle \\
&= \langle 12|\, t_{13}(c_1^\dagger c_3 + c_3^\dagger c_1)\, |23\rangle \\
&= t_{13}\, \langle 0|\, c_2 c_1(c_1^\dagger c_3 + c_3^\dagger c_1)c_2^\dagger c_3^\dagger\, |0\rangle \\
&= t_{13}\, \langle 0|\, c_2 c_1 c_1^\dagger c_3 c_2^\dagger c_3^\dagger\, |0\rangle + t_{13}\, \langle 0|\, c_2 c_1 c_3^\dagger c_1 c_2^\dagger c_3^\dagger\, |0\rangle \\
&= t_{13}\, \langle 0|\, c_2\, \underbrace{c_1 c_1^\dagger}_{1}\, c_3 c_2^\dagger c_3^\dagger\, |0\rangle - t_{13}\, \langle 0|\, c_2 c_3^\dagger\, \underbrace{c_1 c_1}_{0}\, c_2^\dagger c_3^\dagger\, |0\rangle \\
&= t_{13}\, \langle 0|\, \underbrace{c_2 c_2^\dagger}_{1}\, \underbrace{c_3 c_3^\dagger}_{1}\, |0\rangle - 0 \\
&= -t_{13}\, \underbrace{\langle 0|0\rangle}_{1} \\
&= -t_{13}
\end{aligned}$$

Thus, it can be seen that there is an artificial gauge (phase) imposed on t_{13} in the even subspace purely as a result of the ordering of Hamiltonian operators, and

fermionic anticommutation relations. As a result, the even and odd matrix subspace Hamiltonians $\hat{H}_{ET}$ and $\hat{H}_{OT}$, respectively, describing the tunneling Kitaev ring can be written:

$$\hat{H}_{ET} = \begin{bmatrix} 0 & 0 & 0 & 0 \\ 0 & 0 & t & -t_{13} \\ 0 & t & 0 & t \\ 0 & -t_{13} & t & 0 \end{bmatrix} = \begin{bmatrix} 0 & 0 & 0 & 0 \\ 0 & 0 & 1 & -1 \\ 0 & 1 & 0 & 1 \\ 0 & -1 & 1 & 0 \end{bmatrix} \tag{4.8}$$

$$\hat{H}_{OT} = \begin{bmatrix} 0 & t & t_{13} & 0 \\ t & 0 & t & 0 \\ t_{13} & t & 0 & 0 \\ 0 & 0 & 0 & 0 \end{bmatrix} = \begin{bmatrix} 0 & 1 & 1 & 0 \\ 1 & 0 & 1 & 0 \\ 1 & 1 & 0 & 0 \\ 0 & 0 & 0 & 0 \end{bmatrix} \tag{4.9}$$

Thus, through exact diagonalization, even and odd subspace energies and wave-function configurations are calculated as in Fig. (4.2), (4.3) and (4.4), respectively, below.

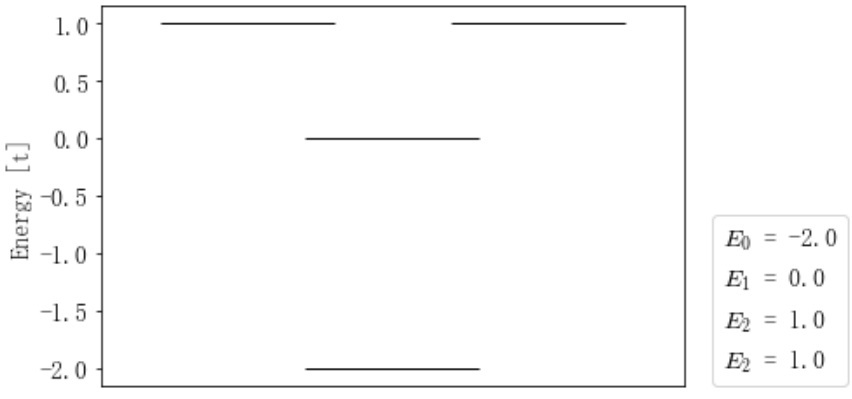

(a)

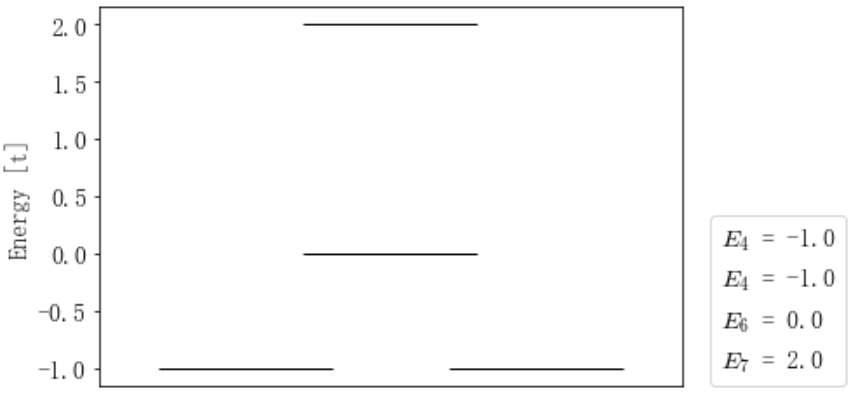

(b)

Figure 4.2: Energy spectra of three-site $\Delta, \mu = 0$ Kitaev ring, (a) even and (b) odd subspaces.

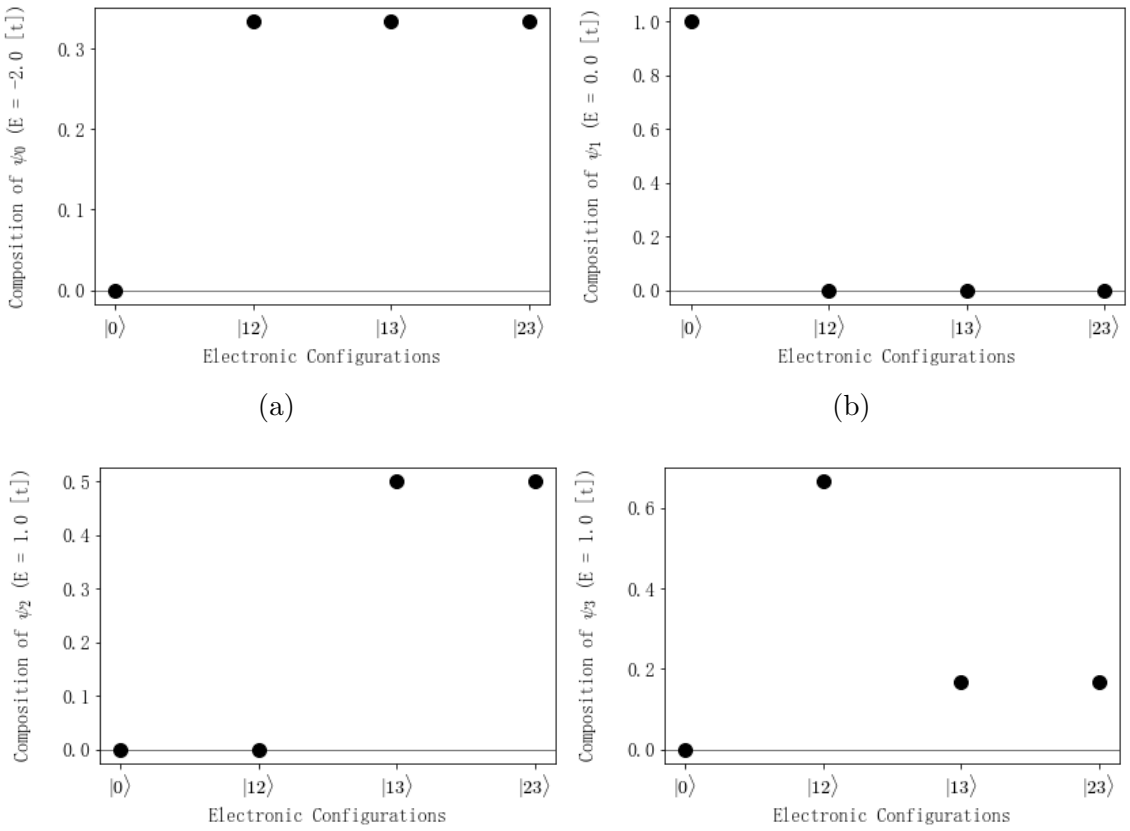

(a) (b)

(c) (d)

Figure 4.3: Wavefunction configurations of three-site $\Delta, \mu = 0$ Kitaev ring, even subspace.

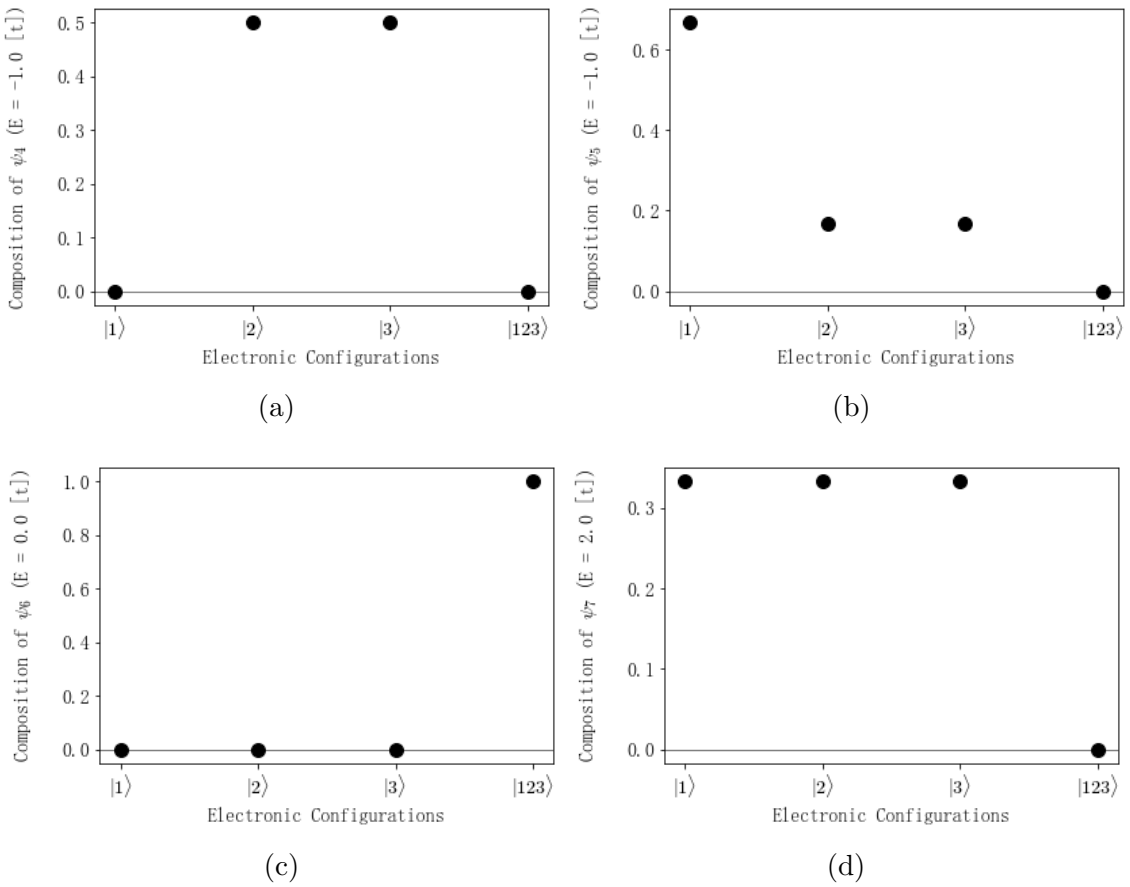

Figure 4.4: Wavefunction configurations of three-site $\Delta, \mu = 0$ Kitaev ring, odd subspace.

Initially, it should be noted that the even and odd subspace energy spectra degeneracy observed in Section 2.2.1 for the tunneling Kitaev chain is no longer present due to the inclusion of ring terms.

In addition, it can be seen by comparison to Fig. (2.3) and (2.4) to Fig. (4.3) and (4.4) that the energy degeneracy of the vacuum state no longer occurs in the ring configuration. In this case, energy degeneracy occurs between multi-electron configurations, and does not occur between differing electron numbers.

4.1.2 Effect of the Pairing Term and Artificial Phase

The pairing term of the Kitaev Hamiltonian can now be introduced to the Kitaev ring. Once again, the $|t| = |\Delta|$ case is considered. The Kitaev Hamiltonian with pairing and tunneling components on a three site ring can be written:

$$\hat{H}_{KR} = t\sum_{i=1}^{3}(c_{i+1}^{\dagger}c_i + c_i^{\dagger}c_{i+1}) + \Delta\sum_{i=1}^{3}(c_{i+1}^{\dagger}c_i^{\dagger} + c_i c_{i+1}) \tag{4.10}$$

Where once again the cases where either site 1 is "greater" in index than site 3, and vice versa, must be considered. Hence, where site 1 is considered "greater" in index than site 3, this Hamiltonian may be written explicitly as:

$$\begin{aligned}\hat{H}_{KR} = {} & t(c_2^{\dagger}c_1 + c_1^{\dagger}c_2 + c_3^{\dagger}c_2 + c_2^{\dagger}c_3) + t_{13}(c_1^{\dagger}c_3 + c_3^{\dagger}c_1) \\ & + \Delta(c_2^{\dagger}c_1^{\dagger} + c_1c_2 + c_3^{\dagger}c_2^{\dagger} + c_2c_3) + \Delta_{13}(c_1^{\dagger}c_3^{\dagger} + c_3c_1)\end{aligned} \tag{4.11}$$

Equivalently, where site 3 is "greater" in index than site 1, the three site Kitaev ring Hamiltonian may be written explicitly as:

$$\begin{aligned}\hat{H}_{KR} = {} & t(c_2^{\dagger}c_1 + c_1^{\dagger}c_2 + c_3^{\dagger}c_2 + c_2^{\dagger}c_3) + t_{13}(c_3^{\dagger}c_1 + c_1^{\dagger}c_3) \\ & + \Delta(c_2^{\dagger}c_1^{\dagger} + c_1c_2 + c_3^{\dagger}c_2^{\dagger} + c_2c_3) + \Delta_{13}(c_3^{\dagger}c_1^{\dagger} + c_1c_3)\end{aligned} \tag{4.12}$$

Initially, the site 1 "greater" in index than site 3 case will be considered. Thus, the subspace matrix Hamiltonians will be the same as those given in Eq. (4.8) and (4.9), with the addition of the pairing elements Δ, and Δ_{13} matrix elements describing the formation of a Cooper pair on sites 1 and 3. These elements, $H_{0,13}^{KR}$ and $H_{2,123}^{KR}$, are calculated explicitly in the derivations below (where recall that $H_{0,13}^{KR} = H_{13,0}^{KR}$ and $H_{2,123}^{KR} = H_{123,2}^{KR}$, thus symmetric matrix elements are not calculated).

Calculation: Pairing element $H_{0,13}^{KR}$ $(= H_{13,0}^{KR})$

The Kitaev Hamiltonian pairing matrix element $H^{KR}_{0,13}$ is calculated as follows, for the case where site 1 is considered "greater" than site 3:

$$\begin{aligned}
H^{KR}_{0,13} &= \langle 0| \hat{H}_{KR} |13\rangle \\
&= \langle 0| \Delta_{13}(c_1^\dagger c_3^\dagger + c_3 c_1) |13\rangle \\
&= \Delta_{13} \langle 0| (c_1^\dagger c_3^\dagger + c_3 c_1) c_1^\dagger c_3^\dagger |0\rangle \\
&= \Delta_{13} \langle 0| c_1^\dagger c_3^\dagger c_1^\dagger c_3^\dagger |0\rangle + \Delta_{13} \langle 0| c_3 c_1 c_1^\dagger c_3^\dagger |0\rangle \\
&= -\Delta_{13} \langle 0| \underbrace{\cancel{c_1^\dagger c_1}}_{0} \underbrace{\cancel{c_3^\dagger c_3}}_{0} |0\rangle + \Delta_{13} \langle 0| c_3 \underbrace{\cancel{c_1 c_1^\dagger}}_{1} c_3^\dagger |0\rangle \\
&= 0 + \Delta_{13} \langle 0| \underbrace{\cancel{c_3 c_3^\dagger}}_{1} |0\rangle \\
&= 0 + \Delta_{13} \underbrace{\langle 0|0\rangle}_{1} \\
&= \Delta_{13}
\end{aligned}$$

Calculation: Pairing element $H^{KR}_{2,123}$ $(= H^{KR}_{123,2})$

The Kitaev Hamiltonian pairing matrix element $H^{KR}_{2,123}$ is calculated as follows, for the case where site 1 is considered "greater" than site 3:

$$\begin{aligned}
H^{KR}_{2,123} &= \langle 2| \hat{H}_{KR} |123\rangle \\
&= \langle 2| \Delta_{13}(c_1^\dagger c_3^\dagger + c_3 c_1) |123\rangle \\
&= \Delta_{13} \langle 0| c_2 (c_1^\dagger c_3^\dagger + c_3 c_1) c_1^\dagger c_2^\dagger c_3^\dagger |0\rangle \\
&= \Delta_{13} \langle 0| c_2 c_1^\dagger c_3^\dagger c_1^\dagger c_2^\dagger c_3^\dagger |0\rangle + \Delta_{13} \langle 0| c_2 c_3 c_1 c_1^\dagger c_2^\dagger c_3^\dagger |0\rangle \\
&= -\Delta_{13} \langle 0| c_2 \underbrace{\cancel{c_1^\dagger c_1}}_{0} c_3^\dagger c_2^\dagger c_3^\dagger |0\rangle + \Delta_{13} \langle 0| c_2 c_3 \underbrace{\cancel{c_1 c_1^\dagger}}_{1} c_2^\dagger c_3^\dagger |0\rangle \\
&= 0 - \Delta_{13} \langle 0| \underbrace{\cancel{c_2 c_2^\dagger}}_{1} \underbrace{\cancel{c_3 c_3^\dagger}}_{1} |0\rangle \\
&= -\Delta_{13} \underbrace{\langle 0|0\rangle}_{1} \\
&= -\Delta_{13}
\end{aligned}$$

Thus, it can be seen that there is an artificial gauge (phase) imposed on Δ_{13} only in the even subspace. As a result, the even and odd matrix subspace Hamiltonians $\hat{H}_{EP1}$ and $\hat{H}_{OP1}$, respectively, describing the Kitaev ring of tunneling and pairing terms can be written:

$$\hat{H}_{EP1} = \begin{bmatrix} 0 & -\Delta & \Delta_{13} & -\Delta \\ -\Delta & 0 & t & -t_{13} \\ \Delta_{13} & t & 0 & t \\ -\Delta & -t_{13} & t & 0 \end{bmatrix} = \begin{bmatrix} 0 & -1 & 1 & -1 \\ -1 & 0 & 1 & -1 \\ 1 & 1 & 0 & 1 \\ -1 & -1 & 1 & 0 \end{bmatrix} \tag{4.13}$$

$$\hat{H}_{OP1} = \begin{bmatrix} 0 & t & t_{13} & -\Delta \\ t & 0 & t & -\Delta_{13} \\ t_{13} & t & 0 & -\Delta \\ -\Delta & -\Delta_{13} & -\Delta & 0 \end{bmatrix} = \begin{bmatrix} 0 & 1 & 1 & -1 \\ 1 & 0 & 1 & -1 \\ 1 & 1 & 0 & -1 \\ -1 & -1 & -1 & 0 \end{bmatrix} \tag{4.14}$$

Thus, through exact diagonalization, even and odd subspace energies and wave-function configurations are calculated as in Fig. (4.5), (4.6) and (4.7) on the following page (respectively).

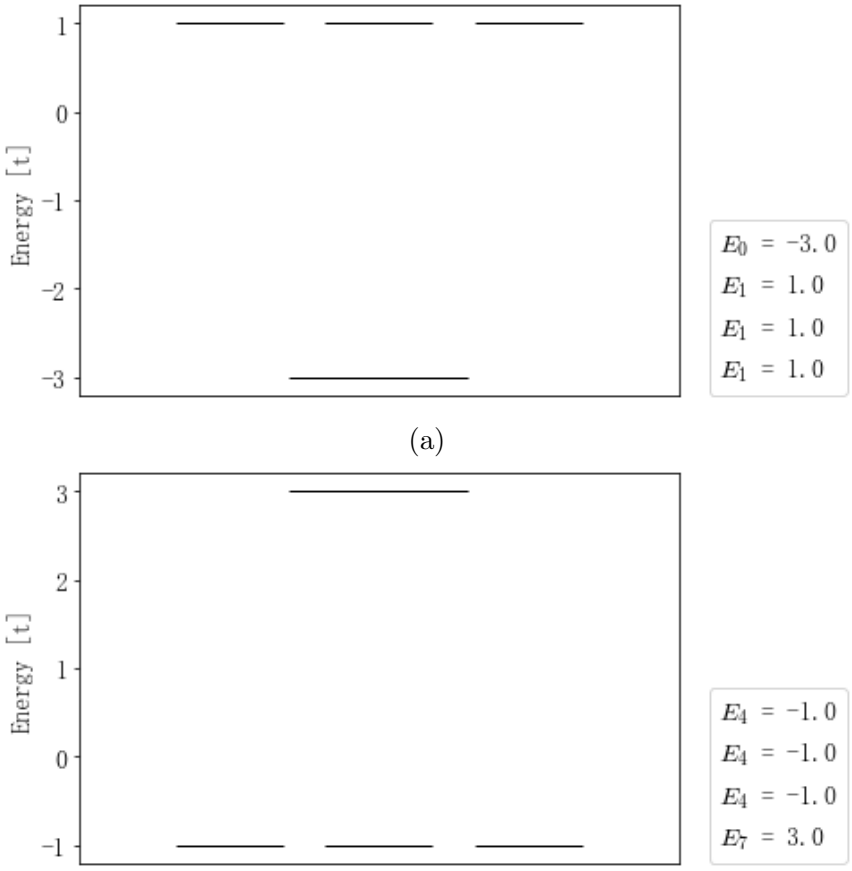

Figure 4.5: Energy spectra of three-site $t = \Delta, \mu = 0$ Kitaev ring, (a) even and (b) odd subspaces, considering site 1 "greater" than site 3.

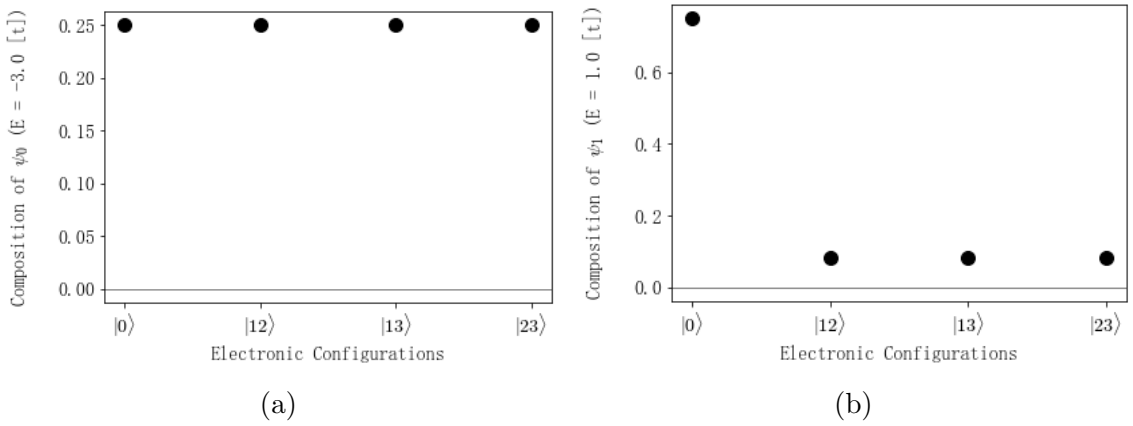

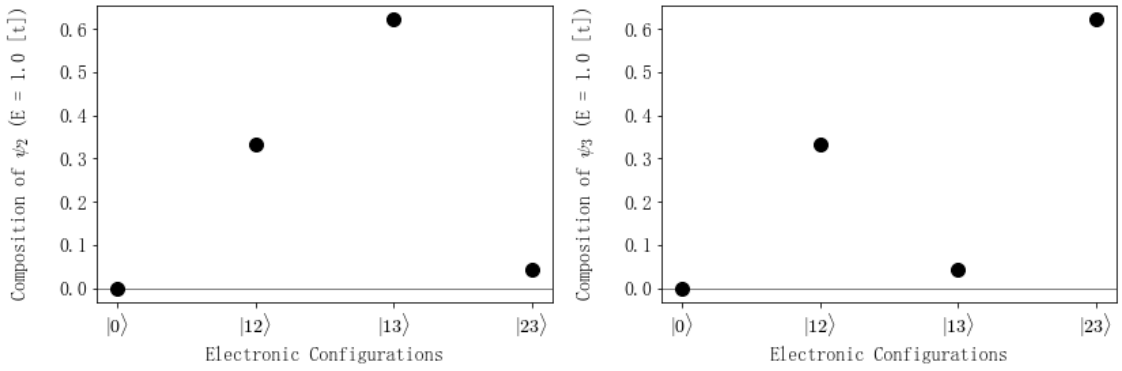

(c) (d)

Figure 4.6: Wavefunction configurations of three-site $t = \Delta, \mu = 0$ Kitaev ring, even subspace, considering site 1 "greater" than site 3.

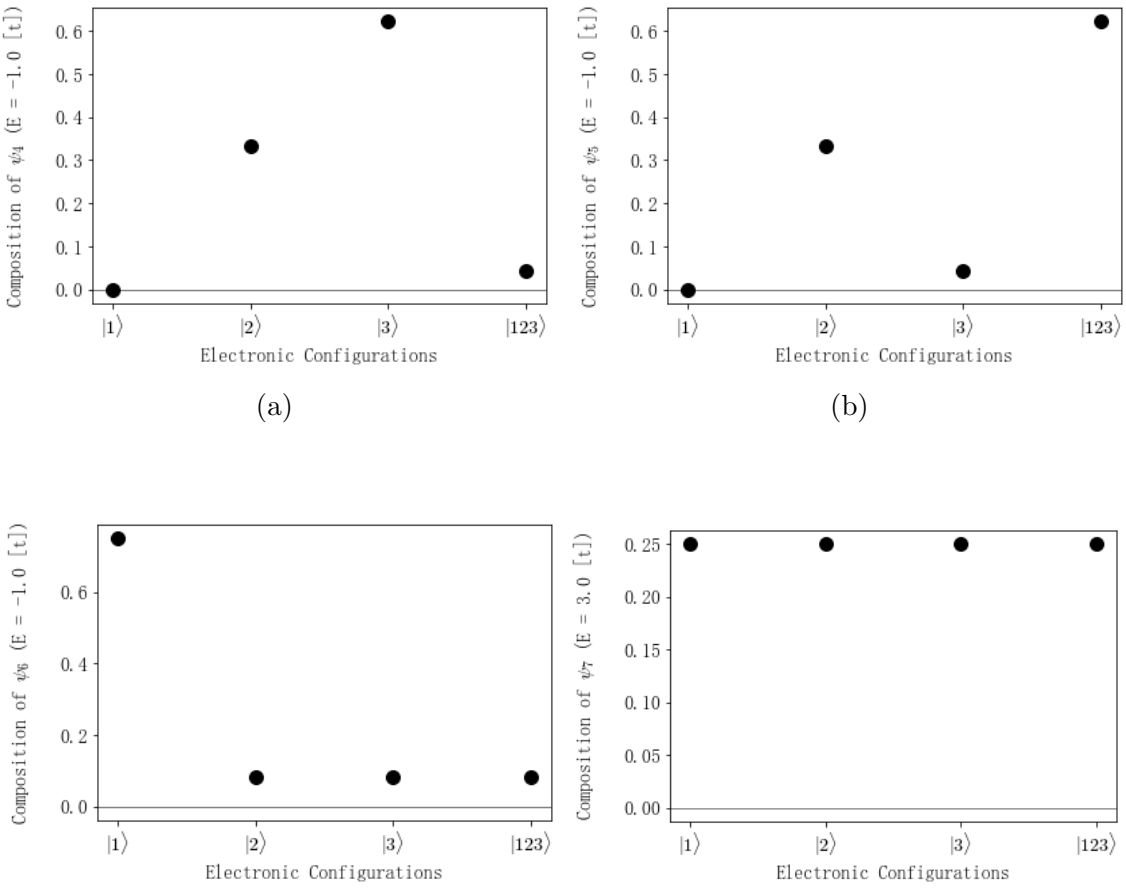

(a) (b)

(c) (d)

Figure 4.7: Wavefunction configurations of three-site $t = \Delta, \mu = 0$ Kitaev ring, odd subspace, considering site 1 "greater" than site 3.

Next, the site 3 "greater" in index than site 1 case will be considered. Thus, the subspace matrix Hamiltonians will be the same as those given in Eq. (4.8) and (4.9), with the addition of the Δ, and Δ_{13} matrix elements describing the formation of a Cooper pair on sites 1 and 3. These elements, $H^{KR}_{0,13}$ and $H^{KR}_{2,123}$, are calculated explicitly in the derivations below.

Calculation: Pairing element $H^{KR}_{0,13}$ $(= H^{KR}_{13,0})$

The Kitaev Hamiltonian pairing matrix element $H^{KR}_{0,13}$ is calculated as follows, for the case where site 3 is considered "greater" than site 1:

$$\begin{aligned}
H^{KR}_{0,13} &= \langle 0| \hat{H}_{KR} |13\rangle \\
&= \langle 0| \Delta_{13}(c_3^\dagger c_1^\dagger + c_1 c_3) |13\rangle \\
&= \Delta_{13} \langle 0| (c_3^\dagger c_1^\dagger + c_1 c_3) c_1^\dagger c_3^\dagger |0\rangle \\
&= \Delta_{13} \langle 0| c_3^\dagger c_1^\dagger c_1^\dagger c_3^\dagger |0\rangle + \Delta_{13} \langle 0| c_1 c_3 c_1^\dagger c_3^\dagger |0\rangle \\
&= \Delta_{13} \langle 0| \underbrace{c_1^\dagger \cancel{c_1}}_{0} \underbrace{c_3^\dagger \cancel{c_3}}_{0} |0\rangle - \Delta_{13} \langle 0| c_3 \underbrace{c_1 \cancel{c_1^\dagger}}_{1} c_3^\dagger |0\rangle \\
&= 0 - \Delta_{13} \underbrace{\langle 0|0\rangle}_{1} \\
&= -\Delta_{13}
\end{aligned}$$

Calculation: Pairing element $H^{KR}_{2,123}$ $(= H^{KR}_{123,2})$

The Kitaev Hamiltonian pairing matrix element $H^{KR}_{2,123}$ is calculated as follows, for the case where site 3 is considered "greater" than site 1:

$$
\begin{aligned}
H^{KR}_{2,123} &= \langle 2|\, \hat{H}_{KR}\, |123\rangle \\
&= \langle 2|\, \Delta_{13}(c_3^\dagger c_1^\dagger + c_1 c_3)\, |123\rangle \\
&= \Delta_{13}\, \langle 0|\, c_2(c_3^\dagger c_1^\dagger + c_1 c_3) c_1^\dagger c_2^\dagger c_3^\dagger\, |0\rangle \\
&= \Delta_{13}\, \langle 0|\, c_2 c_3^\dagger c_1^\dagger c_1^\dagger c_2^\dagger c_3^\dagger\, |0\rangle + \Delta_{13}\, \langle 0|\, c_2 c_1 c_3 c_1^\dagger c_2^\dagger c_3^\dagger\, |0\rangle \\
&= \Delta_{13}\, \langle 0|\, c_2 c_3^\dagger \underbrace{\cancel{c_1 c_1^\dagger}}_{0} c_2^\dagger c_3^\dagger\, |0\rangle - \Delta_{13}\, \langle 0|\, c_2 c_3 \underbrace{\cancel{c_1 c_1^\dagger}}_{1} c_2^\dagger c_3^\dagger\, |0\rangle \\
&= 0 + \Delta_{13}\, \langle 0|\, \underbrace{\cancel{c_2 c_2^\dagger}}_{1} \underbrace{\cancel{c_3 c_3^\dagger}}_{1}\, |0\rangle \\
&= \Delta_{13} \underbrace{\langle 0|0\rangle}_{1} \\
&= \Delta_{13}
\end{aligned}
$$

Thus, it can be seen that there is an artificial gauge (phase) imposed on Δ_{13} in the odd subspace. As a result, the even and odd matrix subspace Hamiltonians $\hat{H}_{EP2}$ and $\hat{H}_{OP2}$, respectively, describing the Kitaev ring of tunneling and pairing terms can be written:

$$
\hat{H}_{EP2} = \begin{bmatrix} 0 & -\Delta & -\Delta_{13} & -\Delta \\ -\Delta & 0 & t & -t_{13} \\ -\Delta_{13} & t & 0 & t \\ -\Delta & -t_{13} & t & 0 \end{bmatrix} = \begin{bmatrix} 0 & -1 & -1 & -1 \\ -1 & 0 & 1 & -1 \\ -1 & 1 & 0 & 1 \\ -1 & -1 & 1 & 0 \end{bmatrix} \tag{4.15}
$$

$$
\hat{H}_{OP2} = \begin{bmatrix} 0 & t & t_{13} & -\Delta \\ t & 0 & t & \Delta_{13} \\ t_{13} & t & 0 & -\Delta \\ -\Delta & \Delta_{13} & -\Delta & 0 \end{bmatrix} = \begin{bmatrix} 0 & 1 & 1 & -1 \\ 1 & 0 & 1 & 1 \\ 1 & 1 & 0 & -1 \\ -1 & 1 & -1 & 0 \end{bmatrix} \tag{4.16}
$$

Then, through exact diagonalization, even and odd subspace energies and wavefunction configurations are calculated as in Fig. (4.8), (4.9) and (4.10) below, respectively.

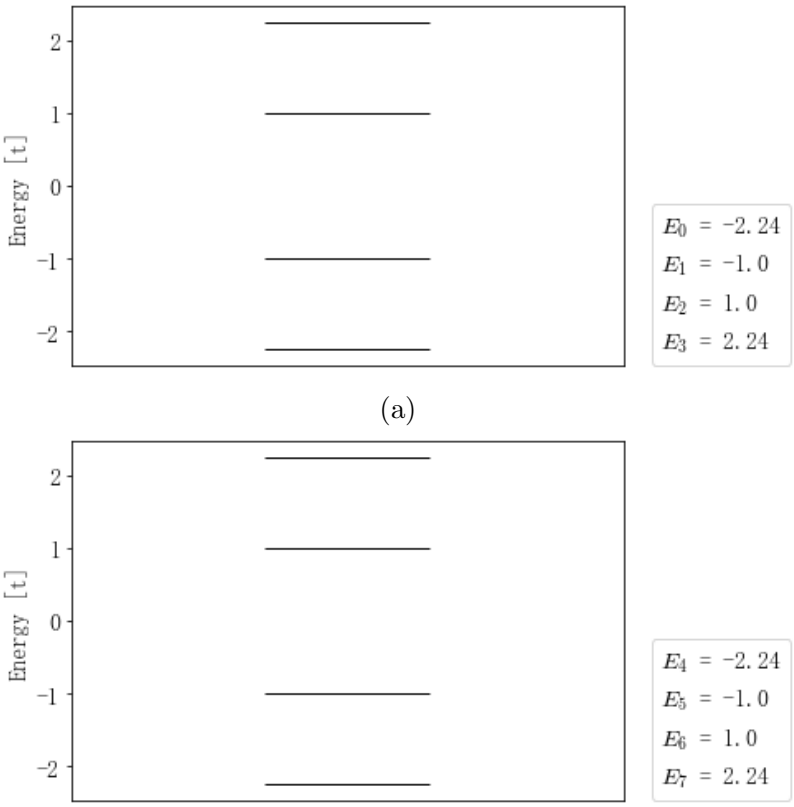

Figure 4.8: Energy spectra of three-site $t = \Delta, \mu = 0$ Kitaev ring, (a) even and (b) odd subspaces, considering site 3 "greater" than site 1.

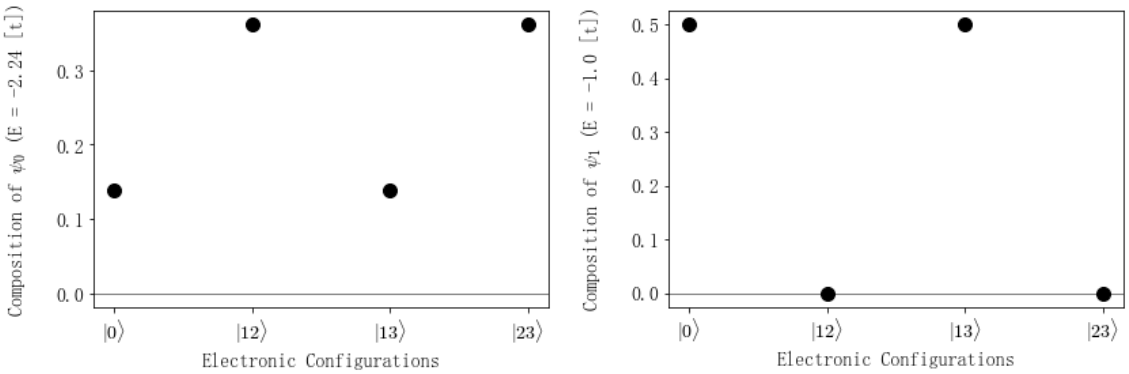

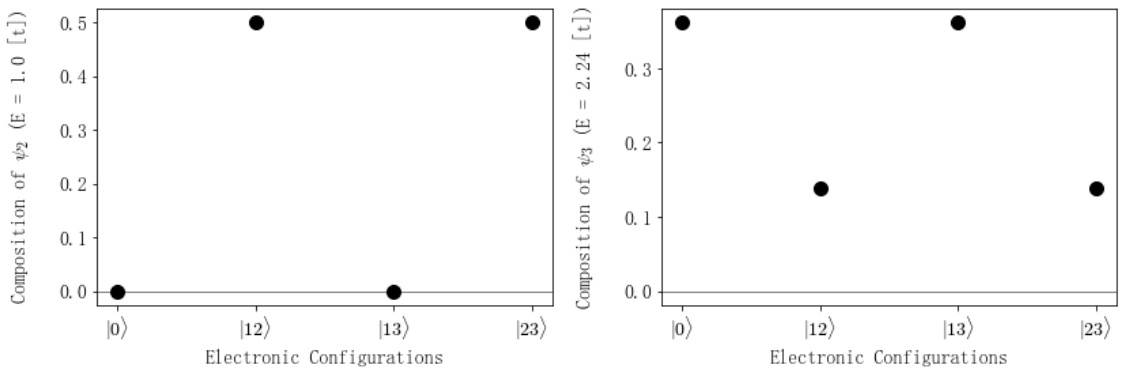

(c) (d)

Figure 4.9: Wavefunction configurations of three-site $t = \Delta, \mu = 0$ Kitaev ring, even subspace, considering site 3 "greater" than site 1.

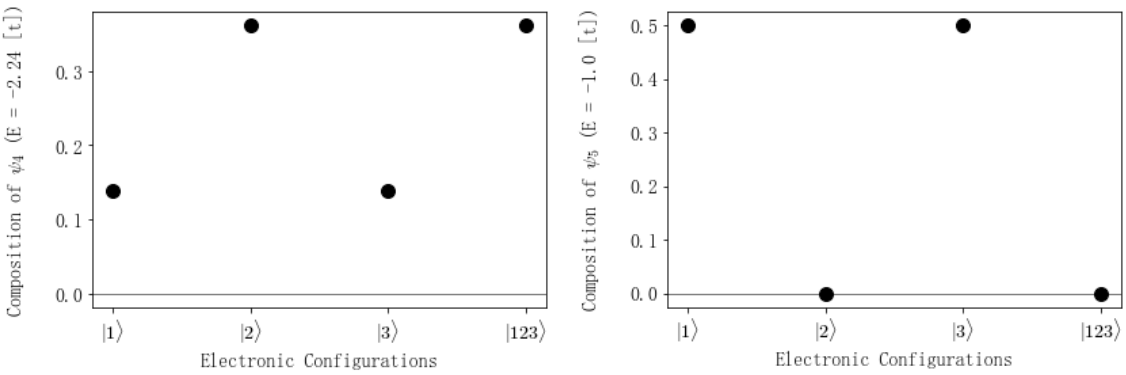

(a) (b)

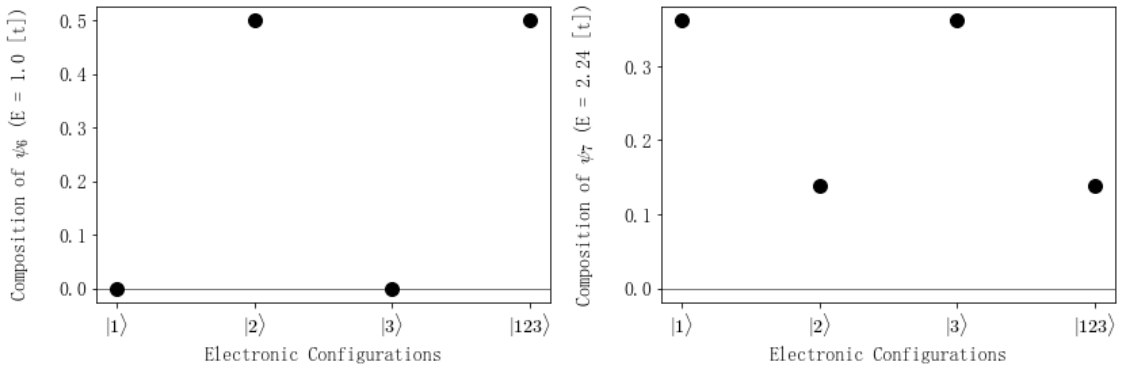

(c) (d)

Figure 4.10: Wavefunction configurations of three-site $t = \Delta, \mu = 0$ Kitaev ring, odd subspace, considering site 3 "greater" than site 1.

Here, it can be seen that inducing an opposite phase in the pairing term of the ring Kitaev Hamiltonian changes the spectra and wavefunctions of the system, when compared to those given in Fig. (4.5), (4.6) and (4.7).

However, comparison with energy spectra calculated in the bond fermion ring is required in order to deduce the correct operator ordering of the pairing term of the ring Kitaev Hamiltonian.

4.2 The Fermionic Kitaev Ring

Within this section, the ring Kitaev Hamiltonian is considered in the bond fermion basis - meaning the formation of the ring will involve consideration of the allowed bond fermion occupation.

Thus, Sec. 4.2.1 will consider the formation of the Kitaev ring in bond fermions, the new role of the "zero energy" bond fermion in the ring topology, and its effect on system energy spectra and configurations. Sec. 4.2.2 will then conclude the analysis of required ordering of the Kitaev Hamiltonian pairing term by comparison of energy spectra, originally beginning in Sec. 4.1.2.

4.2.1 Removal of the Zero Energy State

For the Kitaev Chain in bond fermions, recall that the two unpaired Majoranas at either end of the chain form a single non-local bond fermion, added "by hand" to the system Hamiltonian with zero energy. This zero energy bond fermion, while a necessary representation in the system, does not actually change the Hamiltonian - in the *chain* configuration.

However, in order to convert the system to a ring configuration, the zero energy state is used. Consider the three site, $t = \Delta, \mu = 0$ Kitaev Hamiltonian in bond fermions of Eq. (3.13):

$$\hat{H}_B = \Delta(2a_1^\dagger a_1 - 1) + \Delta(2a_2^\dagger a_2 - 1) + 0(2a_3^\dagger a_3 - 1) \tag{3.13}$$

In the Kitaev chain, the term $0(2a_3^\dagger a_3 - 1)$ is explicitly denoted with a zero coefficient, such that the state's energy to zero. However, in the Kitaev ring, this zero coefficient may be changed to a nonzero "ring pairing energy" denoted Δ_3 (where, similarly, the "ring tunneling energy" becomes t_3, and in this assumption, $t_3 = \Delta_3$). Thus, the ring Kitaev Hamiltonian in bond fermions can be written:

$$\hat{H}_{BR} = \Delta(2a_1^\dagger a_1 - 1) + \Delta(2a_2^\dagger a_2 - 1) + \Delta_3(2a_3^\dagger a_3 - 1) \tag{4.17}$$

Hence, the system becomes as shown in Fig. (4.11) of the following page, where the non-local bond fermion a_3 is now shown to be occupied, and the ring is "connected" through a_3.

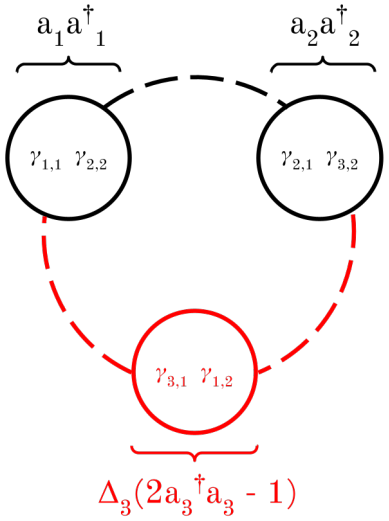

Figure 4.11: Occupation of non-local bond fermion in the simplified $t = \Delta$ Kitaev ring for three sites.

Then, given the diagonal Hamiltonian of Eq. (4.17), it is possible to use this Hamiltonian to calculate the system's energy eigenvalues and wavefunction configurations directly from this equation.

4.2.2 Confirmation of Artificial Phases

The Kitaev ring in bond fermions given by the Hamiltonian of Eq. (4.17) is entirely diagonal, hence it is possible to calculate the system's eigenvalues and eigenvectors analytically. Recall in this case, the eigenvectors will simply be the possible configurations of the system, and its eigenvalues the projection of the Hamiltonian on each possible state.

Hence, the energies of the system may be calculated as in the example calculation of Appendix B.2.2. In combination with the giving the following energy spectra and wavefunctions of the system (where it is assumed $\Delta_3 = \Delta$), as in Fig. (4.12), (4.13), and (4.14) on the following page (respectively).

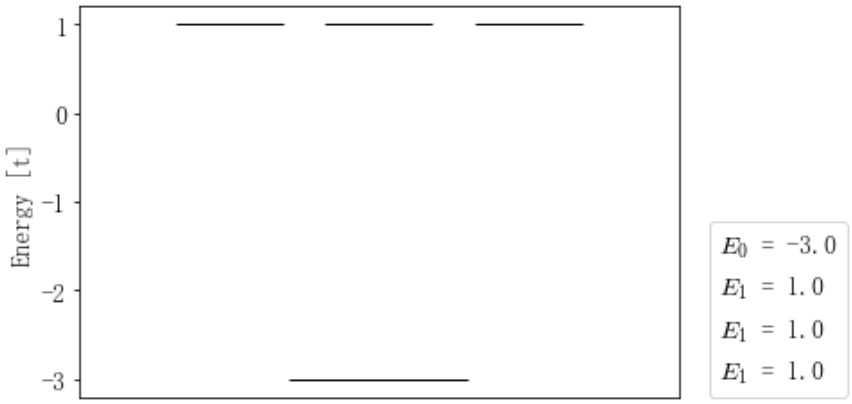

(a)

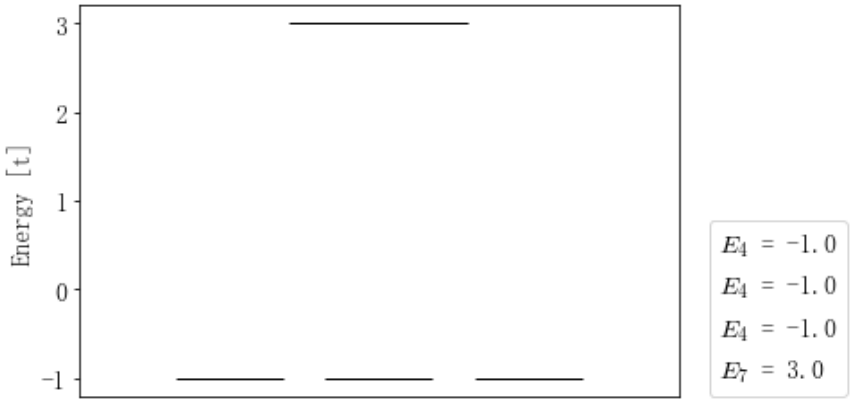

(b)

Figure 4.12: Energy spectra of three-site $t = \Delta, \mu = 0$ Kitaev ring in bond fermions, (a) even and (b) odd subspaces.

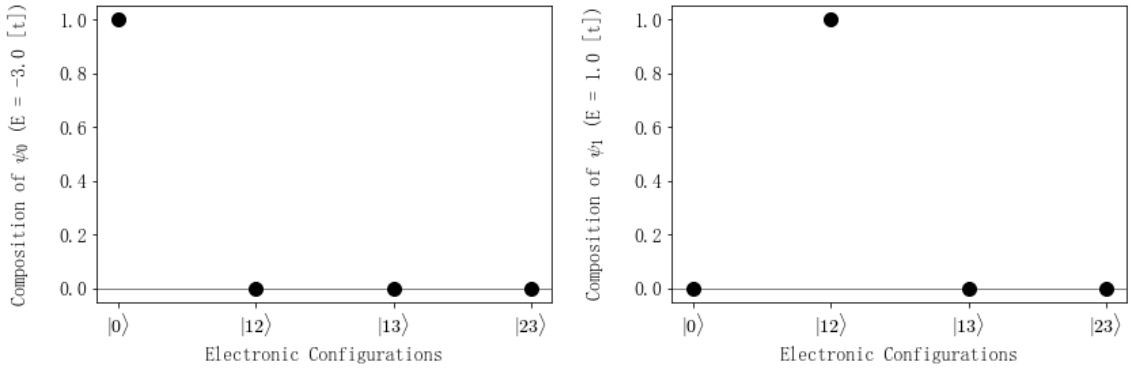

(a) (b)

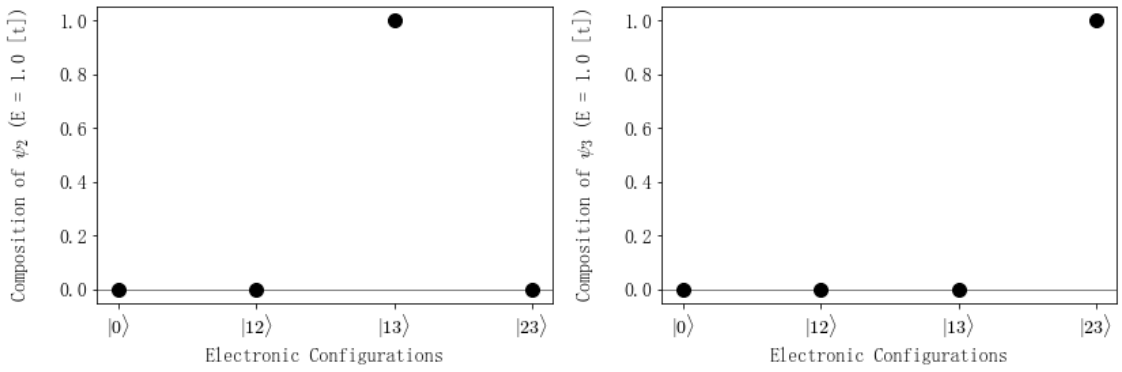

(c) (d)

Figure 4.13: Wavefunction configurations of three-site $t = \Delta, \mu = 0$ Kitaev ring in bond fermions, even subspace.

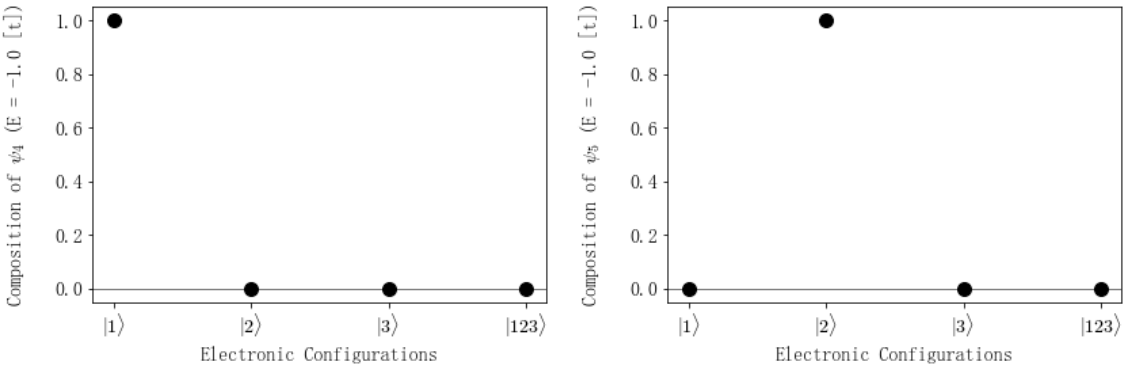

(a) (b)

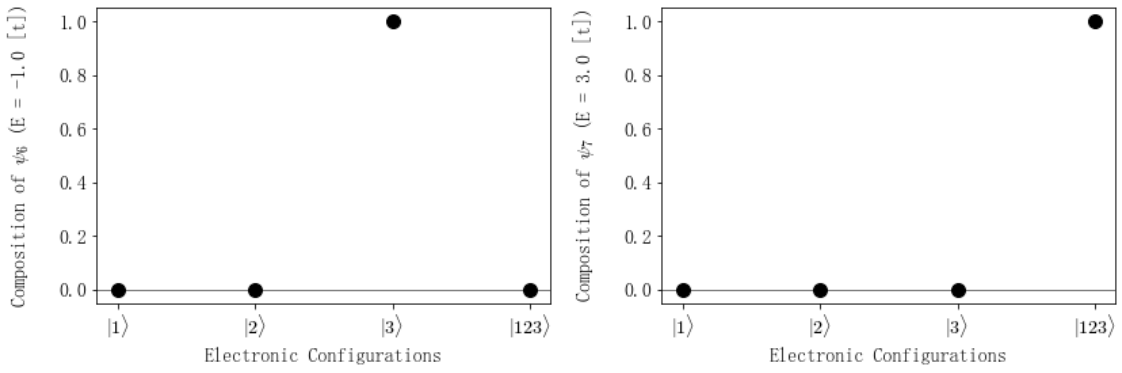

(c) (d)

Figure 4.14: Wavefunction configurations of three-site $t = \Delta, \mu = 0$ Kitaev ring in bond fermions, odd subspace.

In this case, it is of note that the degenerate energies of configurations as seen in Sec. 3.2.3 as a result of the zero energy bond fermion are no longer present.

Degenerate energy states are present in the spectra, however, these occur in the one and two site occupations, and do not occur with differing occupation numbers.

It is also noted that this is the only allowed spectra given by the ring Kitaev Hamiltonian of Eq. (4.17) - there is only one possible Hamiltonian of the system given by this derivation, therefore the energy spectra given above for the Kitaev ring in bond fermions must be correct. Thus, the spectra of Fig. (4.12) is used to confirm the correct ordering of the fermionic system by direct comparison.

By considering Fig. (4.12), Fig. (4.5) and (4.8), it is observed that the $t = \Delta, \mu = 0$ Kitaev ring spectra in the fermion and bond fermion bases match only in the case where site 1 is considered "greater" in index than site 3. The spectra given by the Kitaev ring in bond fermions, and by the Kitaev ring in fermions of Eq. (4.11) is as shown in Fig. (4.15) below.

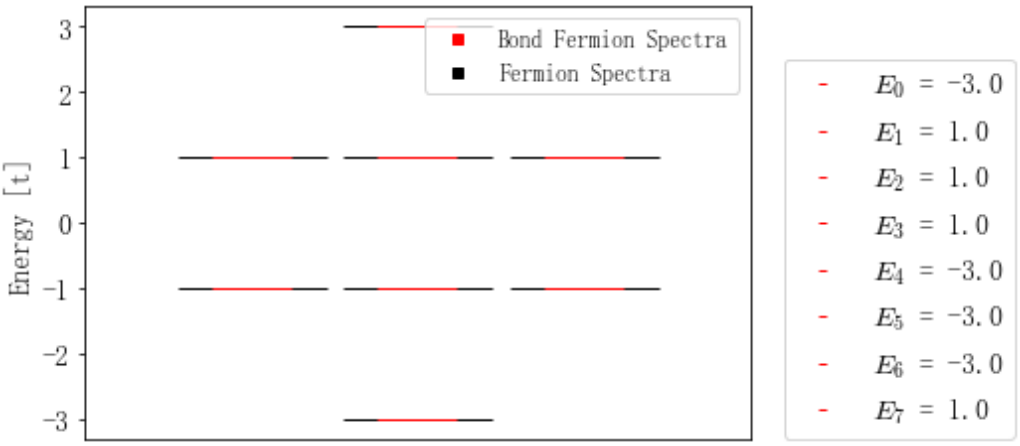

Figure 4.15: Degenerate energy spectra of three-site $t = \Delta, \mu = 0$ Kitaev ring in fermions and in bond fermions, considering site 1 "greater" in index than site 3.

As a result, it must be considered that the correct ordering of operators in the fermionic system is:

$$t_{13}(c_1^\dagger c_3 + c_3^\dagger c_1)$$
$$\Delta_{13}(c_1^\dagger c_3^\dagger + c_3 c_1) \tag{4.3}$$

Therefore, the correct three-site ring Kitaev Hamiltonian is (explicitly) written as:

$$\begin{aligned}\hat{H}_{KR} = & t(c_2^\dagger c_1 + c_1^\dagger c_2 + c_3^\dagger c_2 + c_2^\dagger c_3) + t_{13}(c_1^\dagger c_3 + c_3^\dagger c_1) \\ & + \Delta(c_2^\dagger c_1^\dagger + c_1 c_2 + c_3^\dagger c_2^\dagger + c_2 c_3) + \Delta_{13}(c_1^\dagger c_3^\dagger + c_3 c_1) \\ & - \mu(c_1^\dagger c_1 + c_2^\dagger c_2 + c_3^\dagger c_3)\end{aligned} \tag{4.18}$$

Importantly, this result depends on the presence of the artificial phase of Δ_{13}. By comparison of Eq. (4.13), (4.14), and Eq. (4.15), (4.16), it can be seen that the only difference in these matrices is the sign of Δ_{13}.

In the case where site 1 is considered to be "greater" in index than site 3, the Cooper pairing matrix element is given by:

$$\begin{cases} \Delta_{13} & \text{in even subspace} \\ -\Delta_{13} & \text{in odd subspace} \end{cases} \tag{4.19}$$

Representing a phase change in the even subspace compared to the chain pairing matrix elements Δ, which are usually given as $-\Delta$ in both the even and odd subspace matrix Hamiltonians.

The dependence of the artificial gauge to matching spectra between the fermion and bond fermion Kitaev rings implies that the presence of this artificial gauge is necessary in the fermionic ring system. However, the physical significance of the artificial gauge is not yet known - although this phase affects the movement of Cooper pairs in the ring, such a concept must be further studied in order to realize its full implications.

Chapter 5

Conclusions

In this thesis, an analysis of Kitaev's chain and ring of spinless fermions on a quantum wire, as well as the resultant emergent Majorana zero modes and artificial gauges, has been presented.

Within this work, Chapter 2 discusses the Kitaev system in the fermionic basis, where initial energy spectra and wavefunctions are calculated through exact diagonalization. In Sec. 3.2, the Kitaev chain is transformed into a chain of Majoranas, and Majoranas are paired on neighboring sites to form "bond fermions", creating a diagonal Hamiltonian. Emergent Majorana zero modes - two zero energy, dangling Majoranas on either end of the chain - are found to be necessary to find degenerate energy states, and in turn, allow the energy spectra of the Kitaev chain in fermions and bond fermions to match exactly. In this case, matching spectra occur only when considering the zero-energy eigenvalue given by the non-local bond fermion (consisting of the two MZMs). In addition, degenerate energy wavefunctions occur only when the difference in two states is the occupation of the non-local bond fermion.

Under expansion to the ring system in Chapter 4, it is noted that one must determine a correct ordering of fermionic operators, where an emergent "artificial gauge" occurs under specific orderings. From exact diagonalization results in the fermion basis compared to those of the bond fermion basis, it is found that the order of operators affects the energy spectra of the ring. An artificial phase on tunneling and Cooper

pairing Hamiltonian matrix elements emerges, describing transitions at the "ends" of the ring. As a result, is determined that site 1 must be considered "greater" in index than site N (of an N site ring) in order for the energy spectra of the Kitaev ring in fermions and bond fermions to match. These results suggest that the movement of Cooper pairs on a fermionic ring occur in a particular manner, and are affected by the emergent artificial gauge.

In conclusion, the purposes of exploring the Kitaev chain and ring systems, observing emergent MZMs, and deriving the origin of the ring's artificial gauges, were achieved by analytical derivation and matching of energy spectra across transformations via exact diagonalization. Properties of electronic Hamiltonians are explored, considering the effect of artificial gauges and fermion statistics, and serving as a starting point for future research and discussion about these physical implications. Overall, these results contribute to the understanding of Kitaev chains and rings, and the origins of MZMs in 1D chains, which may have future applications in topologically protected quantum computing.

Bibliography

[1] J. Alicea, "New directions in the pursuit of majorana fermions in solid state systems," *Reports on Progress in Physics*, vol. 75, no. 7, p. 076 501, 2012.

[2] R. Pawlak, S. Hoffman, J. Klinovaja, D. Loss, and E. Meyer, "Majorana fermions in magnetic chains," *Progress in Particle and Nuclear Physics*, vol. 107, 1–19, 2019.

[3] L. Borsten and M. J. Duff, "Majorana fermions in particle physics, solid state and quantum information," *The Future of Our Physics Including New Frontiers*, 77–121, 2017.

[4] S. R. Elliott and M. Franz, "Colloquium: Majorana fermions in nuclear, particle, and solid-state physics," *Reviews of Modern Physics*, vol. 87, no. 1, 137–163, 2015.

[5] B. Jaworowski and P. Hawrylak, "Quantum bits with macroscopic topologically protected states in semiconductor devices," *Applied Sciences*, 2019.

[6] A. Y. Kitaev, "Unpaired majorana fermions in quantum wires," *Physics-Uspekhi*, vol. 44, no. 10S, 131–136, 2001.

[7] R. M. Lutchyn, J. D. Sau, and S. Das Sarma, "Majorana fermions and a topological phase transition in semiconductor superconductor heterostructures," *Physical Review Letters*, vol. 105, no. 7, 2010.

[8] M. Leijnse and K. Flensberg, "Introduction to topological superconductivity and majorana fermions," *Semiconductor Science and Technology*, vol. 27, no. 12, p. 124 003, 2012.

[9] C. Beenakker, "Search for majorana fermions in superconductors," *Annual Review of Condensed Matter Physics*, vol. 4, no. 1, 113–136, 2013.

[10] L. Herviou, C. Mora, and K. Le Hur, "Phase diagram and entanglement of two interacting topological kitaev chains," *Physical Review B*, vol. 93, no. 16, 2016.

[11] H.-Y. Hui, P. M. R. Brydon, J. D. Sau, S. Tewari, and S. D. Sarma, "Majorana fermions in ferromagnetic chains on the surface of bulk spin-orbit coupled s-wave superconductors," *Scientific Reports*, vol. 5, 2015.

[12] S. Nadj-Perge *et al.*, "Observation of majorana fermions in ferromagnetic atomic chains on a superconductor," *Science*, vol. 346, pp. 602–607, 2014.

[13] B. Jäck, Y. Xie, and A. Yazdani, "Detecting and distinguishing majorana zero modes with the scanning tunneling microscope," *Nature*, 541–554, 2021.

[14] H. Zhang *et al.*, "RETRACTED ARTICLE: Quantized majorana conductance," *Nature*, vol. 556, pp. 74–79, 2018.

[15] S. B. Bravyi and A. Y. Kitaev, "Fermionic quantum computation," *Annals of Physics*, vol. 298, no. 1, 210–226, 2002.

[16] A. Kitaev, "Fault-tolerant quantum computation by anyons," *Annals of Physics*, vol. 303, no. 1, 2–30, 2003.

[17] S. D. Sarma, M. Freedman, and C. Nayak, "Majorana zero modes and topological quantum computation," *npj Quantum Information*, vol. 1, no. 1, 2015.

[18] H. Soller, "Dissipative quantum computing with majorana fermions," *Journal of Applied Mathematics and Physics*, vol. 04, pp. 227–232, Jan. 2016.

[19] M. A. Nielsen, "The fermionic canonical commutation relations and the jordan-wigner transform," 2005.

[20] O. Derzhko, "Jordan-wigner fermionization for spin-1/2 systems in two dimensions: A brief review," *Journal of Physical Studies*, vol. 5, pp. 49–64, 2001.

[21] D. De Falco and D. Tamascelli, "An introduction to quantum annealing," *RAIRO - Theoretical Informatics and Applications*, vol. 45, pp. 99–116, 2011.

[22] P. Hauke, H. G. Katzgraber, W. Lechner, H. Nishimori, and W. D. Oliver, "Perspectives of quantum annealing: Methods and implementations," *Reports on Progress in Physics*, vol. 83, 2020.

[23] "D-wave problem-solving handbook (d-wave user manual 09-1171b-i)," *D-Wave Systems Inc.*, 2021.

[24] "Qpu solver datasheet (d-wave user manual 09-1109b-e)," *D-Wave Systems Inc.*, 2021.

[25] "What is quantum annealing?" *D-Wave System Documentation*, 2022.

[26] J. Tilly *et al.*, *The variational quantum eigensolver: A review of methods and best practices*, 2021.

[27] M. Horowitz and E. Grumbling, *Quantum Computing: Progress and Prospects*. The National Academies Press, 2019.

[28] Y. Cao *et al.*, "Quantum chemistry in the age of quantum computing," *Chemical Reviews*, vol. 119, no. 19, pp. 10 856–10 915, 2019.

[29] R. Miceli and M. McGuigan, "Quantum computation and visualization of hamiltonians using discrete quantum mechanics and ibm qiskit," *2018 New York Scientific Data Summit (NYSDS)*, pp. 1–6, 2018.

[30] S. Kwon, A. Tomonaga, G. L. Bhai, S. J. Devitt, and J.-S. Tsai, "Gate-based superconducting quantum computing," *Journal of Applied Physics*, vol. 129, no. 4, p. 041 102, 2021.

[31] X. Yuan, S. Endo, Q. Zhao, Y. Li, and S. C. Benjamin, "Theory of variational quantum simulation," *Quantum*, vol. 3, p. 191, 2019.

[32] "Simulating molecules using vqe," *Qiskit, International Business Machines (IBM) Corporation*, 2022.

[33] R. Wiersema, "How to construct and load hamiltonians in pennylane," *Pennylane Blog, Xanadu Quantum Technologies*, 2021.

[34] "Building molecular hamiltonians," *Pennylane Demos, Xanadu Quantum Technologies*, 2022.

[35] "A brief overview of vqe," *Pennylane Demos, Xanadu Quantum Technologies*, 2021.

[36] P. B. Pal, "Dirac, majorana, and weyl fermions," *American Journal of Physics*, vol. 79, no. 5, 485–498, 2011.

[37] N. G. Marchuk, *Dirac gamma-equation, classical gauge fields and clifford algebra*, 1998. arXiv: math-ph/9811022 [math-ph].

[38] C.-B. Hua, R. Chen, D.-H. Xu, and B. Zhou, "Disorder-induced majorana zero modes in a dimerized kitaev superconductor chain," *Physical Review B*, vol. 100, 2019.

[39] X.-L. Yu *et al.*, "Topological phase transitions, majorana modes, and quantum simulation of the su-schrieffer-heeger model with nearest-neighbor interactions," *Physical Review B*, vol. 101, 2020.

[40] J. Alicea, Y. Oreg, G. Refael, F. von Oppen, and M. P. A. Fisher, "Non-abelian statistics and topological quantum information processing in 1d wire networks," *Nature Physics*, vol. 7, pp. 412–417, 2011.

[41] E. M. Stoudenmire, J. Alicea, O. A. Starykh, and M. P. Fisher, "Interaction effects in topological superconducting wires supporting majorana fermions," *Physical Review B*, vol. 84, 2011.

[42] A. Peruzzo *et al.*, "A variational eigenvalue solver on a quantum processor," *Nature Communications*, vol. 5, no. 1, 2014. eprint: arXiv:1304.3061.

[43] S. E. Smart and D. A. Mazziotti, "Quantum solver of contracted eigenvalue equations for scalable molecular simulations on quantum computing devices," *Physical Review Letters*, vol. 126, no. 7, 2021.

[44] A. Papageorgiou and H. Wozniakowski, *The sturm-liouville eigenvalue problem and np-complete problems in the quantum setting with queries*, 2007.

[45] L. Bittel and M. Kliesch, "Training variational quantum algorithms is np-hard," *Physical Review Letters*, vol. 127, 2021.

[46] P. W. Shor, "Fault-tolerant quantum computation," *37th Symposium on Foundations of Computing*, no. 1, pp. 56–65, 1996.

[47] D. Aharonov and M. Ben-Or, "Fault-tolerant quantum computation," *29th Annual ACM Symposium on Theory of Computing (STOC)*, no. 1, 1997.

[48] A. M. Steane, "Efficient fault-tolerant quantum computing," *Nature*, vol. 399, no. 6732, 124–126, 1999.

[49] D. G. Cory *et al.*, "Experimental quantum error correction," *Physical Review Letters*, vol. 81, no. 10, 2152–2155, 1998.

[50] E. Knill, "Quantum computing with realistically noisy devices," *Nature*, vol. 434, no. 7029, 39–44, 2005.

[51] C. Nayak, S. H. Simon, A. Stern, M. Freedman, and S. Das Sarma, "Non-abelian anyons and topological quantum computation," *Reviews of Modern Physics*, vol. 80, no. 3, 1083–1159, 2008.

[52] T. D. Stanescu, R. M. Lutchyn, and S. Das Sarma, "Majorana fermions in semiconductor nanowires," *Physical Review B*, vol. 84, no. 14, 2011.

[53] S. Rao, *Introduction to abelian and non-abelian anyons*, 2016. arXiv: 1610.09260 [cond-mat.mes-hall].

[54] E. Génetay Johansen and T. Simula, "Fibonacci anyons versus majorana fermions: A monte carlo approach to the compilation of braid circuits in su(2)k anyon models," *PRX Quantum*, vol. 2, no. 1, 2021.

[55] J. Sau, S. Simon, S. Vishveshwara, and J. R. Williams, "From anyons to majoranas," *Nature Reviews Physics*, vol. 2, no. 12, 667–668, 2020.

Appendix A: Methodology

In order to compare and confirm mappings of Kitaev's "toy chain" in various bases, system wavefunctions and energy spectra are calculated using analytical and numerical methods. This section describes various methodology used in obtaining results throughout this work.

A.1 Second Quantization and Coherent Summation

Second quantization notation is an occupation notation taking advantage of many-particle systems consisting of identical particles. In particular, second quantization defines systems based simply on the occupation of states, taking into account only the number of identical particles in any given state, rather than attempting to distinguish between particles. Essentially, the occupation number basis does not consider if a specific particle is in a particular state, only if there is *some* particle (or particles) in a particular state.

Beginning with the wavefunctions and eigenenergies of some Hamiltonian $\hat{H}$ (for some α in the set of possible eigenstates with associated eigenvalues):

$$\hat{H}\left|\psi_\alpha\right\rangle = E_\alpha\left|\psi_\alpha\right\rangle \tag{A.1}$$

The eigenstates of the system can be written in terms of the occupation number states. Consider a system with a complete set of M distinct states, or particle configurations:

$$|1\rangle, |2\rangle, |3\rangle, ... |m\rangle, ... |M\rangle \tag{A.2}$$

This system may hence contain some number of particles n_m in each state $|m\rangle$, where the allowed number of particles in a given state will depend on particle type:

$$n_m = \begin{cases} 0, 1 & \text{if fermions} \\ 0, 1, 2, ... \in \mathbb{N} & \text{if bosons} \end{cases} \tag{A.3}$$

Then, the state $|\phi_m\rangle$, can be defined in terms of the occupation numbers n_m as:

$$|\phi_m\rangle = |n_1, n_2, n_3, ...n_M\rangle \tag{A.4}$$

Where $|\phi_m\rangle$ is some state with n_1 particles in the state $|1\rangle$, n_2 particles in the state $|2\rangle$, etc.

It is then possible to write down any state of the system $|\psi_\alpha\rangle$ as a linear combination of multi-particle occupation number states using coherent summation. Coherent summation assumes that all quantum states $|\phi_m\rangle$ may be present in a given state of the system, regardless of the total number of particles $N_m = \sum_i n_i$ in any given $|\phi_m\rangle$. Thus, under this assumption, eigenstates of the system $|\psi_\alpha\rangle$ may be written:

$$|\psi_\alpha\rangle = \sum_m A_m |\phi_m\rangle \tag{A.5}$$

Where A_m is some normalization coefficient corresponding to the multi-particle state $|\phi_m\rangle$, and allowed multi-particle states and wavefunctions are defined by the given system and its constituent particles.

Hence, this is the basis for second quantization - a language of multi-particle systems which takes into account only the occupation numbers n_m of any given state (site, orbital, etc.). Importantly, second quantization also does not distinguish between individual particles when defining the Hamiltonian, operators, or mathematical relationships of a given system - allowing the entire system and its various properties

to be written consistently in the occupation number basis, as will be used throughout this thesis.

A.2 Spinless Fermions

Essentially, a spinless fermion is a particle which, while still considered to follow Fermi-Dirac statistics and the Pauli exclusion principle (resulting in restrictions upon occupation numbers and symmetry), no longer takes spin into account. As a result, spinless fermions may only singly-occupy sites.

It is now possible to further define the second quantized number and multi-particle states (from the previous section) in accordance with this condition. Firstly, the occupation number n_m of a given single particle state $|m\rangle$ must be:

$$n_m = \begin{cases} 1 & \text{if } |m\rangle \text{ occupied} \\ 0 & \text{if } |m\rangle \text{ unoccupied} \end{cases} \tag{A.6}$$

As a result, any multi-particle occupation number state of the system $|\phi_m\rangle$ will only contain $n_m \in \{0, 1\}$. As the single particle states are now distinguished simply by whether they are occupied or not, in order to more easily distinguish occupation of states, occupied single particle states can be given simply by their state number m, and unoccupied single particle states can be omitted from the multi-particle state. Then, $|\phi_m\rangle$ as described in Eq. (A.4) may be rewritten as:

$$|\phi_m\rangle = |m_1, m_2, m_3, ...m_M\rangle \tag{A.7}$$

Where:

$$m_m = \begin{cases} m & \text{if } |m\rangle \text{ occupied} \\ Omitted & \text{if } |m\rangle \text{ unoccupied} \end{cases} \tag{A.8}$$

Example: Explicit State Representation

Consider a system of 3 sites in a state $|\phi_\beta\rangle$, of which sites 1 and 3 are occupied. In this notation, the occupation of each site may be written:

$$\begin{aligned} m_1 \text{ occupied } &\implies m_1 = 1 \\ m_2 \text{ unoccupied } &\implies m_2 \text{ omitted} \\ m_3 \text{ occupied } &\implies m_3 = 3 \end{aligned}$$

Then, plugging in the above to the state representation of $|\phi_\beta\rangle$:

$$|\phi_\beta\rangle = |m_1, m_2, m_3\rangle = |13\rangle$$

Note that for any system, the vacuum state $|\phi_0\rangle$ of zero occupied sites is written simply as:

$$|\phi_0\rangle = |0\rangle \tag{A.9}$$

Then, a system with M distinct single particle states, or sites, may have all possible electronic states written explicitly in terms of the occupied sites. Here it is assumed the number of particles of the system N may fluctuate such that $0 \leq N \leq M$. In this case, the number of possible electronic configurations k is given by:

$$k = \binom{M}{0} + \binom{M}{1} + ... + \binom{M}{M-1} + \binom{M}{M} \tag{A.10}$$

Where the binomial coefficient "M choose N" for some N particles on M possible sites is represented as the binomial coefficient for combinations without repetition:

$$\binom{M}{N} = \frac{M!}{N!(M-N)!} \tag{A.11}$$

Where for a system of M sites, which may be either occupied or unoccupied by a single particle, the binomial coefficient gives the number of possible electronic configurations to be:

$$k = 2^M \tag{A.12}$$

Thus, the system wavefunction can now be written as a linear combination of all k possible configurations of spinless fermions, $|\psi_\alpha\rangle$ (as described in Eq. (A.5)):

$$|\psi_\alpha\rangle = \sum_{\alpha=0}^{k-1} A_\alpha \, |\phi_\alpha\rangle \tag{A.13}$$

Written explicitly for all k electronic configurations:

$$|\psi_\alpha\rangle = A_0^\alpha \, |0\rangle + A_1^\alpha \, |1\rangle + ... + A_{k-1}^\alpha \, |12...M\rangle \tag{A.14}$$

In a fermionic system, the occupation number states may also be represented by the action of the fermionic creation operators on the vacuum state $|0\rangle$. Starting with the fermionic creation and annihilation operators acting on some site $i \in M$ of an M-site system:

$$c_i^\dagger, c_i \tag{A.15}$$

Where it should be noted that the fermionic creation and annihilation operators on some sites $i, j \in M$ obey the following commutation relations:

$$\begin{aligned} \{c_i^\dagger, c_j^\dagger\} &= 0 \\ \{c_i, c_j\} &= 0 \\ \{c_i, c_j^\dagger\} &= \delta_{ij} \end{aligned} \tag{A.16}$$

Hence, the action of the fermionic creation and annihilation operators on a state $|i\rangle$ representing the occupation of a single site $i \in M$ by a single spinless fermion, and the vacuum state $|0\rangle$ are:

$$\begin{aligned} c_i^\dagger |0\rangle = |i\rangle \, , c_i^\dagger |i\rangle = 0 \\ c_i |i\rangle = |0\rangle \, , c_i |0\rangle = 0 \end{aligned} \tag{A.17}$$

Following directly from the above equations, the following relation can be written:

$$\begin{aligned} \langle 0| \, c_i c_i^\dagger \, |0\rangle &= \langle 0| \, c_i \, |i\rangle \\ &= \langle 0|0\rangle \\ \implies c_i c_i^\dagger &= 1 \end{aligned} \tag{A.18}$$

In this thesis, for some state consisting of N particles, these states are written in the following notation and ordering of fermionic operators:

$$\begin{aligned} |1, 2, ..., N-1, N\rangle &= c_1^\dagger c_2^\dagger ... c_{N-1}^\dagger c_N^\dagger \, |0\rangle \\ \langle 1, 2, ..., N-1, N| &= \langle 0| \, c_N c_{N-1} ... c_2 c_1 \end{aligned} \tag{A.19}$$

Where it should be noted that the decided and maintained canonical ordering, ie. the ordering of the fermionic creation and annihilation operators in state representation, is maintained consistently throughout this work.

A.3 Configuration Interaction and The Matrix Hamiltonian Representation

The configuration interaction method is used for determining electronic system and excitation energies. The configuration interaction method is an alternative to the Hartree-Fock method, and operates in second quantization formalism, considering system wavefunctions as a linear combination of all possible states.

Eq. (A.14) of the previous section is already defined in the configuration interaction based formalism, where by writing the single and multi-particle occupation states $|\phi_\alpha\rangle$

as fermionic operators acting on the vacuum state, configuration interaction methods can be used to solve for further information about the given system. Recall Eq. (A.14) describing a wavefunction ψ_α of some system of spinless fermions:

$$|\psi_\alpha\rangle = A_0^\alpha |0\rangle + A_1^\alpha |1\rangle + ... + A_{k-1}^\alpha |12...M\rangle \tag{A.14}$$

For a given system described by a Hamiltonian $\hat{H}$ (again, as described in Eq (A.1) of the previous section) of which ψ_α is a wavefunction, ψ_α is dependant on the allowed electronic configurations determined by this Hamiltonian. For instance, any given Hamiltonian defined in second quantization in terms of fermionic creation and annihilation operators may allow only certain particle numbers N, number of sites M, transitions between particle numbers, etc. In order to know the allowed wavefunctions of any given system, the coefficients A^α of the above equation must be determined in terms of the specific Hamiltonian of the system described.

Hence, by acting on Eq. (A.14) with the Hamiltonian $\hat{H}$, the following matrix equation is obtained:

$$\sum_\beta \langle\phi_\gamma| \hat{H} |\phi_\beta\rangle A_\beta^\alpha = E^\alpha A_\gamma^\alpha \tag{A.20}$$

By the configuration interaction methodology, in order to solve for the allowed wavefunctions and energies of the system, it is hence sufficient to diagonalize the Hamiltonian matrix $\sum_\beta \langle\phi_\gamma| \hat{H} |\phi_\beta\rangle$. This matrix represents the Hamiltonian in terms of the orthonormal basis states, $|\phi_\alpha\rangle$, of the system, and can be written explicitly in terms of the occupation number basis states given in Eq. (A.14) as:

$$\hat{H} = \begin{bmatrix} H_{0,0} & H_{0,1} & \dots & H_{0,12...M} \\ H_{1,0} & \ddots & & \\ \vdots & & & \\ H_{12...M,0} & & & H_{12...M,12...M} \end{bmatrix} \tag{A.21}$$

Where the matrix element $\langle\phi_\gamma| \hat{H} |\phi_\beta\rangle$ is written as $H_{\gamma,\beta}$ for simplicity.

By diagonalizing the Hamiltonian matrix above, the configuration interaction method returns the energy eigenvalues E^α and corresponding eigenvectors, or wavefunctions $|\psi_\alpha\rangle$. In this case, the system wavefunction is given in terms of coefficients A^α as the eigenvector:

$$|\psi_\alpha\rangle = \begin{bmatrix} A_0^\alpha \\ A_1^\alpha \\ \vdots \\ A_{k-1}^\alpha \end{bmatrix} \tag{A.22}$$

Hence, allowing the energy values and wavefunctions of a given system to be found (relatively painlessly), provided the matrix Hamiltonian can be constructed either analytically or computationally through calculation of the Hamiltonian matrix elements.

A.4 Matrix Element Calculation

In order to prepare matrices for diagonalization, it is required to perform the explicit matrix element calculations for all k^2 elements $H_{\gamma,\beta}$. Although it is possible to write programs to generate Hamiltonian matrices computationally, the initial calculations must be done analytically to ensure correct computational results.

Matrix element calculations are done simply by writing matrix elements explicitly using Eq. (A.19), and simplifying using Eq. (A.16). As a result, any elements of a second quantized Hamiltonian with constant coefficients (as given by the configuration interaction method, and where coefficient integrals are not computed within this thesis) will either be a combination of matrix coefficients, or will be 0.

As this is a difficult concept to explain and be understood generally, an example matrix element calculation is shown below.

Example: Generalized Matrix Element Calculation

Consider a system of three arbitrary sites p, q, r, such that $p, q, r \in \mathbb{Z}^+$, and $p < q < r$. In addition, consider an example Hamiltonian written in second quantization formalism describing tunneling of a single spinless fermion between sites p and q of such a system of singly-occupied sites to be:

$$\hat{H}_{ex} = t(c_q^\dagger c_p + c_p^\dagger c_q)$$

Where t is the constant nearest-neighbor tunneling (or hopping) coefficient, and $c_i^\dagger, c_i$ for $i \in \{p, q\}$ are the spinless fermion creation and annihilation operators.

Then, the matrix element calculation of an element $H_{pr,qr}^{ex}$ is performed as follows, using the fermionic relations in Eq. (A.19) and Eq. (A.16):

$$\begin{aligned}
H_{pr,qr}^{ex} &= \langle pr| \hat{H}_{ex} |qr\rangle \\
&= \langle pr| t(c_q^\dagger c_p + c_p^\dagger c_q) |qr\rangle \\
&= t \langle 0| c_r c_p (c_q^\dagger c_p + c_p^\dagger c_q) c_q^\dagger c_r^\dagger |0\rangle \\
&= t \langle 0| c_r c_p c_q^\dagger c_p c_q^\dagger c_r^\dagger |0\rangle + t \langle 0| c_r c_p c_p^\dagger c_q c_q^\dagger c_r^\dagger |0\rangle \\
&= -t \langle 0| c_r c_q^\dagger \underbrace{\cancel{c_p c_p}}_{0} c_q^\dagger c_r^\dagger |0\rangle + t \langle 0| c_r \underbrace{\cancel{c_p c_p^\dagger}}_{1} \underbrace{\cancel{c_q c_q^\dagger}}_{1} c_r^\dagger |0\rangle \\
&= 0 + t \langle 0| \cancel{c_r c_r^\dagger} |0\rangle \\
&= t \underbrace{\langle 0|0\rangle}_{1} \\
&= t
\end{aligned}$$

A.5 Computational Generation of Matrix Hamiltonians

Although is it possible to derive matrix Hamiltonians for a given system of M sites analytically by calculating matrix elements by hand, it is a rather tedious process given a number of k^2 matrix elements (where k is the number of possible electronic configurations).

One possible method of increasing the efficiency of this process is to generate the matrix Hamiltonian computationally by using differences in occupation number states represented by computational arrays (or vectors) to infill elements directly.

Essentially, terms in a second quantized Hamiltonian describe changes to fermion occupation of sites, eg. an exchange of particles on neighboring sites, creation of a cooper pair on neighboring sites, etc. By mapping occupation number states to computational arrays, iterating through each possible combination of states, and comparing them, Hamiltonian coefficients can be mapped to each comparison and placed in a corresponding empty array representing the matrix Hamiltonian.

Although each generation program is required to be tailored to the individual Hamiltonian represented due to the large number of possible terms and operator combinations, an example of one possible occupation state comparison method is shown below.

Example: Computational Mapping of Hamiltonian Matrix Tunneling Element

Consider the matrix element $H_{12,13} = t$ describing the tunneling of a spinless fermion from site 2 to site 3. Computationally, the states $|12\rangle$ and $|13\rangle$ can be represented by the vectors:

$$|12\rangle = (1, 2)$$
$$|13\rangle = (1, 3)$$

By noting that the length of each vector is identical, and that the norm of (1,3) - (1,2) = 1, the "rule" can be made that for each set of two configurations p, q where the lengths are identical and the norm of their difference is 1, the corresponding Hamiltonian matrix element $H_{p,q} = t$.

(It should be noted that for proper mapping, a casual application of "proof by induction" should be used, where numerous coefficients are calculated analytically for each Hamiltonian term to ensure any given "rules" are correct for all elements k^2 in any given system of M sites.)

A generalized algorithm and program structure are shown as a flow chart in Fig. (A.1) below, where Fig. (A.1) a). describes the general function call for Hamiltonian generation, and Fig. (A.1) b). describes the Hamiltonian generation function.

The generalized mapping procedure and analytical Hamiltonian terms are used in the generalized algorithm of Fig. (A.1) to determine the exact if and if-else statements as shown in the figure. These 'if' and 'if-else' statements are used (as shown in the example above) to add Hamiltonian coefficients to the rows p and columns q of the computationally generated matrix Hamiltonian, where these correspond directly to elements p and q of the list of all possible electronic configurations.

An explicit example of such a Hamiltonian matrix generation function is described in detail in Section 2.1.2, with source code in Appendix C.1, where the matrix Hamiltonian of Kitaev's "toy chain" is generated computationally.

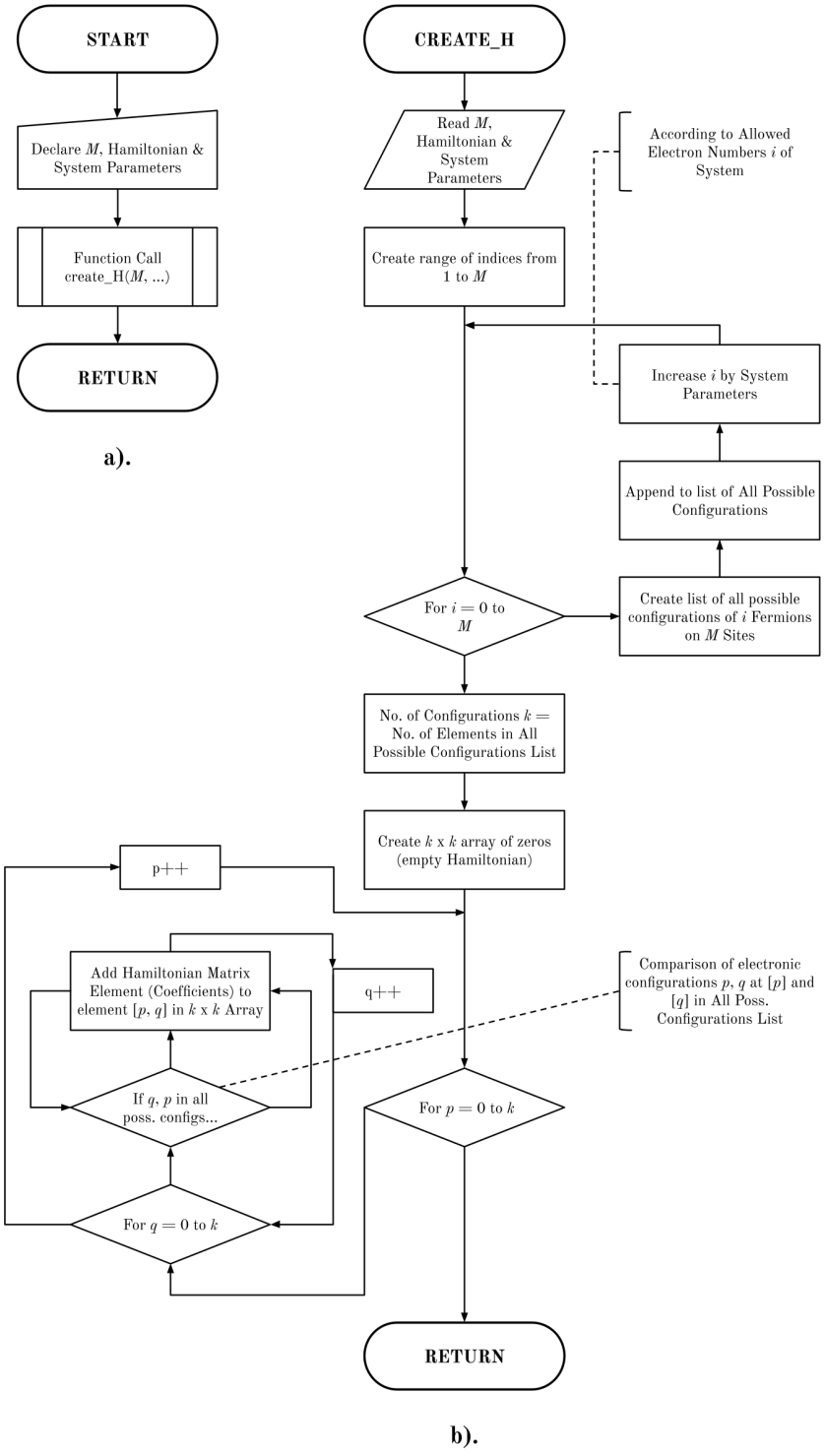

Figure A.1: Program flowchart for computational generation of a Hamiltonian matrix of M sites. a). Main function call, b). main function.

A.6 Exact Diagonalization, Energy Spectra, and Wavefunctions

In general, to know information about the probability of the system being in certain states (eg. in the case of this thesis, the focus is on the occurrence of the system being in such a state such that unpaired majorana fermions may emerge), it is first necessary to solve the eigenvalue problem of the system given by Eq. (A.1):

$$\hat{H}\,|\psi_\alpha\rangle = E_\alpha\,|\psi_\alpha\rangle \tag{A.1}$$

As per Sec. A.3 and the configuration-interaction method, it is possible to perform diagonalization upon a given matrix representation of a Hamiltonian, where the returned eigenvalues of the matrix will be the energy spectra of configurations, and the returned eigenvectors will be the system wavefunctions - hence, allowing the eigenvalue equation Eq. (A.1) to be solved.

In general, any Hamiltonian matrix representing a system of k possible configurations will be a square k x k matrix, where such a square matrix is said to be diagonalizable if and only if it has k linearly independent eigenvectors. Such a diagonalizable matrix can be written in the form:

$$\hat{H} = WDW^{-1} \tag{A.23}$$

Where D is a k x k diagonal matrix consisting of the eigenvalues of $\hat{H}$, and W is a k x k matrix consisting of the associated eigenvectors.

Depending on the characteristics of such a Hamiltonian matrix $\hat{H}$, various diagonalization methods (either analytical or computational) may be used, with varying degrees of difficulty, problem scope, and accuracy. The calculations and computational work in this thesis were performed in Python 3, therefore pre-built diagonalization methods were available through Python's packages and functions, and it was not required to explicitly write any eigenvalue calculators.

Within Python 3, if $\hat{H}$ is a Hermitian matrix of this form, the eigenvalue problem can be solved exactly by decomposing $\hat{H}$ into its constituents of Eq. (A.23),

and returning the eigenvalues $\hat{H}$ given by D. The function `linalg.eigh` of the `numpy` package performs this matrix decomposition through spectral factorization on a given Hermitian matrix, returning a complete list of eigenvalues. Alternately, if both eigenvalues and eigenvectors are calculated, `eigh` uses an iterative QR decomposition instead. In general, the `eigh` function uses symmetry of Hermitian matrices to reduce computational time, where recall a Hermitian matrix $\hat{H}$ and its matrix elements $H_{\gamma,\beta}$ are defined by the symmetry relations:

$$\begin{aligned} \hat{H}^\dagger &= \hat{H} \\ H^*_{\gamma,\beta} &= H_{\beta,\gamma} \\ \langle\phi_\gamma|\,\hat{H}\,|\phi_\beta\rangle^* &= \langle\phi_\beta|\,\hat{H}^\dagger\,|\phi_\gamma\rangle \end{aligned} \tag{A.24}$$

Where † represents the Hermitian conjugate, and in the case of scalar matrix elements, will simply be equivalent to the complex conjugate *.

In this thesis, the Hamiltonians studied are all Hermitian operators. From the definition of states in the occupation number basis, the matrix elements $H_{\gamma,\beta}$ will also follow the condition of Eq. (A.24). This can be shown using the canonically ordered definition of occupation number states of Eq. (A.19), and conventional Hermitian conjugation rules for operators:

$$\begin{aligned} (c)^\dagger &= c^\dagger \\ (c^\dagger)^\dagger &= c \\ (c_a c_b)^\dagger &= c_b^\dagger c_a^\dagger \end{aligned} \tag{A.25}$$

Where it should be noted that in general, for any product of multiple bras, kets, and operators, the Hermitian conjugate can be taken by taking the Hermitian conjugate of each individual component, and swapping the order of all components.

Hence, using these relations, any matrix element $H_{\gamma,\beta}$ in the occupation number basis can be written:

$$
\begin{aligned}
H^*_{\gamma,\beta} &= \langle\phi_\gamma| \hat{H} |\phi_\beta\rangle^\dagger \\
&= \langle 0| ...c_{\gamma+1}c_\gamma c_{\gamma-1}...\hat{H}...c^\dagger_{\beta-1}c^\dagger_\beta c^\dagger_{\beta+1}... |0\rangle^\dagger \\
&= \langle 0| (...c_{\gamma+1}c_\gamma c_{\gamma-1}...\hat{H}...c^\dagger_{\beta-1}c^\dagger_\beta c^\dagger_{\beta+1}...)^\dagger |0\rangle \\
&= \langle 0| ...(c^\dagger_{\beta+1})^\dagger (c^\dagger_\beta)^\dagger (c^\dagger_{\beta-1})^\dagger ...(\hat{H})^\dagger ...(c_{\gamma-1})^\dagger (c_\gamma)^\dagger (c_{\gamma+1})^\dagger ... |0\rangle \\
&= \langle 0| ...c_{\beta+1}c_\beta c_{\beta-1}...\hat{H}^\dagger ...c^\dagger_{\gamma-1}c^\dagger_\gamma c^\dagger_{\gamma+1}... |0\rangle \\
&= \langle\phi_\beta| \hat{H}^\dagger |\phi_\gamma\rangle
\end{aligned}
$$

As it is already known that the Hamiltonian $\hat{H}$ is Hermitian such that $\hat{H} = \hat{H}^\dagger$, it follows that the above may be written:

$$
\begin{aligned}
\langle\phi_\beta| \hat{H}^\dagger |\phi_\gamma\rangle &= \langle\phi_\beta| \hat{H} |\phi_\gamma\rangle \\
&= H_{\beta,\gamma} \\
\therefore H^*_{\gamma,\beta} &= H_{\beta,\gamma}
\end{aligned}
\tag{A.26}
$$

Thus, for any matrix element $H_{\gamma,\beta}$ of a Hermitian Hamiltonian $\hat{H}$ in the occupation number basis with canonical ordering as defined in Eq. (A.19), it can be said that the corresponding matrix representation of $\hat{H}$ is also Hermitian.

Hence, by using the Python 3 function `eigh` on such Hermitian Hamiltonians, exact diagonalization was performed in order to calculate energy eigenvalues and wavefunction eigenvectors of the given systems. These eigenvalues could then be plotted through the use of Python 3's `matplotlib` package, generating visual representations of energy spectra.

Similarly, by taking the square of each eigenvector of the system (where `eigh` returns the normalized eigenvectors), the system probability densities $|\,|\psi_\alpha\rangle\,|^2$ (or probabilities of each configuration occurring in each state of the system) could then also be plotted using the `matplotlib` package.

A.7 Accuracy of Numerical Methods

In order to ensure accuracy of numerical and computational methods used, several methods have been employed to minimize error and prevent inaccurate reporting of

results.

For results reported in the publication described in Sec. 1.4, analytical results and derivations were compared with those of publication co-authors and were found to match exactly. These analytical results compared consisted of matrix Hamiltonian representations of Kitaev's chain in the fermion and bond fermion representations described in Chapters 2, 3, and 4.

For generalized eigenvalue calculations, Python's `eigh` function of the `numpy` package returns results with double-precision floating point accuracy, ie. performs calculations with up to 64-bit precision, or roughly 15-17 digits of precision.

This is confirmed with the comparison of returned eigenvalues after basis mapping, where a set of example system eigenvalues (for a Kitaev chain of 3 sites) on the order of 0.5×10^1 were compared and found to be exact to minimum 15 digits of accuracy, as shown in Fig. (A.2) below. The compared matrix Hamiltonians in the example case are not equivalent, however the eigenvalue calculations for each of the four matrix Hamiltonians converge to the same values with minimum 15 digits of precision.

This error found is minimal in comparison to the order of magnitude of calculated eigenvalues, where eigenvalues on the order of 0.5×10^1 gave a greatest error on the order of 4.0×10^{-15}. As a result, any computational error as a result of Python's exact diagonalization routines can be considered insignificant on the scale of these results, and are not considered to affect the results and conclusions of this work.

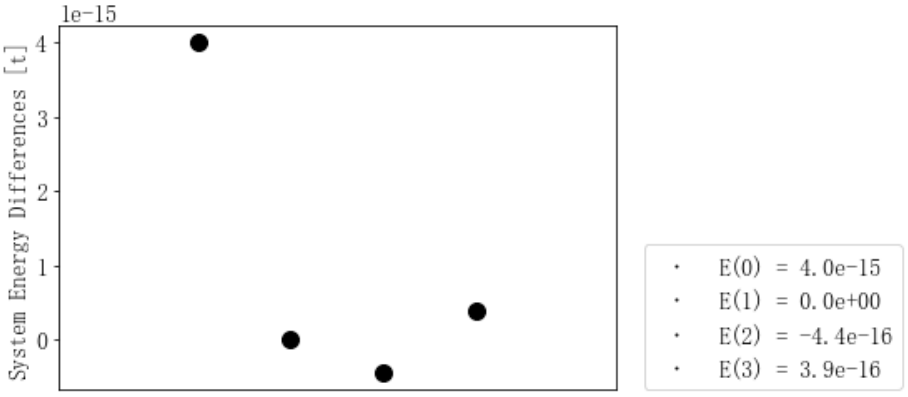

Figure A.2: Example comparison of energy spectra of three-site t, Δ, μ finite Kitaev chain, odd subspace, between fermionic and bond fermion bases.

Appendix B: Derivations and Example Calculations

B.1 Derivation of the Kitaev Hamiltonian in Majorana Fermions

By using the fermionic and Majorana fermion relations in Eq. (3.2) and (3.3), the original Kitaev chain Hamiltonian for N sites given by Eq. (1.1) can be transformed into the Majorana basis. Beginning with Eq. (1.1):

$$\hat{H}_K = t\sum_{i=1}^{N-1}(c_{i+1}^\dagger c_i + c_i^\dagger c_{i+1}) + \Delta\sum_{i=1}^{N-1}(c_{i+1}^\dagger c_i^\dagger + c_i c_{i+1}) - \mu\sum_{i=1}^{N}(c_i^\dagger c_i) \tag{1.1}$$

Beginning with only the tunneling term, subbing in Majorana operators:

$$\begin{aligned}
t\sum_{i=1}^{N-1} c_{i+1}^\dagger c_i + c_i^\dagger c_{i+1} &= t\sum_{i=1}^{N-1}\{\frac{1}{2}(\gamma_{i+1,1} - i\gamma_{i+1,2})\frac{1}{2}(\gamma_{i,1} + i\gamma_{i,2}) \\
&\qquad + \frac{1}{2}(\gamma_{i,1} - i\gamma_{i,2})\frac{1}{2}(\gamma_{i+1,1} + i\gamma_{i+1,2})\} \\
&= \frac{t}{4}\sum_{i=1}^{N-1}\gamma_{i+1,1}\gamma_{i,1} - i\gamma_{i+1,2}\gamma_{i,1} + i\gamma_{i+1,1}\gamma_{i,2} - i^2\gamma_{i+1,2}\gamma_{i,2} \\
&\qquad + \gamma_{i,1}\gamma_{i+1,1} - i\gamma_{i,2}\gamma_{i+1,1} + i\gamma_{i,1}\gamma_{i+1,2} - i^2\gamma_{i,2}\gamma_{i+1,2} \\
&= \frac{t}{4}\sum_{i=1}^{N-1}\cancel{\gamma_{i+1,1}\gamma_{i,1}} + i\gamma_{i,1}\gamma_{i+1,2} + i\gamma_{i+1,1}\gamma_{i,2} - \cancel{i^2\gamma_{i+1,2}\gamma_{i,2}} \\
&\qquad - \cancel{\gamma_{i+1,1}\gamma_{i,1}} + i\gamma_{i+1,1}\gamma_{i,2} + i\gamma_{i,1}\gamma_{i+1,2} + \cancel{i^2\gamma_{i,2}\gamma_{i+1,2}\gamma_{i,2}} \\
&= \frac{t}{4}\sum_{i=1}^{N-1} 2i\gamma_{i,1}\gamma_{i+1,2} + 2i\gamma_{i+1,1}\gamma_{i,2} \\
&= \frac{it}{2}\sum_{i=1}^{N-1}\gamma_{i,1}\gamma_{i+1,2} + \gamma_{i+1,1}\gamma_{i,2}
\end{aligned}$$

Then, the process is repeated with only the pairing term:

$$\begin{aligned}
\Delta\sum_{i=1}^{N-1} c_{i+1}^{\dagger}c_i^{\dagger} + c_i c_{i+1} &= \Delta\sum_{i=1}^{N-1}\{\frac{1}{2}(\gamma_{i+1,1} - i\gamma_{i+1,2})\frac{1}{2}(\gamma_{i,1} - i\gamma_{i,2}) \\
&\qquad + \frac{1}{2}(\gamma_{i,1} + i\gamma_{i,2})\frac{1}{2}(\gamma_{i+1,1} + i\gamma_{i+1,2})\} \\
&= \frac{\Delta}{4}\sum_{i=1}^{N-1}\gamma_{i+1,1}\gamma_{i,1} - i\gamma_{i+1,2}\gamma_{i,1} - i\gamma_{i+1,1}\gamma_{i,2} + i^2\gamma_{i+1,2}\gamma_{i,2} \\
&\qquad + \gamma_{i,1}\gamma_{i+1,1} + i\gamma_{i,2}\gamma_{i+1,1} + i\gamma_{i,1}\gamma_{i+1,2} + i^2\gamma_{i,2}\gamma_{i+1,2} \\
&= \frac{\Delta}{4}\sum_{i=1}^{N-1}\gamma_{i+1,1}\gamma_{i,1} + i\gamma_{i,1}\gamma_{i+1,2} - i\gamma_{i+1,1}\gamma_{i,2} + i^2\gamma_{i+1,2}\gamma_{i,2} \\
&\qquad - \gamma_{i+1,1}\gamma_{i,1} - i\gamma_{i+1,1}\gamma_{i,2} + i\gamma_{i,1}\gamma_{i+1,2} - i^2\gamma_{i+1,2}\gamma_{i,2} \\
&= \frac{\Delta}{4}\sum_{i=1}^{N-1}\cancel{\gamma_{i+1,1}\gamma_{i,1}} + i\gamma_{i,1}\gamma_{i+1,2} - i\gamma_{i+1,1}\gamma_{i,2} + \cancel{i^2\gamma_{i+1,2}\gamma_{i,2}} \\
&\qquad - \cancel{\gamma_{i+1,1}\gamma_{i,1}} - i\gamma_{i+1,1}\gamma_{i,2} + i\gamma_{i,1}\gamma_{i+1,2} - \cancel{i^2\gamma_{i+1,2}\gamma_{i,2}} \\
&= \frac{\Delta}{4}\sum_{i=1}^{N-1} 2i\gamma_{i,1}\gamma_{i+1,2} - 2i\gamma_{i+1,1}\gamma_{i,2} \\
&= \frac{i\Delta}{2}\sum_{i=1}^{N-1}\gamma_{i,1}\gamma_{i+1,2} - \gamma_{i+1,1}\gamma_{i,2}
\end{aligned}$$

Where it can be noted that the tunneling and pairing terms contain the same terms, and are contained over the same summation. Therefore, combining the tunneling and pairing terms to further simplify:

$$\begin{aligned}
&\frac{it}{2}\sum_{i=1}^{N-1}(\gamma_{i,1}\gamma_{i+1,2} + \gamma_{i+1,1}\gamma_{i,2}) + \frac{i\Delta}{2}\sum_{i=1}^{N-1}(\gamma_{i,1}\gamma_{i+1,2} - \gamma_{i+1,1}\gamma_{i,2}) \\
&\qquad = \frac{i}{2}\sum_{i=1}^{N-1}\{t(\gamma_{i,1}\gamma_{i+1,2} + \gamma_{i+1,1}\gamma_{i,2}) + \Delta(\gamma_{i,1}\gamma_{i+1,2} - \gamma_{i+1,1}\gamma_{i,2})\} \\
&\qquad = \frac{i}{2}\sum_{i=1}^{N-1}\{(t+\Delta)\gamma_{i,1}\gamma_{i+1,2} + (t-\Delta)\gamma_{i+1,1}\gamma_{i,2}\} \\
&\qquad = \frac{i(t+\Delta)}{2}\sum_{i=1}^{N-1}\gamma_{i,1}\gamma_{i+1,2} + \frac{i(t-\Delta)}{2}\sum_{i=1}^{N-1}\gamma_{i+1,1}\gamma_{i,2}
\end{aligned}$$

Hence, the pairing and tunneling terms of the Kitaev chain Hamiltonian in Majorana fermions can be written as above.

Finally, the chemical potential term can be derived (once again in the same process as above):

$$\begin{aligned}
-\mu \sum_{i=1}^{N} c_i^\dagger c_i &= -\mu \sum_{i=1}^{N} \frac{1}{2}(\gamma_{i,1} - i\gamma_{i,2})\frac{1}{2}(\gamma_{i,1} + i\gamma_{i,2}) \\
&= -\frac{\mu}{4} \sum_{i=1}^{N} \gamma_{i,1}\gamma_{i,1} - i\gamma_{i,2}\gamma_{i,1} + i\gamma_{i,1}\gamma_{i,2} - i^2\gamma_{i,2}\gamma_{i,2} \\
&= -\frac{\mu}{4} \sum_{i=1}^{N} \gamma_{i,1}^2 + i\gamma_{i,1}\gamma_{i,2} + i\gamma_{i,1}\gamma_{i,2} + \gamma_{i,2}^2 \\
&= -\frac{\mu}{4} \sum_{i=1}^{N} 2 + 2i\gamma_{i,1}\gamma_{i,2} \\
&= -\frac{\mu}{2} \sum_{i=1}^{N} 1 + i\gamma_{i,1}\gamma_{i,2} \\
&= -\frac{N\mu}{2} - \frac{i\mu}{2} \sum_{i=1}^{N} \gamma_{i,1}\gamma_{i,2}
\end{aligned}$$

Then, combining all three terms above gives the final form of the Kitaev chain Hamiltonian in Majorana fermion operators (as in Eq. (3.4)):

$$\hat{H}_M = \frac{i(t+\Delta)}{2} \sum_{i=1}^{N-1} \gamma_{i,1}\gamma_{i+1,2} + \frac{i(t-\Delta)}{2} \sum_{i=1}^{N-1} \gamma_{i+1,1}\gamma_{i,2} - \frac{i\mu}{2} \sum_{i=1}^{N} \gamma_{i,1}\gamma_{i,2} - \frac{N\mu}{2} \quad (3.4)$$

B.2 Derivation of the Kitaev Hamiltonian in Bond Fermions

B.2.1 Simplified Kitaev Hamiltonian in Bond Fermions

In order to transform the simplified Kitaev Hamiltonian into the basis of bond fermions, consider the simplified Kitaev Hamiltonian in the basis of Majorana fermions as given by Eq. (3.8):

$$\hat{H}_M = i\Delta \sum_{i=1}^{N-1} \gamma_{i,1}\gamma_{i+1,2} \tag{3.8}$$

As the bond fermionic operators are defined in terms of two Majorana operators γ, using the bond fermion operator definitions of Eq. (3.5) and Majorana operator relations of Eq. (3.3), firstly calculate the bond fermion number operator:

$$\begin{aligned} a_i^\dagger a_i &= \frac{1}{2}(\gamma_{i,1} - i\gamma_{i+1,2})\frac{1}{2}(\gamma_{i,1} + i\gamma_{i+1,2}) \\ &= \frac{1}{4}(\gamma_{i,1}\gamma_{i,1} - i\gamma_{i+1,2}\gamma_{i,1} + i\gamma_{i,1}\gamma_{i+1,2} - i^2\gamma_{i+1,2}\gamma_{i+1,2}) \\ &= \frac{1}{4}(1 + i\gamma_{i,1}\gamma_{i+1,2} + i\gamma_{i,1}\gamma_{i+1,2} + 1) \\ &= \frac{1}{4}(2i\gamma_{i,1}\gamma_{i+1,2} + 2) \\ &= \frac{1}{2}(i\gamma_{i,1}\gamma_{i+1,2} + 1) \end{aligned} \tag{B.1}$$

Where it is noted that the term $i\gamma_{i,1}\gamma_{i+1,2}$ is exactly the one which appears in our Majorana Hamiltonian above. Hence, solving for $i\gamma_{i,1}\gamma_{i+1,2}$ in terms of the bond fermionic number operator:

$$\begin{aligned} a_i^\dagger a_i &= \frac{1}{2}(i\gamma_{i,1}\gamma_{i+1,2} + 1) \\ 2a_i^\dagger a_i - 1 &= i\gamma_{i,1}\gamma_{i+1,2} \end{aligned} \tag{B.2}$$

Thus, substituting the above relation into the simplified Kitaev Hamiltonian:

$$i\Delta \sum_{i=1}^{N-1} \gamma_{i,1}\gamma_{i+1,2} = \Delta \sum_{i=1}^{N-1} (2a_i^\dagger a_i - 1)$$

Which gives the final form of the simplified Kitaev Hamiltonian in bond fermions (as in Eq. (3.9)):

$$\hat{H}_B = \Delta \sum_{i=1}^{N-1} (2a_i^\dagger a_i - 1) \tag{3.9}$$

B.2.2 Example of (Simplified) Kitaev Hamiltonian Eigenvalue Calculation in the Bond Fermion Basis

For the Kitaev Hamiltonian on three sites in the bond fermion basis, of Eq. (3.13):

$$\hat{H}_B = \Delta(2a_1^\dagger a_1 - 1) + \Delta(2a_2^\dagger a_2 - 1) + 0(2a_3^\dagger a_3 - 1) \tag{3.13}$$

An example eigenvalue calculation is computed below, using the bond fermionic relations in Eq. (3.6) and Eq. (3.7).

Example: Pairing Term (Two-Electron Configuration)

The Kitaev Hamiltonian eigenvalue corresponding to bond fermion occupation state $|13\rangle$ is calculated as follows:

$$H_B\,|13\rangle = [\Delta(2a_1^\dagger a_1 - 1) + \Delta(2a_2^\dagger a_2 - 1) + 0(2a_3^\dagger a_3 - 1)]\,|13\rangle$$

Where recall the number operator $a_i^\dagger a_i = 1$ if acting on an occupied site, or $= 0$ if acting on an unoccupied site:

$$H_B\,|13\rangle = [\Delta(2\underbrace{a_1^\dagger a_1}_{1} - 1) + \Delta(2\underbrace{a_2^\dagger a_2}_{0} - 1) + 0(2\underbrace{a_3^\dagger a_3}_{1} - 1)]\,|13\rangle$$

$$
\begin{aligned}
H_B\,|13\rangle &= [\Delta(2-1) + \Delta(0-1) + 0(2-1)]\,|13\rangle \\
&= [\Delta - \Delta + 0]\,|13\rangle \\
&= 0\,|13\rangle
\end{aligned}
$$

Thus, the energy of the configuration $|13\rangle$ is $0\,[\Delta]$.

B.2.3 Full Kitaev Hamiltonian in Bond Fermions

In order to transform the chain Kitaev Hamiltonian into the basis of bond fermions, consider the chain Kitaev Hamiltonian in the basis of Majorana fermions as given by Eq. (3.4):

$$
\hat{H}_M = \frac{i(t+\Delta)}{2}\sum_{i=1}^{N-1}\gamma_{i,1}\gamma_{i+1,2} + \frac{i(t-\Delta)}{2}\sum_{i=1}^{N-1}\gamma_{i+1,1}\gamma_{i,2} - \frac{i\mu}{2}\sum_{i=1}^{N}\gamma_{i,1}\gamma_{i,2} - \frac{N\mu}{2} \tag{3.4}
$$

As the bond fermionic operators are defined in terms of two Majorana operators γ, using the bond fermion operator definitions of Eq. (3.5) and Majorana operator relations of Eq. (3.3), firstly recall the bond fermion number operator from the previous Appendix B.2.1:

$$
2a_i^\dagger a_i - 1 = i\gamma_{i,1}\gamma_{i+1,2} \tag{B.2}
$$

Thus, the first term of $\hat{H}_M$ becomes (straightforwardly):

$$
\frac{i(t+\Delta)}{2}\sum_{i=1}^{N-1}\gamma_{i,1}\gamma_{i+1,2} = \frac{(t+\Delta)}{2}\sum_{i=1}^{N-1}(2a_i^\dagger a_i - 1)
$$

Then, in order to transform the other terms of the Hamiltonian, an expression must be found for $\gamma_{i,2}$ and $\gamma_{i+1,1}$. Firstly, consider the bond fermionic relations in terms of Majorana fermions, as given in Eq. (3.5), and letting index $i \longrightarrow i+1$:

$$\begin{aligned} a_{i+1} &= \frac{1}{2}(\gamma_{i+1,1} + i\gamma_{i+2,2}) \\ a_{i+1}^{\dagger} &= \frac{1}{2}(\gamma_{i+1,1} - i\gamma_{i+2,2}) \end{aligned} \tag{B.3}$$

Thus:

$$\begin{aligned} a_{i+1} + a_{i+1}^{\dagger} &= \frac{1}{2}(\gamma_{i+1,1} + i\gamma_{i+2,2}) + \frac{1}{2}(\gamma_{i+1,1} - i\gamma_{i+2,2}) \\ &= \frac{1}{2}(\gamma_{i+1,1} + \cancel{i\gamma_{i+2,2}} + \gamma_{i+1,1} - \cancel{i\gamma_{i+2,2}}) \\ a_{i+1} + a_{i+1}^{\dagger} &= \gamma_{i+1,1} \end{aligned} \tag{B.4}$$

Repeating these calculations for a further index:

$$\begin{aligned} a_{i-1} &= \frac{1}{2}(\gamma_{i-1,1} + i\gamma_{i,2}) \\ a_{i-1}^{\dagger} &= \frac{1}{2}(\gamma_{i-1,1} - i\gamma_{i,2}) \end{aligned} \tag{B.5}$$

Thus:

$$\begin{aligned} a_{i-1} - a_{i-1}^{\dagger} &= \frac{1}{2}(\gamma_{i-1,1} + i\gamma_{i,2}) - \frac{1}{2}(\gamma_{i-1,1} - i\gamma_{i,2}) \\ &= \frac{1}{2}(\cancel{\gamma_{i-1,1}} + i\gamma_{i,2} - \cancel{\gamma_{i-1,1}} + i\gamma_{i,2}) \\ a_{i-1} - a_{i-1}^{\dagger} &= i\gamma_{i,2} \end{aligned} \tag{B.6}$$

Finally, in order to derive the $\gamma_{i,1}$ operator required to calculate the chemical potential term of the Hamiltonian, consider Eq. (3.5):

$$\begin{aligned} a_i &= \frac{1}{2}(\gamma_{i,1} + i\gamma_{i+1,2}) \\ a_i^{\dagger} &= \frac{1}{2}(\gamma_{i,1} - i\gamma_{i+1,2}) \end{aligned} \tag{3.5}$$

Thus:

$$\begin{aligned} a_i + a_i^\dagger &= \frac{1}{2}(\gamma_{i,1} + i\gamma_{i+1,2}) + \frac{1}{2}(\gamma_{i,1} - i\gamma_{i+1,2}) \\ &= \frac{1}{2}(\gamma_{i,1} + \cancel{i\gamma_{i+1,2}} + \gamma_{i,1} - \cancel{i\gamma_{i+1,2}}) \\ a_i + a_i^\dagger &= \gamma_{i,1} \end{aligned} \tag{B.7}$$

Then, as all required operators have been derived, plugging in to the required terms of the Hamiltonian:

$$\begin{aligned} \frac{i(t-\Delta)}{2}\sum_{i=1}^{N-1}\gamma_{i+1,1}\gamma_{i,2} &= \frac{(t-\Delta)}{2}\sum_{i=1}^{N-1}(a_{i+1} + a_{i+1}^\dagger)(a_{i-1} - a_{i-1}^\dagger) \\ \frac{i\mu}{2}\sum_{i=1}^{N}\gamma_{i,1}\gamma_{i,2} &= \frac{\mu}{2}\sum_{i=1}^{N}(a_i + a_i^\dagger)(a_{i-1} - a_{i-1}^\dagger) \end{aligned}$$

Finally, plugging all terms back into Eq. (3.4), the full chain Kitaev Hamiltonian in the bond fermion basis becomes:

$$\begin{aligned} H_B = &\frac{(t+\Delta)}{2}\sum_{i=1}^{N-1}(2a_i^\dagger a_i - 1) \\ &+ \frac{(t-\Delta)}{2}\sum_{i=1}^{N-1}(a_{i+1} + a_{i+1}^\dagger)(a_{i-1} - a_{i-1}^\dagger) \\ &- \frac{\mu}{2}\sum_{i=1}^{N}(a_i + a_i^\dagger)(a_{i-1} - a_{i-1}^\dagger) - \frac{\mu N}{2} \end{aligned} \tag{B.8}$$

Appendix C: Source Codes

C.1 Generation of the Matrix Kitaev Hamiltonian

```
def create_numerical_H(N, t_n, Delta_n, mu_n, evenodd, ring):

    #Create range of indices from 1 to N.
    indices = range(1,N+1)

    #Making sure all our values are okay... these are simply the
    conventions we use to submit to code.
    t_n = -1*abs(t_n)
    Delta_n = -1*abs(Delta_n)
    mu_n = abs(mu_n)

    #Create the list of possible site occupations, where these are
    combinations without repetition.
    #These are of course different for the even and odd subspaces of the
     Hamiltonian...

    if evenodd == "Even":
        site_indices = list(itertools.combinations(indices, 2))

        #Note we need to insert the vacuum state when considering
        #even occupation.
        site_indices.insert(0,(0,))
        if N >= 4:
            for i in range(4,N+1,2):
                site_indices_2 = list(itertools.combinations(indices,i))
                for j in range(len(site_indices_2)):
                    site_indices.append(site_indices_2[j])

    elif evenodd == "Odd":
        site_indices = list(itertools.combinations(indices, 1))
        if N >= 3:
            for i in range(3,N+1,2):
                site_indices_2 = list(itertools.combinations(indices,i))
                for j in range(len(site_indices_2)):
                    site_indices.append(site_indices_2[j])

    #Create an empty Hamiltonian which we can then fill with our
    numerical parameters.
    site_indices = np.asarray(site_indices)
    print(site_indices)
```

```
no_config = len(site_indices)
H = np.zeros((no_config,no_config))

#Fill the elements of the matrix Hamiltonian by iterating over sites
.
#For the "normal" fermion Hamiltonian, this is relatively simple.
for i in range(no_config):
    for j in range(no_config):
        if len(site_indices[i]) == len(site_indices[j]):

            #No change in the electron occupation indicates
            #tunneling if one site is changed to NN.
            if la.norm(np.asarray(site_indices[i])
            - np.asarray(site_indices[j])) == 1:
                H[i][j] = t_n

            if (evenodd == "Even") and (ring == "Ring")
            and (N >= 3):
                if (set(np.setxor1d(site_indices[i],
                site_indices[j])) == set([1,N])) and
                (len(np.intersect1d(site_indices[i],
                site_indices[j])) == (len(site_indices[i]) - 1)):
                    H[i][j] = -1*t_n

            elif (evenodd == "Odd") and (ring == "Ring")
            and (N >= 3):
                if (set(np.setxor1d(site_indices[i],
                site_indices[j])) == set([1,N])) and
                (len(np.intersect1d(site_indices[i],
                site_indices[j])) == (len(site_indices[i]) - 1)):
                    H[i][j] = t_n

        #Next consider the case where the lengths differ by 2:
        elif len(site_indices[i]) == len(site_indices[j]) - 2:

            #When site index j has two more elements than i,
            #indicates creation or annihilation of cooper pair.
            diffelements = np.setdiff1d(site_indices[j],
            site_indices[i])

            if (abs(diffelements[1] - diffelements[0]) == 1)
            and (len(diffelements) == 2):
                H[i][j] = Delta_n
                H[j][i] = Delta_n

            elif (evenodd == "Odd") and (ring == "Ring")
            and (N >= 3) and (len(diffelements) == 2)
            and ((diffelements[0] == 1) and diffelements[1] == N):
                H[i][j] = Delta_n
                H[j][i] = Delta_n

            elif (evenodd == "Even") and (ring == "Ring")
            and (N >= 3) and (len(diffelements) == 2)
            and ((diffelements[0] == 1) and diffelements[1] == N):
```

```
                H[i][j] = Delta_n
                H[j][i] = Delta_n

        if np.asarray(site_indices[0][0]) == 0:
            if len(site_indices[j]) == 2:

                diffelements = np.setdiff1d(site_indices[j],
                site_indices[0])

                if (abs(diffelements[1] - diffelements[0]) == 1)
                and (len(diffelements) == 2):
                    H[0][j] = Delta_n
                    H[j][0] = Delta_n

                elif (evenodd == "Even") and (ring == "Ring")
                and (N >= 3) and (len(diffelements) == 2)
                and ((diffelements[0] == 1)
                and diffelements[1] == N):
                    H[0][j] = -1*Delta_n
                    H[j][0] = -1*Delta_n

                elif (evenodd == "Odd") and (ring == "Ring")
                and (N >= 3) and (len(diffelements) == 2)
                and ((diffelements[0] == 1)
                and diffelements[1] == N):
                    H[0][j] = Delta_n
                    H[j][0] = Delta_n

        #Now let's add in chemical potential...
        if i == j:
            H[i][j] = -1*mu_n*len(site_indices[i])

            if np.asarray(site_indices[0][0]) == 0:
                H[0][0] = 0
return H
```